A Thesis

For the Degree of Master of Science

Anti-oxidant, anti-inflammatory and anti-melanogenesis effects of Narcissus extracts

Department of Veterinary Medicine

GRADUATE SCHOOL

JEJU NATIONAL UNIVERSITY

Chanuri Yashara Dissanayake

June, 2018

Anti-oxidant, anti-inflammatory and anti-melanogenesis

effects of Narcissus extracts

Chanuri Yashara Dissanayake

(Supervised by Professor Chang-Hoon Han)

A thesis submitted in partial fulfillment of the requirement

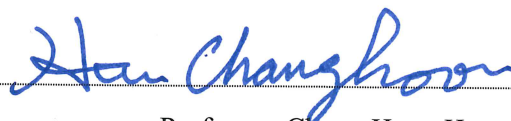for the degree of Master of Science

2018. 06. 01

This thesis has been examined and approved by

Professor, Youngheun Jee

College of Veterinary Medicine

Professor, Young-Jae Lee

College of Veterinary Medicine

Professor, Chang-Hoon Han

College of Veterinary Medicine

Date

Department of Veterinary Medicine

Graduate School, Jeju National University

ii

TABLE OF CONTENTS

ABSTRACT

The present study was performed to evaluate the inhibitory activity of extracts of *Narcissus tazetta* var. *Chinensis* on inflammation in RAW 264.7 and melanin synthesis in B16-F10 melanoma cells. Functional effects of Narcissus flower extract (NFE), Narcissus stem extract (NSE), and Narcissus root extract (NRE) were analyzed. Narcissus extracts (NE) displayed DPPH free radical scavenging activity in a dose-dependent manner. Based on cell viability assay, NFE, NSE and NRE had no cytotoxicity up to 10, 4, 20 µg/mL concentrations in RAW 264.7 cells and 20, 5, 20 µg/mL concentrations in B16-F10 melanoma cells respectively. Based on Western blot analysis, NE significantly inhibited the production of inducible nitric oxide synthase (iNOS) and cyclooxygenase-2 (COX-2) protein expression levels, with concomitant reductions in the production of nitric oxide (NO) in LPS stimulated RAW 264.7 cells. In addition, NE inhibited pro-inflammatory cytokine levels including TNF-α, IL-1β, and IL-6 in LPS stimulated RAW 264.7 cells. NE inhibited both melanin synthesis and tyrosinase activity in α-MSH stimulated B16-F10 melanoma cells in a dose dependent manner. RNA sequencing analysis showed differential gene expression patterns in genes related to immune response, inflammatory response and antioxidant activity in LPS stimulated RAW 264.7 macrophage cells. LPS stimulated differentially expressed 39 genes related to inflammatory response including NF-κB2, AXL, APOE, LDL, TLR4, NF-κB1, IFNB1, IRAK2, NR1H4, Cxcr2, Cxcr6, Ccl28 and Cxcl9 were normalized to the control level by each NE. Overall results suggest that NE scavenged DPPH free radicles dose dependently, exhibited anti-inflammatory effects via attenuating iNOS, COX-2 protein expression, TNF-α, IL-6 and IL-1β pro-inflammatory cytokines expression and normalizing the expression of genes related to inflammation which were perturbed by LPS in RAW 264.7 macrophage cells, and showed anti-melanogenesis effects on α-MSH stimulated B16-F10 melanoma cells by suppressing the cellular tyrosinase activity and melanin synthesis in B16-F10 melanoma cells. Bioactive compounds in NE can

be applied for the development of anti-inflammatory drugs in pharmaceutical industry and for the development of anti-melanogenesis drugs in cosmetic industry.

LIST OF ABBREVIATIONS

AEAC	Ascorbic acid Equivalent Antioxidant Capacity
ANOVA	One-way analysis of variance
COX-2	Cyclooxygenase-2
DMEM	Dulbecco's Modified Eagle Medium
DPPH	2,2-diphenyl-1-picryl-hydrazyl-hydrate
EC50	Effective concentration
ELISA	Enzyme-linked immunosorbent assay
FBS	Fetal bovine serum
HPLC	High-performance liquid chromatography
LPS	Lipopolysaccharides
L-DOPA	L-3,4-dihydroxyphenylalanine
IL-1β	Interleukin 1β
IL-6	Interleukin 6
iNOS	Inducible nitric oxide synthase
NF-κb	Nuclear factor-κB
NE	Narcissus extracts
NFE	Narcissus flower extracts
NRE	Narcissus root extracts
NSE	Narcissus stem extracts
PrepLC	Preparative high-performance liquid chromatography
TNF-α	Tumor Necrosis Factor-α
α-MSH	α-Melanocyte stimulating hormone

LIST OF FIGURES

LIST OF TABLES

INTRODUCTION

Narcissus belong to the family of Amaryllidaceous are widely used as medicinal plants due to their biological properties including anti-inflammation, anti-oxidant and anti-melanogenesis activities [46, 64]. *Narcissus tazetta var. Chinensis* species have flavonoids and phytochemicals including glucomannan, pseudolycorine, lycorine, and tazettine which have biological activities [21, 34, 43]. The present study was performed to evaluate the diverse biological activities including anti-oxidant, anti-inflammatory, and anti-melanogenesis effects of phytochemicals in Narcissus *tazetta var. Chinensis.*

Inflammation is a complex biological process and a part of the defense mechanism of organisms in response to noxious stimuli including pathogens, chemicals or microbiological toxins which results in various pathologies [1, 27, 54]. Inflammation could be divided into two major groups as acute or chronic. Acute inflammation is the initial response of the body in the presence of harmful stimuli which is short term. Chronic inflammation is known to be the prolonged inflammatory response which is caused by pro-inflammatory mediators and involved in changing the types of cells present at inflamed site [42].

During inflammation, the influx of neutrophils and macrophages into the site of inflammation causes the pathogenesis of inflammatory conditions [38]. Macrophages become activated in response to microbial infections and rapidly differentiate to express several inflammatory responses including phagocytosis, secretion of cytokines and chemokines [30, 68, 76]. Lipopolysaccharide (LPS), cell wall component of gram-negative bacteria stimulates through Toll-like receptor 4 (TLR4), a membrane- bound pattern recognition receptor, resulting in the activation of a series of signaling events including NF-κB, and triggers inflammation through the production and release of pro-inflammatory

mediators and cytokines which initiate and maintain the inflammatory response [20]. Inflammatory mediators and cytokines induce the recruitment of neutrophils and increase the ROS production with mitochondrial interaction [6, 81]. Neutrophils abundantly express myeloperoxidase, which increase the bacterial lysis and amplifies the LPS release during gram-negative bacteria infection and subsequently promotes inflammation. Hence, attenuating macrophage activation could be a potential therapeutic target in inflammatory diseases [31].
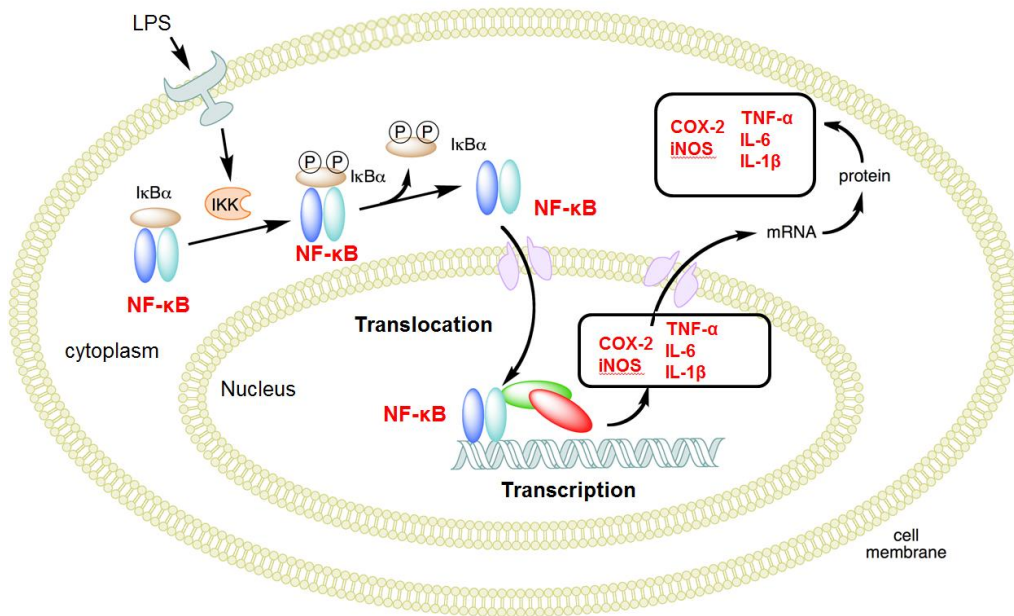
Figure 1. Mechanism of iNOS and COX-2 expression

Typically, NF-κB retains in a latent cytoplasmic form bound to nuclear factor of kappa light polypeptide gene enhancer in B-cells inhibitor, alpha (IκBα) and beta (IκBβ) inhibitor proteins, which prevent nuclear translocation of NF-κB [2]. Following cell stimulation, IκBα inhibitor protein is rapidly phosphorylated and degraded, and NF-κB is activated [15]. Activated NF-κB regulates the transcription of immune and inflammatory related genes including IL-1β, IL-6, and TNF-α like pro-inflammatory cytokines, and COX-2 and iNOS like inflammatory mediators [3, 25, 35] [Figure 1].

iNOS is induced in response to LPS, and a variety of pro-inflammatory cytokines increase the NO production intensifying inflammation [50]. NO, a pro-inflammatory mediator, and is significantly elevated during inflammation in LPS-stimulated macrophages by nitric oxide synthase (NOS) converting L- arginine into citrulline, and then peroxynitrite (ONOO$^-$) is synthesized. Presence of large amount of cytotoxic ONOO$^-$ leads to tissue damage as a consequence of oxidative stress and DNA damage [28] [Figure 2].
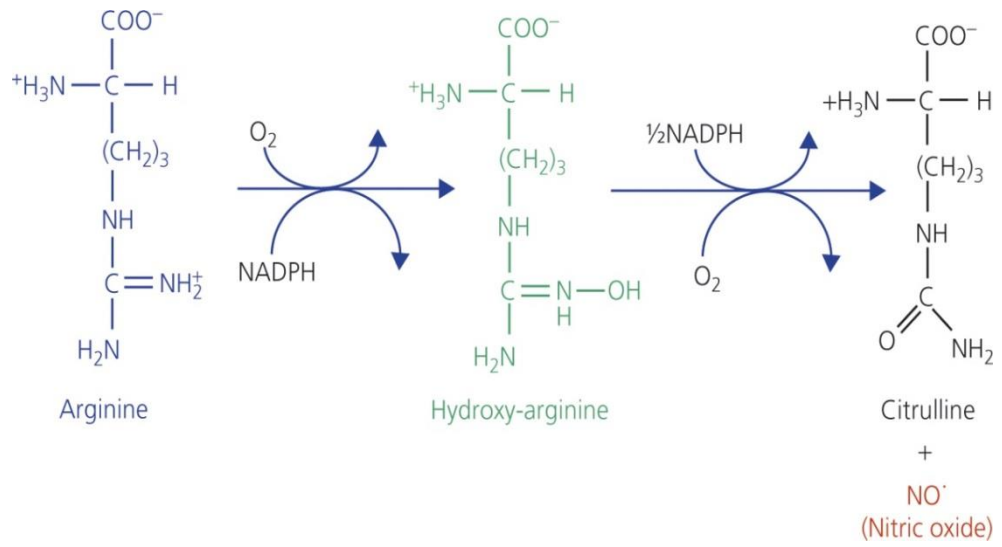
Figure 2. Production of nitric oxide from arginine as catalyzed by nitric oxide synthase (NOS)

The expression of COX-2 is induced by inflammatory stimulus, inflammatory cytokines or growth factors. COX-2 is important for the production of pro-inflammatory factor PGE2 which further contributes to inflammation. [44, 77]. Therefore, discovery of therapeutic agents that can inhibit pro-inflammatory cytokines (TNF-α, IL-1β, and IL-6), NO, iNOS, COX-2, and NF-κB translocation are critical for the treatment of inflammation. The present study was performed to evaluate the anti-inflammatory effect of NE on LPS stimulated RAW 264.7 macrophage cells.

Mitochondrial respiration, NADPH oxidase and the xanthine/xanthine oxidase system, generates. superoxide (O_2^-) which can either react with NO to form highly reactive peroxynitrite (ONOO$^-$) or converts into H_2O_2 under the influence of SOD (superoxide dismutase). Oxidative stress can have both direct and indirect effects on macrophage function [37]. Oxidative stress affects pro-inflammatory chemokine and cytokine production, and macrophage recruitment and inflammation [61].

UV induces photo-aging with uneven pigment distribution, and induces cutaneous melanomas and melanocyte dysplasia in chronically sun-exposed skin [53]. UVR-induced photo damage, and its repair signals induce melanogenesis in skin [4]. Antioxidants which scavenge free radicals have a potential whitening effect on skin [87].

Melanogenesis is a physiological process resulting the synthesis and distributing melanin pigments [19]. Melanin is produced in melanocytes within membrane-bound organelles known as melanosomes and provide colour to skin, hair and eyes of animals while protecting the underlying tissues from UV damage [39, 74]. Since abnormal melanism including freckles, solar lentigines and dark spots are considered to be aesthetically undesired, introduction of an effective melanin inhibitor has a great attention in the field of cosmetics [91].

10

Melanogenesis can be directly stimulated by ultraviolet radiation (UV) of solar light or indirectly by keratinocyte-derived factors including α-MSH (α-melanocyte stimulating hormone) endothelins, growth factors, and cytokines [12]. α-MSH is released by keratinocytes, and binds with melanocortin 1 receptor (MC1R), which increases cAMP levels within the melanocytes and increases the transcription of microphthalmia-associated transcription factor (MITF). MITF triggers transcription of numerous pigmentation genes essential for melanin synthesis including tyrosinase, TRP1, and TRP2 [10] [Figure 4].
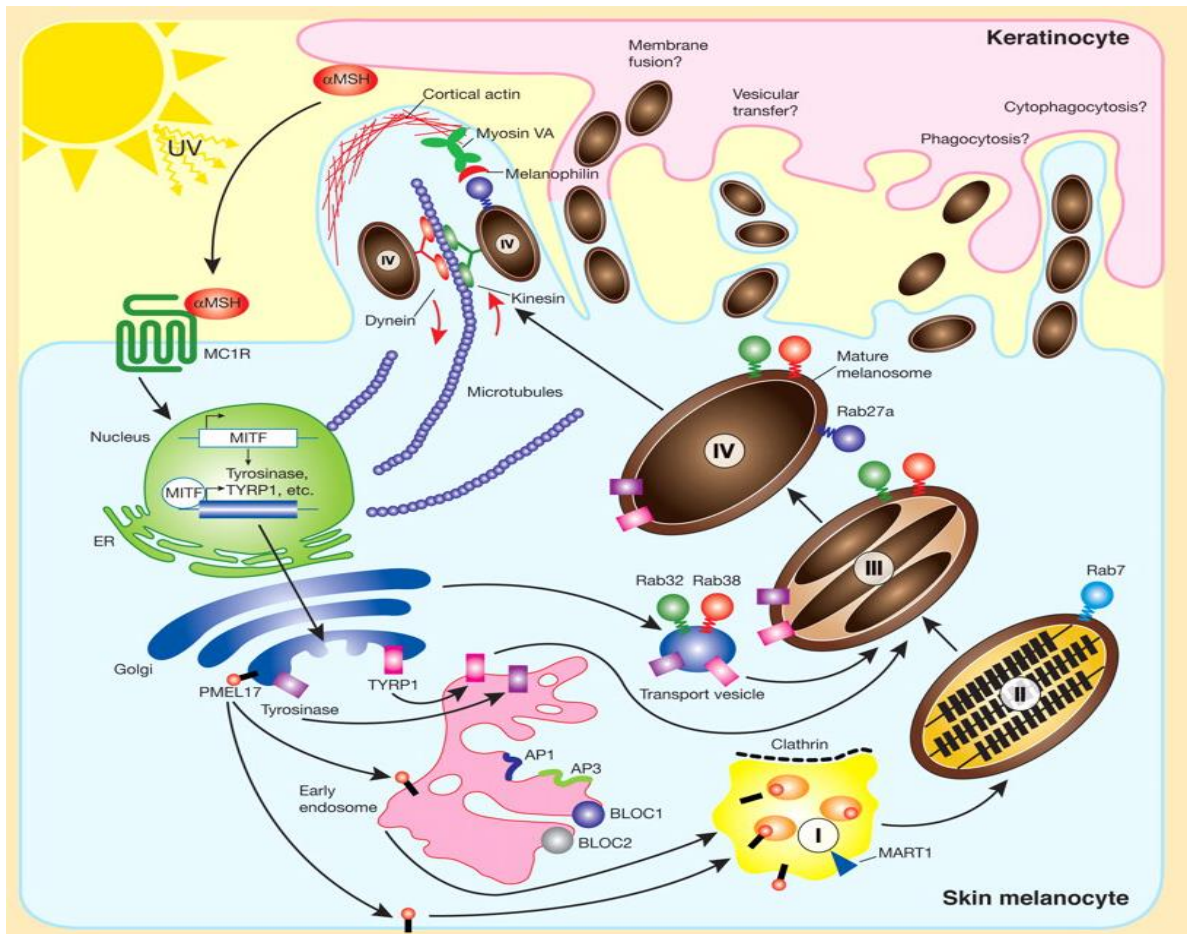
Figure 3. Melanin synthesis pathway [88].
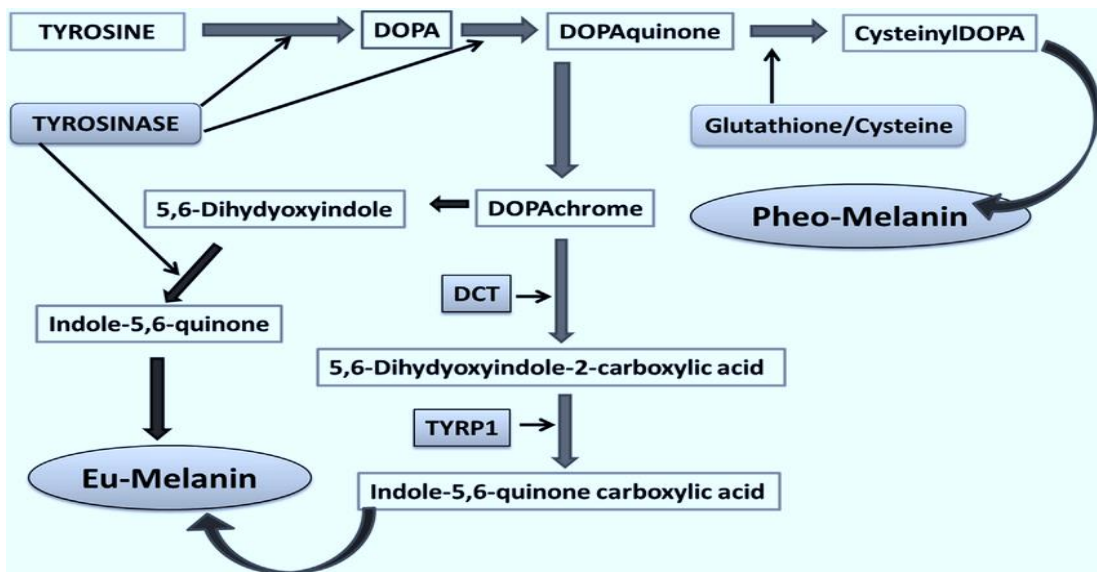
Figure 4. Melanin biosynthesis [82]

Melanin synthesis is mainly controlled by tyrosinase, TRP1, and TRP2 enzymes among which tyrosinase is a bi-functional rate-limiting enzyme that modulates melanin production by catalyzing the first and rate limiting steps, the hydroxylation of tyrosine to L-DOPA and the oxidation of L-DOPA in dopaquinone [19]. Therefore, inhibition of tyrosinase, is a common target for depigmenting agents in modulating skin pigmentary abnormalities. The present study revealed inhibitory effect of *Narcissus tazetta var. Chinensis* against melanogenesis via inhibition of tyrosinase in α-MSH stimulated B16-F10 melanoma cells [Figure 4].

MATERIALS AND METHODS

Materials

α-melanocyte stimulating hormone (α-MSH), 2,2-diphenyl-1-picrylhydrazyl (DPPH), L-Ascorbic Acid (AA), L-3,4-dihydroxyphenylalanine (L-DOPA), mushroom tyrosinase, phenylmethylsulfonyl fluoride (PMSF) Lipopolysaccharides (LPS), iNOS and COX-2 primary antibodies were purchased from Sigma Aldrich [40]. Beta Actin primary antibody was purchased from Thermofisher [40], Griess Reagent System from Promega [40] and Mouse IL-2, Mouse IL-1β, Mouse IL-6 ELISA Complete Kit and Tris-Glycine-PAG non SDS Precast Gel (10%) from Koma biotech (Korea). B16-F10 mouse melanoma cell line was purchased from ATCC [40] and RAW 264.7 cells from the Korean Cell Line Bank (Korea). Triton X-100 was purchased from Bio-Rad Laboratories [40], Dulbecco's modified Eagle's medium (DMEM) from Life Technologies [40] EZ-Western Lumi Pico, and EZ-Cytox from DogenBio (Korea). All other reagents were purchased from commercial sources and were of the analytical grade.

Sample preparation

Narcissus tazetta var. *Chinensis* was collected and samples were washed and rinsed carefully in fresh water and allowed to dry at room temperature. Dried samples were separated into flower, stem, and root and fifty grams of Narcissus powder was soaked in 1 L of 80% ethanol (ethanol/water=80/20, v/v) and was incubated for 24 hrs at room temperature to facilitate extraction. The extract was filtered using Whatman 0.45 µm pore sized filter paper, and the filtrate was diluted to final concentration of 16mg/mL (w/v).

Chromatographic analysis

Ethanolic NE with final concentration of 16mg/mL (w/v) was rotary evaporated to remove ethanol and 80mg/mL (w/v) of aqueous NE was obtained. Waters 2998 photodiode array detector (Waters, UK) with SunFire C18 column was used to identify HPLC chromatograms. Following identification of peaks using HPLC, 80mg/mL NE was filtered and diluted into 30mg/mL using Methanol. 500 μL of the 30mg/mL standard solutions were injected into the column set at 30 ℃. The analysis was carried out using YMC-PACK ODS-A column in Agilent Technologies 1229 Infinity II LC preparative LC machine (Agilent Technologies, USA).

Table 1. Chromatographic conditions in Agilent 1220 Infinity II LC

Chromatographic condition	
Solvent	Acetonitrile
Flow rate	2,000mL/min
Retention time	90 Min
Injection Volume	30.00μL
Temperature	30˚C
VWD (Variable wavelength detector)	230nm

Cell culture and treatment

Murine macrophage cell (RAW 264.7) cells and murine melanoma cell B16-F10 melanoma cells were cultured in DMEM supplemented with 10% FBS and 1% penicillin-streptomycin. Cells were maintained and incubated in modified atmospheric condition of 5% CO_2 and at 37˚C ambient temperature. Cells were sub-cultured within two days intervals. Cultured cells in exponential phase at 80% confluence from passage 4-6 were used for the experiments.

DPPH assay

The antioxidant activity of Narcissus extracts were determined by measuring the DPPH scavenging ability of Narcissus extracts according to Sanchez-Moreno et al. with slight modifications [71]. Various concentrations of Narcissus extracts dissolved in DMSO were incubated with ethanolic 0.1mM DPPH at room temperature for 30 minutes. DPPH free radicals react with antioxidants in samples, turn violet colour DPPH in to a colourless form decreasing the absorbance at 525 nm in UV spectrophotometer (Mecasys, Korea). Results were expressed as percentages of control (100%), and the concentration of extracts required to cause a 50% decrease in the absorbance was calculated as EC50 value. The radical scavenging ability (%) of the samples was calculated as [1 − (Absorbance of a group added to sample/ Absorbance of a group non-added to sample)] x 100 and calculated as EC50, the concentration of sample needed to scavenge DPPH free radicals by 50%. EC50 of GTFE was expressed as ascorbic acid equivalent antioxidant capacity (AEAC). AEAC (mg AA/100g sample) = EC50 (AA) / EC50 (sample) $\times$ 10^5 [63]. The EC50 of AA used for the calculation of AEAC was 0.0062 mg/Ml

Cell viability assay (MTT assay)

The commonly used cytotoxicity assay, MTT assay proved the cytocompatibility of NE with RAW 264.7 macrophage and B16-F10 melanoma cells. RAW 264.7 macrophage and B16-F10 melanoma cells were cultured separately in 5×10^4 cells/well cell density in 96 well plates. After 24 hrs of cell seeding, cells were treated with various concentrations of Narcissus samples for 24 hrs. Cell media was removed using a suction valve and 10 µl of EZ-Cytox Cell Viability Assay Kit solution mixed with 90 µL DMEM was then added into each well followed by 2 hrs incubation at 37 °C in a 5% CO2 incubator, and the absorbance at 450 nm was determined in a ELISA micro plate reader (Gordig, Austria). The percentage of cell viability was calculated.

Cell viability (%) = (mean absorbency in test wells)/(mean absorbency in control wells) $\times$ 100.

Measurement of Nitric oxide levels

RAW 264.7 cells were seeded in 6 well plates at a cell density of 1×10^6 cells/well for 24 hrs. Cells were treated with Narcissus samples for 1 hr, and then incubated with LPS for 24 hrs. Culture supernatant 50 µL from each sample was mixed with an equal volume of sulfanilamide and N-1-naphthylethylenediamine dihydrochloride (Griess Reagent System) under acidic (phosphoric acid) conditions and incubated for 10 min at room temperature (RT) [49]. The absorbance was measured against a standard sodium nitrite curve at 550 nm wavelength in a ELISA micro plate reader [13].

Western blot analysis

RAW 264.7 cells were seeded in 6 well plates at a cell density of 1×10^6 cells/well for 24 hrs. Cells were treated with Narcissus samples for 1 hr, and then incubated with LPS for 24 hrs. Following incubation, the cells were washed with PBS and frozen at -80℃ for 30 min and RIPA buffer with protease inhibitor was added at RT. Then, the whole-cell lysate was transferred to micro-centrifuge tubes and centrifuged at 12,000 rpm at 4℃ for 10 min. The supernatant was separated and sample protein concentrations were assessed by Bradford assay. Cellular proteins were mixed with loading buffer and boiled at 94℃ for 5 min. Based on the Bradford assay equal amount of proteins were loaded into Tris-Glycine-Polyacrylamide gels, non-sodium dodecyl sulfate precast gel (10%). After electrophoresis (100 V, 120 min), cellular proteins were transferred onto a nitrocellulose membrane (Koma Biotech, Korea) and subjected to immunoblotting for overnight at 4℃. Then membranes were blocked with 5 % skim milk and incubated with primary antibodies in various dilutions suggested by manufactures. After three washes (10 min/wash) with TBST, blots were further

incubated with an anti-mouse or anti-rabbit IgG-horseradish peroxidase-conjugate antibody at a 1:3000 dilution for 1 h at RT and were developed using EZ-Westeren Lumi Pico solution (Dogen, Korea) in an enhanced Chemi-luminescence Bioimaging Instrument (NeoScience Co., Ltd., Korea). Protein expression of COX-2, iNOS and Beta-actin proteins were determined by western blot analysis [36].

Enzyme-linked immunosorbent assay (ELISA)

RAW 264.7 cells were cultured and treated with Narcissus samples and stimulated with LPS for 24 hrs as they were for the western blot analysis. The concentration of TNF-α, Interleukin-1, Interleukin-1β and Interleukin-6 production were assayed using an enzyme-linked immunosorbent assay (ELISA) kits (Koma biotech, Korea) according to the manufacturer's instructions. Briefly plate was prewashed with washing solution and incubated with samples for 2 hrs, detection antibody for 2 hrs, colour development enzyme for 30 min at RT following 4 times washing at each step. Then colour development solution was added and reaction was stopped by adding stop solution based on visual observation. Absorbance was measured using a micro titer plate reader at 450nm wavelength.

Total RNA isolation, library preparation, sequencing and data analysis

RAW 264.7 cells were cultured in 6 well plates (1×10^6 cells/well) and incubated at 37°C, for 48 hrs. Cells were exposed to α-MSH and different concentrations of NE. Following RAW 264.7 cell cultivation and NE sample treatment, total RNA was collected by dissolving cells by addition of 500 μL of Trizol reagent/well (Invitrogen, USA) according to manufacturer's instructions, and were stored at -80℃ until use. RNA quality was evaluated by Agilent 2100 bioanalyzer using the RNA 6000 Nano Chip (Agilent Technologies, Netherlands), and RNA quantification was carried out using ND-2000 Spectrophotometer (Thermofisher, USA). Based on manufacturer's instructions a library for control and test RNAs was constructed using SENSE 3' mRNA-Seq Library Prep Kit (Lexogen, Austria).

Total RNA 500 ng was prepared and an oligo-dT primer containing an Illumina-compatible sequence at its 5' end was hybridized to the RNA and reverse transcription was performed. Following RNA degradation complimentary strand synthesis was started by random primer containing an Illumina-compatible linker sequence at its 5' end. Magnetic beads were used to remove all reaction components. The library was amplified to add the complete adapter sequences required for cluster generation. The completed library was purified from PCR components. High-throughput sequencing was performed as single-end 75 sequencing using NextSeq 500 (Illumina, USA). SENSE 3' mRNA-Seq reads were aligned using Bowtie2 version 2.1.0 [41]. Bowtie2 indices were either generated from genome assembly sequence or the representative transcript sequences for aligning to the genome and transcriptome. The alignment file was used for assembling transcripts, estimating their abundances and detecting differential expression of genes. Differentially expressed genes were determined based on counts from unique and multiple alignments using EdgeR within R version 3.2.2 (R development Core Team, 2011) using Bioconductor version 3.0 [24]. The RT (Read Count)data were processed based on Quantile normalization method using the Genowiz ™ version 4.0.5.6 (Ocimum Biosolutions, India). Cytoscape (version 2.7), an open source bioinformatics platform developed by the Institute of Systems Biology, Seattle, WA, was used to construct network diagrams and to illustrate clustering of the genes in our dataset within specific pathways. Gene classification was based on searches done by Medline databases (National Centre for Biotechnology Information, USA).
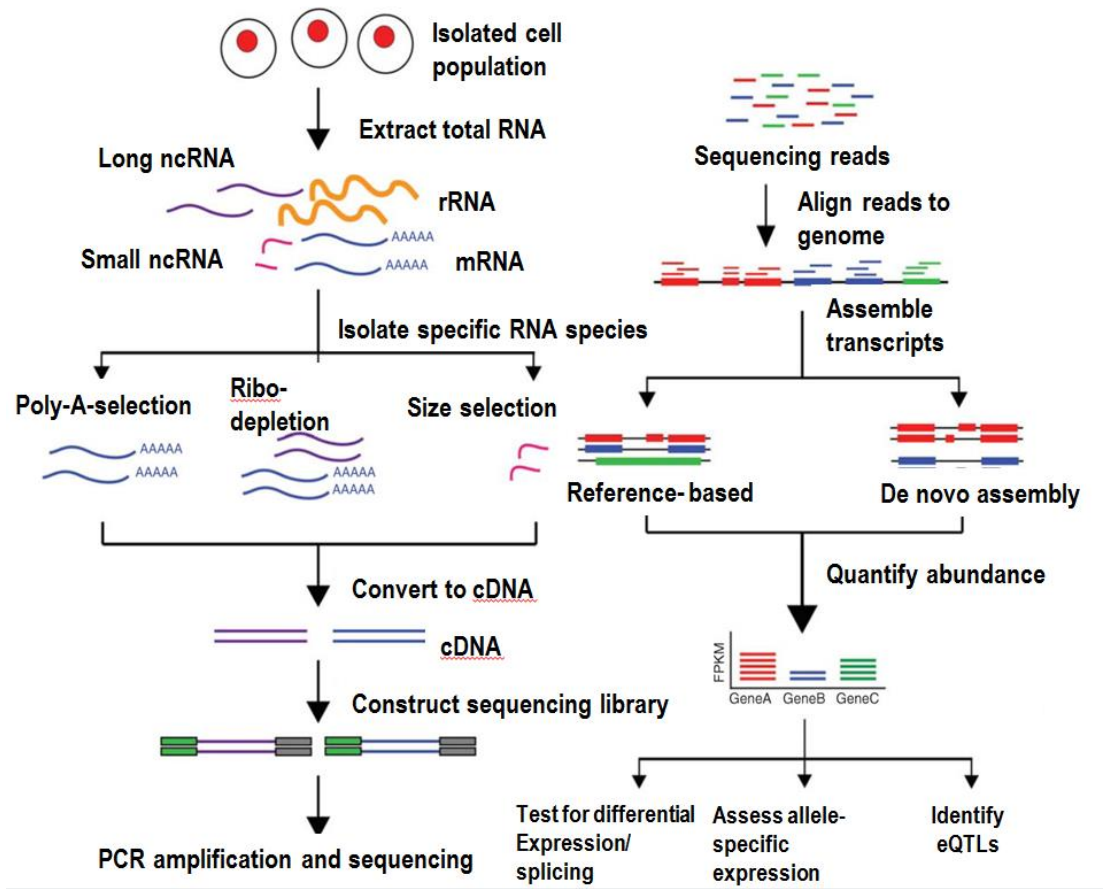
Figure 5. RNA Sequencing

Mushroom tyrosinase inhibition assay

The inhibitory effect of NE on, mushroom tyrosinase activity was measured as described previously. 130 µL of varying concentrations of NE samples 0, 250, 500, 1,000, 2,000, 4,000 and 8,000 µg/mL were mixed with 20 µL of mushroom tyrosinase (1250 U/mL) in 96-well micro plate. Mixtures were incubated with 120 µL of 1.5 mM L-DOPA at 37℃ for 5 min and absorbance was measured at 490 nm using ELISA micro plate reader.

Cellular tyrosinase inhibition assay

Cellular tyrosinase activity was determined as described previously with slight modifications [84]. Briefly, B16-F10 melanoma cells were incubated at a density of 1×10^6 cells in 6 well plates for 24 hrs. Cells were treated with increasing concentrations of Narcissus samples for 1 hr, and then incubated with 20nM α-MSH for 48 hrs. Then the cells were washed twice with ice-cold PBS and lysed in 500 µL of PBS containing 1% Triton X-100 and 2 mM PMSF by freezing and thawing. The cell lysates were centrifuged at 15,000 rpm for 30 min at 4 ℃. Then 150 µL of the supernatant was mixed with 150 µL of reaction solution 2 mM L-DOPA, incubated at 37℃ for 10 min, and the absorbance at 490 nm was measured using an ELISA plate reader.

Cellular melanin synthesis inhibition assay

Melanin contents were measured as previously described with slight modifications [72]. B16-F10 murine melanocytes were seeded at 1×10^6 cells/well cell density for overnight in 6 well plates and then treated Narcissus samples for 1 hr, and then incubated with 20nM α-MSH for 48 hrs. Cells were washed with PBS, harvested by trypsinization, and centrifuged for 5 min at 1200 × g. The cell pellets were oven dried at 60℃ and then pellets were dissolved in 500 µL of 1.0 M NaOH containing 10% DMSO for 30 min at 80 ℃

heating block. Melanin wad dissolved by vortexing and then melanin contents of 300 μL supernatants were measured at 490 nm.

Data analysis

Data were expressed as means ± S.D. from minimum three independent experiments. Data were statistically analyzed with IBM SPSS Statistics (Ver.17.0; USA). The statistical differences among groups were analyzed with one way analysis (ANOVA) followed by Turkey's test. *$p<0.01$, **$p<0.001$ and ***$p<0.0001$ indicate statistically significant differences from the control group.

STRING analysis was done using STRING software version 9.0 and IPA data were analyzed through the use of QIAGEN's Ingenuity® Pathway Analysis (IPA®, QIAGEN Redwood City, www.qiagen.com/ingenuity).

RESULTS

Radical scavenging activity

DPPH radical scavenging activity assay was conducted to evaluate the antioxidant activity of NE. NE expressed DPPH free radical scavenging activity concentration dependently. DPPH radical scavenging activities of 100, 200, 400, and 800 µg/mL of NFE were estimated to be 35%, 70%, 89%, and 93% respectively (Fig. 6A). DPPH radical scavenging activities of 100, 200, 400, and 800 µg/mL of NSE was estimated to be 19%, 33%, 61%, and 91% respectively (Fig. 6B). For NRE, DPPH radical scavenging activities of 100, 200, 400, and 800 µg/mL was estimated to be 4%, 9%, 17%, and 29% respectively (Fig. 6C). The EC50 values of NFE, NSE, and NRE for 0.1Mm DPPH were estimated to be 182 µg/mL, 319 µg/mL, and 1155 µg/mL which are corresponding to 3,406, 1,943, and 536 mg of ascorbic acid / g based on the ascorbic acid equivalent antioxidant capacity (AEAC) calculation as described in Materials and Methods.
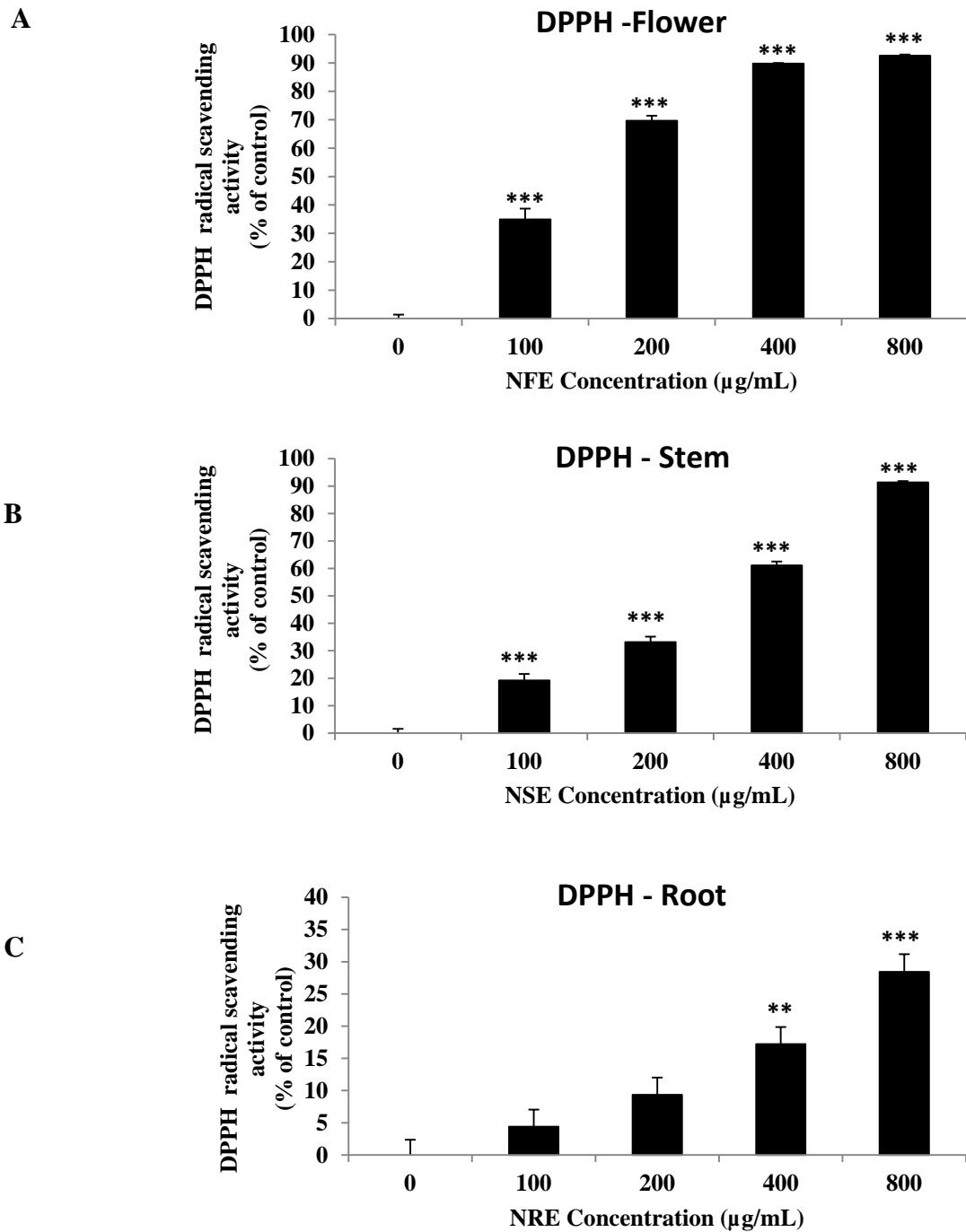
Figure 6. Effects of NE on DPPH radical scavenging

(**A**) DPPH radical scavenging activity of NFE, (**B**) NSE, and (**C**) NRE. Data are the means of ± S.E. for three independent experiments. (*p < 0.01, **p < 0.001, and ***p < 0.0001 compared with the control).

Cellular toxicity

To determine whether Narcissus samples have a cytotoxic effect, RAW 264.7 macrophage cells were treated with indicated concentrations of samples for 24 hrs, and cell viabilities were observed using an MTT assay. No cytotoxicity was observed with NFE in RAW 264.7 cells upto the concentrations of 10 μg/mL, whereas the cellular cytotoxicity was increased significantly by 24% at the concentrations of 15 μg/mL in RAW 264.7 cell (Fig. 7A). NSE showed cytotoxicity which was increased significantly by 42% at the concentrations of 5 μg/mL in RAW 264.7 cell (Fig. 7B). In addition, cellular cytotoxicity was significantly increased in exposure to NRE by 40% at the concentration of 40 μg/mL in RAW 264.7 cell (Fig. 7C).

.
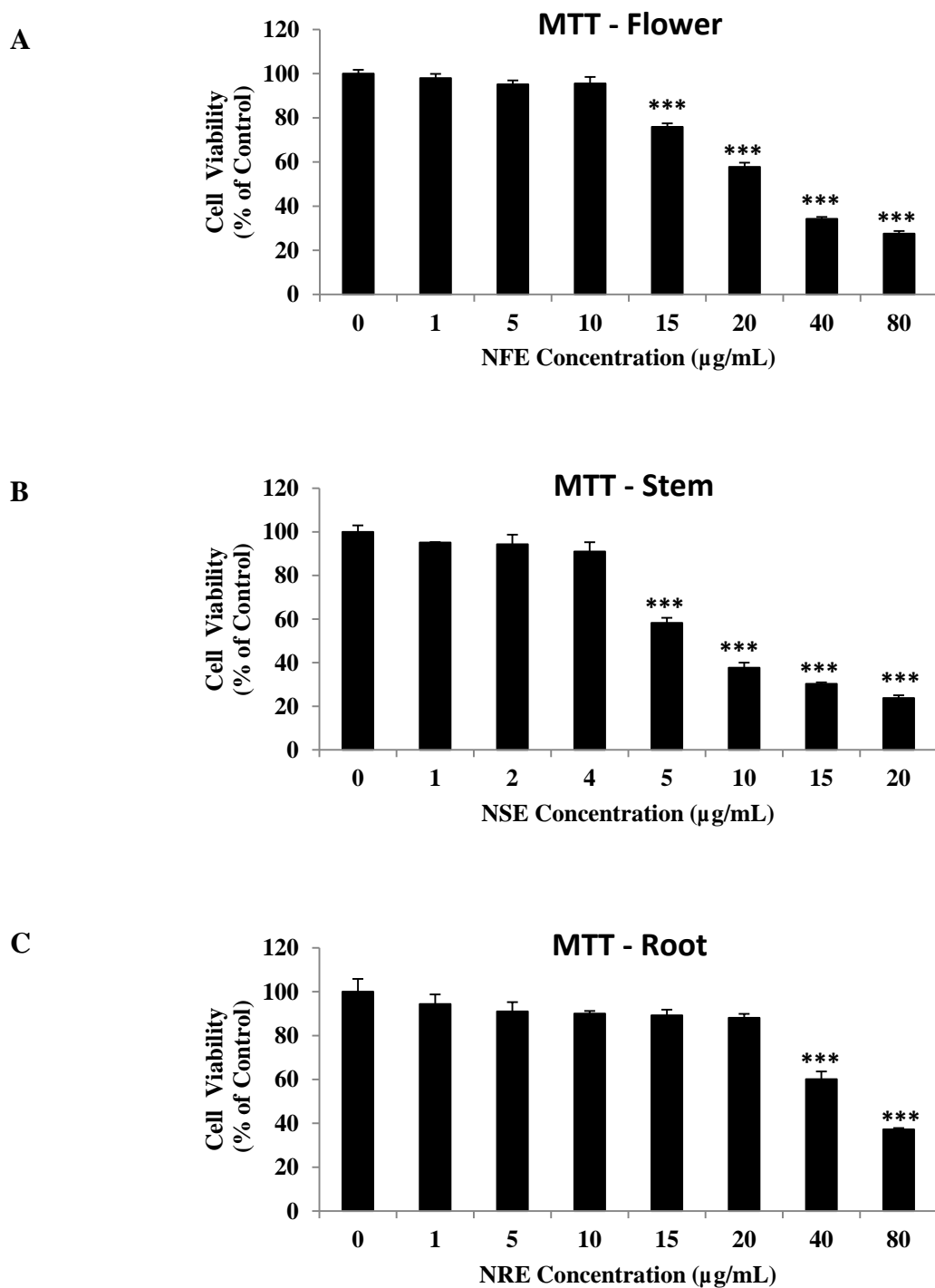
Figure 7. Effects of NE on RAW 264.7 macrophage cell viability.

(A) RAW 264.7 macrophage cell viability in different concentrations of NFE,. **(B)** RAW NSE, and **(C)** NRE. Data are the means of ± S.E. for three independent experiments. (*p < 0.01, **p < 0.001 and ***p < 0.0001 compared with the control).

제주대학교 중앙도서관
JEJU NATIONAL UNIVERSITY LIBRARY

Nitric oxide suppression in RAW264.7 cells

Since multiple intracellular mechanisms make NO to act as a pro-inflammatory mediator, the present study examined the effects of NE on NO production in LPS stimulated RAW264.7 cells. As shown in Fig. 8, NO level in media was markedly increased following LPS treatment. However, NO production was decreased by 12%, 60%, 64% and 66% by addition of 1, 5, 10 and 20 µg/mL of NFE. By addition of 1, 2, 5 and 10 µg/mL of NSE 17%, 43%, 63% and 66% of NO productions were inhibited. 28%, 57%, 66% and 67% of NO productions were attenuated by addition of 5, 10, 20 and 30 µg/mL of NRE respectively.
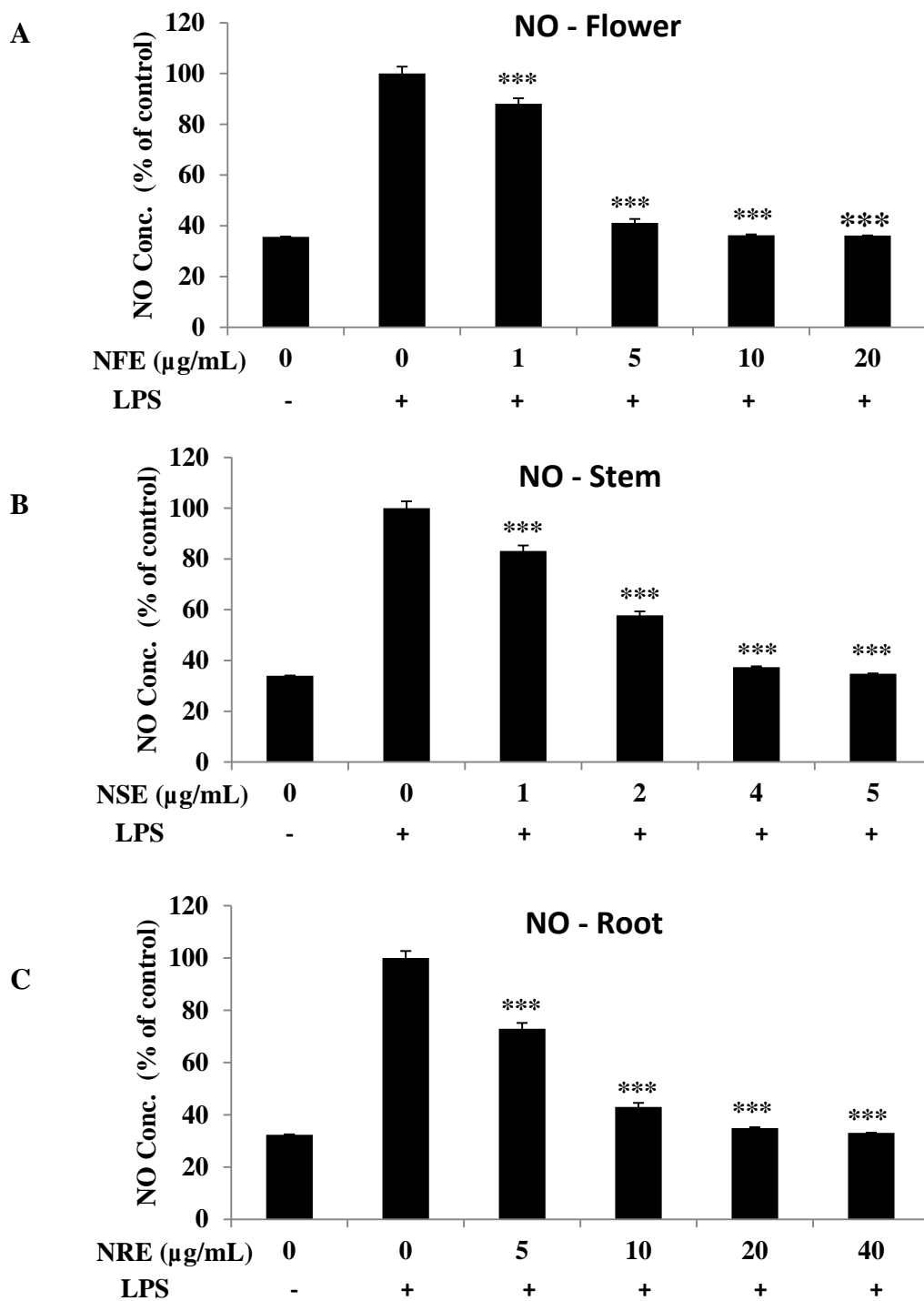
Figure 8. Inhibitory effects of Effects of NE on NO production in LPS-stimulated Raw 264.7 macrophage cells.

Inhibition of NO production with different concentrations of (A) NFE, (B) NSE, and (C) NRE. Data are the means of ± S.E. for three independent experiments. (*p < 0.01, and ***p < 0.0001 compared with the control).

Inhibitory effects of NE on COX-2 and iNOS protein levels

The effects of NE on COX-2 and iNOS protein expression levels were investigated by Western blotting. Based on densitometry, NE markedly suppressed COX-2 and iNOS protein expression levels concentration dependently. LPS-induced COX-2 expressions were reduced by 42%, 58%, 70%, and 85% at 1, 5, 10 and 20 µg/mL of NFE; 15%, 30%, 50%, and 65%, at 1, 2, 4 and 5 µg/mL of NSE; and 10%, 18%, 60%, and 90% at 5, 10, 20 and 30 µg/mL of NRE respectively. LPS-induced iNOS expressions were reduced by 15%, 30%, 50%, and 90% at 1, 5, 10 and 20 µg/mL of NFE; 10%, 18%, 32%, and 45%, at 1, 2, 4 and 5 µg/mL of NSE; and 23%, 76%, 83%, and 95% at 5, 10, 20 and 30 µg/mL of NRE respectively (Fig. 9, 10, 11).
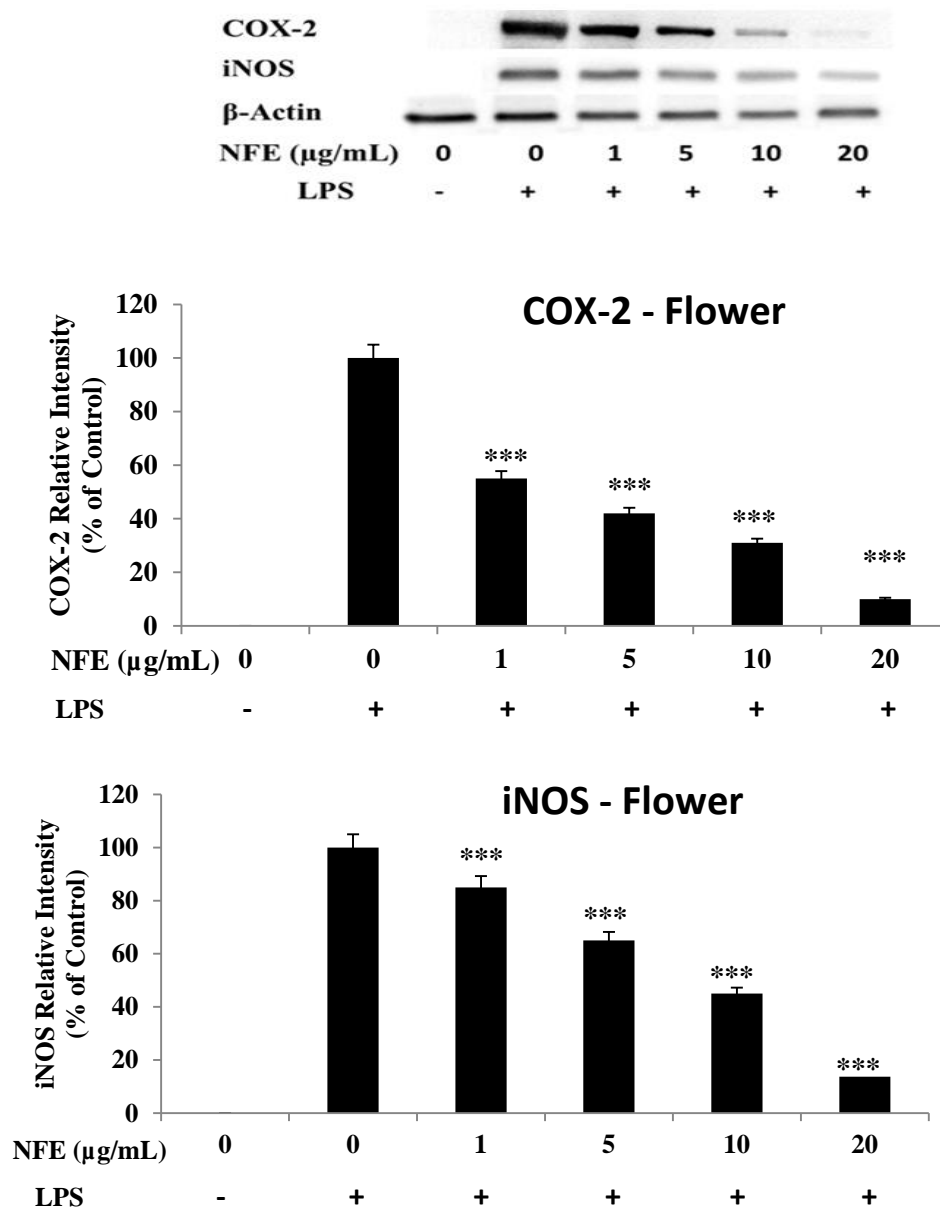
Figure 9. Effects of NFE on COX-2 and iNOS production in LPS-stimulated Raw 264.7 macrophage cells.

Raw 264.7 cells were preincubated with LPS for 24 h, and then incubated without or with indicated concentrations of NFE for 24 h. Cell lysates were resolved by 10% SDS–PAGE, transferred to nitrocellulose membranes, and probed with antibodies against iNOS and COX-2. Band intensities were measured by ImageJ software. Relative amounts of iNOS and COX-2 (B) compared to β-actin. Data are the means of ± S.E. for three independent experiments.

31
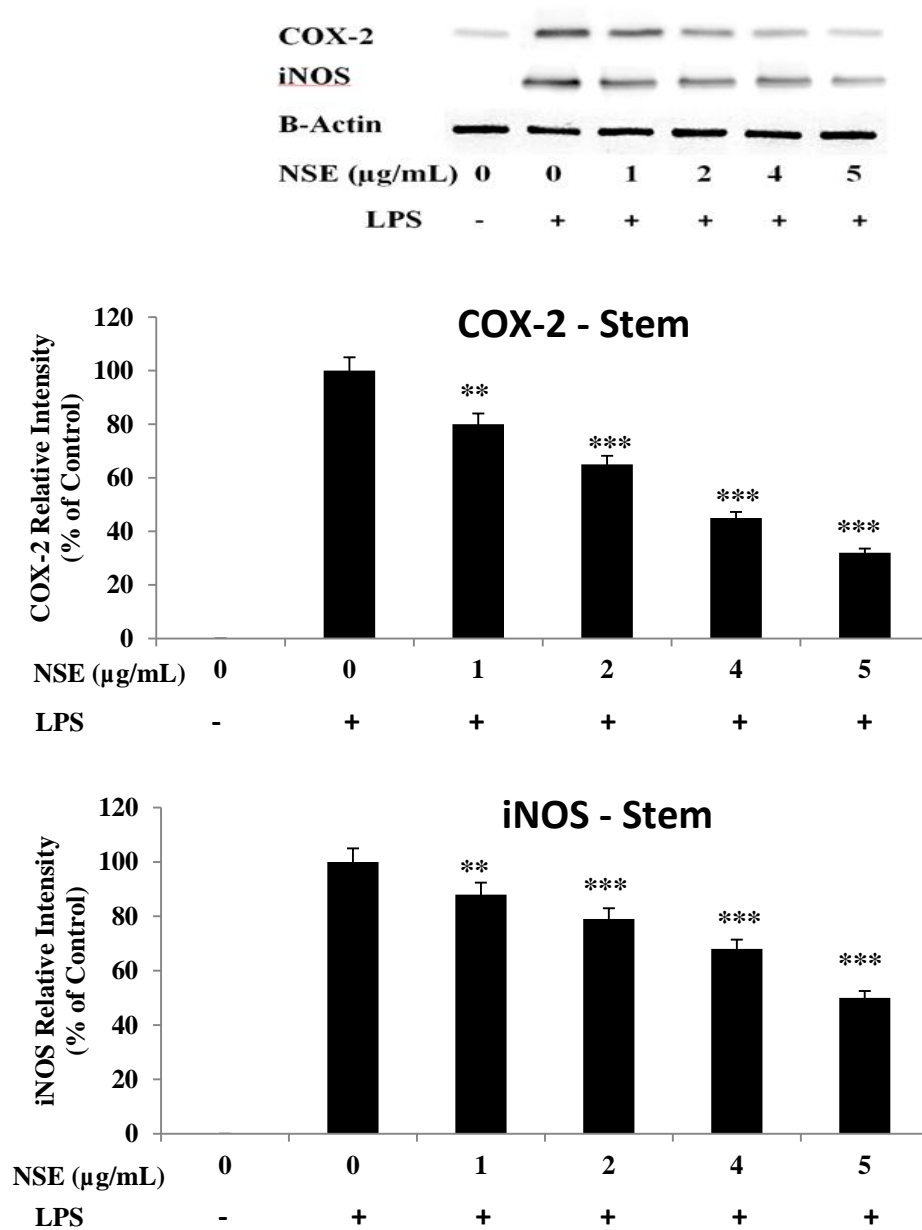
Figure 10. Effects of NSE on COX-2 and iNOS production in LPS-stimulated Raw 264.7 macrophage cells.

Raw 264.7 cells were preincubated with LPS for 24 h, and then incubated without or with indicated concentrations of NFE for 24 h. Cell lysates were resolved by 10% SDS–PAGE, transferred to nitrocellulose membranes, and probed with antibodies against iNOS and COX-2. Band intensities were measured by ImageJ software. Relative amounts of iNOS and COX-2 (B) compared to β-actin. Data are the means of ± S.E. for three independent experiments.
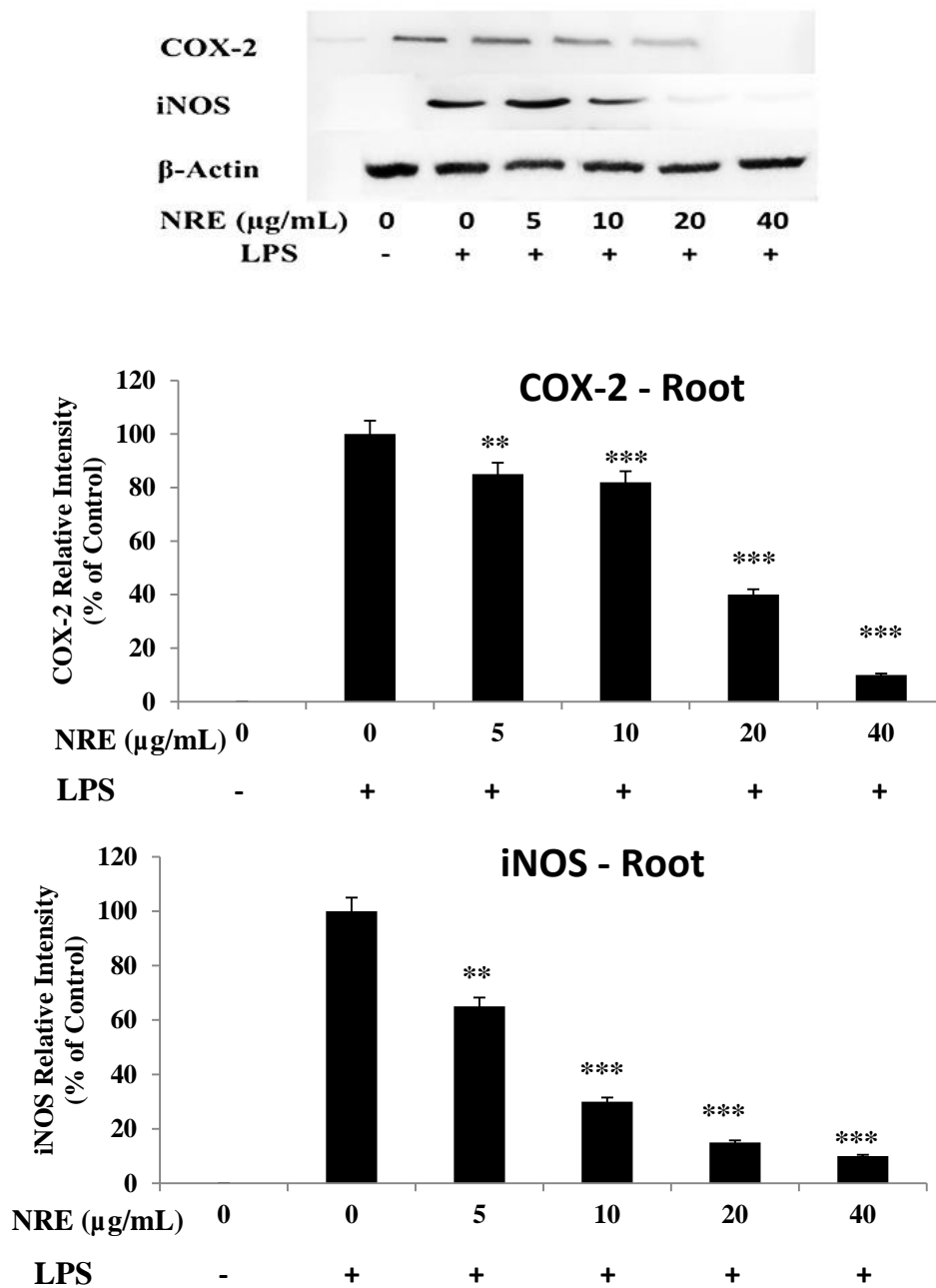
Figure 11. Effects of NRE on COX-2 and iNOS production in LPS-stimulated Raw 264.7 macrophage cells.

Raw 264.7 cells were preincubated with LPS for 24 h, and then incubated without or with indicated concentrations of NFE for 24 h. Cell lysates were resolved by 10% SDS–PAGE, transferred to nitrocellulose membranes, and probed with antibodies against iNOS and COX-2. Band intensities were measured by ImageJ software. Relative amounts of iNOS and COX-2 (B) compared to β-actin. Data are the means of ± S.E. for three independent experiments.

Inhibitory effects of NE on TNF-α, IL-6 and IL-1β

The effects of NE on TNF-α, IL-6 and IL-1β pro-inflammatory cytokines production were investigated by ELISA. NE markedly suppressed TNF-α, IL-6 and IL-1β pro-inflammatory cytokines production concentration dependently. LPS-induced TNF-α production was reduced by 10%, 33%, 54% and 78%, by 1, 5, 10 and 20 µg/mL of NFE; 49%, 58%, 60% and 79% by 1, 2, 4 and 5 µg/mL of NSE; and 31%, 48%, 50% and 86% by 5, 10, 20 and 30 µg/mL of NRE respectively. LPS-induced IL-6 production was reduced by 7%, 10%, 22% and 45% by 1, 5, 10 and 20 µg/mL of NFE; 7%, 11%, 23% and 38% by 1, 2, 4 and 5 µg/mL of NSE; and 6%, 23%, 41% and 52% by 5, 10, 20 and 30 µg/mL of NRE respectively. LPS-induced IL-1β production was reduced by 11%, 28%, 21% and 23% by 1, 5, 10 and 20 µg/mL of NFE; 6%, 13%, 15% and 29% by 1, 2, 4 and 5 µg/mL of NSE; and 20%, 24%, 27% and 43% by 5, 10, 20 and 30 µg/mL of NRE respectively (Fig. 12, 13, 14).
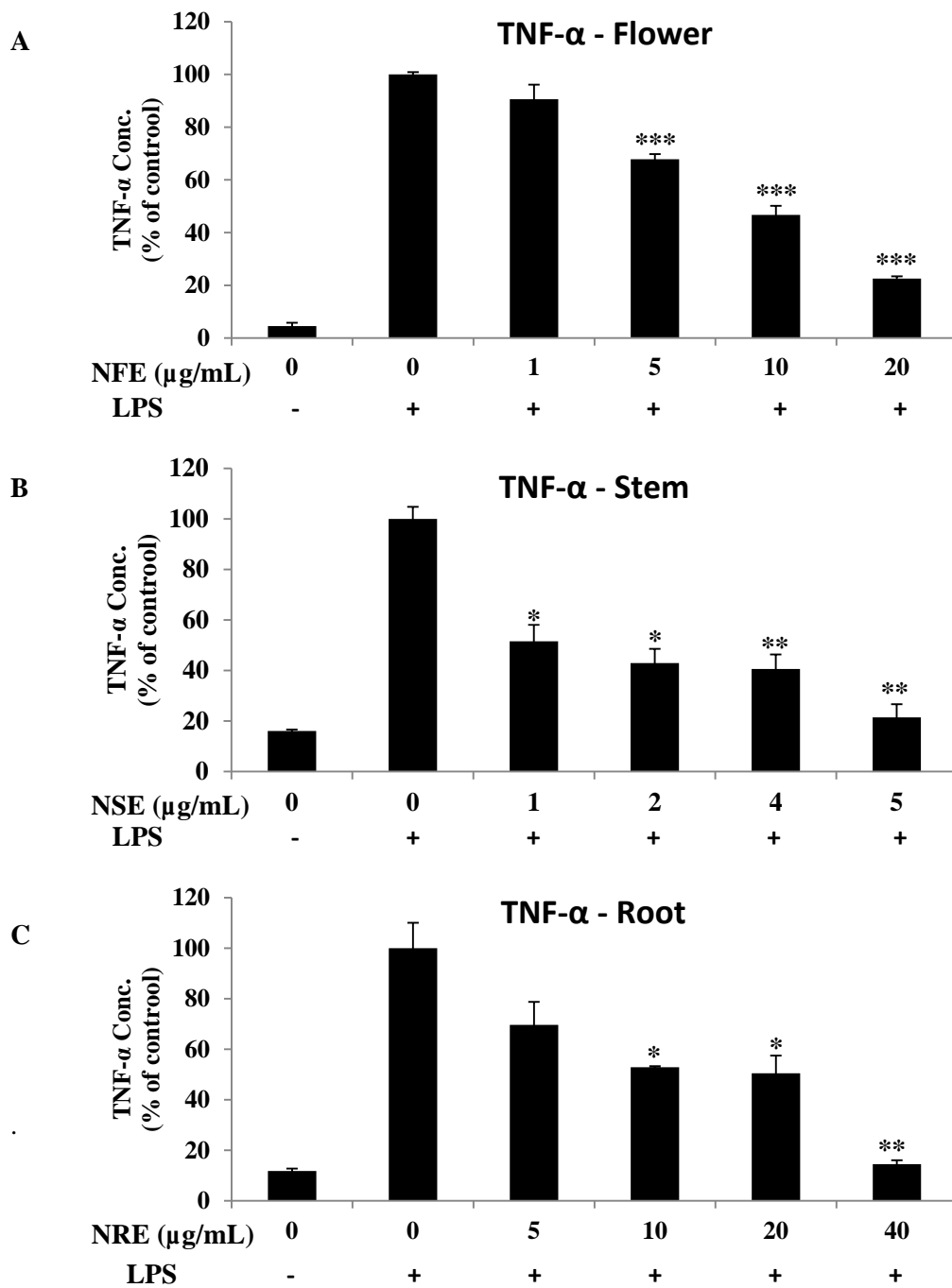
Figure 12. Inhibitory effect of NE on the proinflammatory cytokine production in LPS stimulated RAW 264.7 macrophage cells

The production of TNF-α in LPS stimulated RAW 264.7 cells was determined by ELISA using the supernatant. Data are the means of ± S.E. for three independent experiments. (*p < 0.01, **p < 0.001, and ***p < 0.0001 compared with the control). (A) NFE (B) NSE (C) NRE
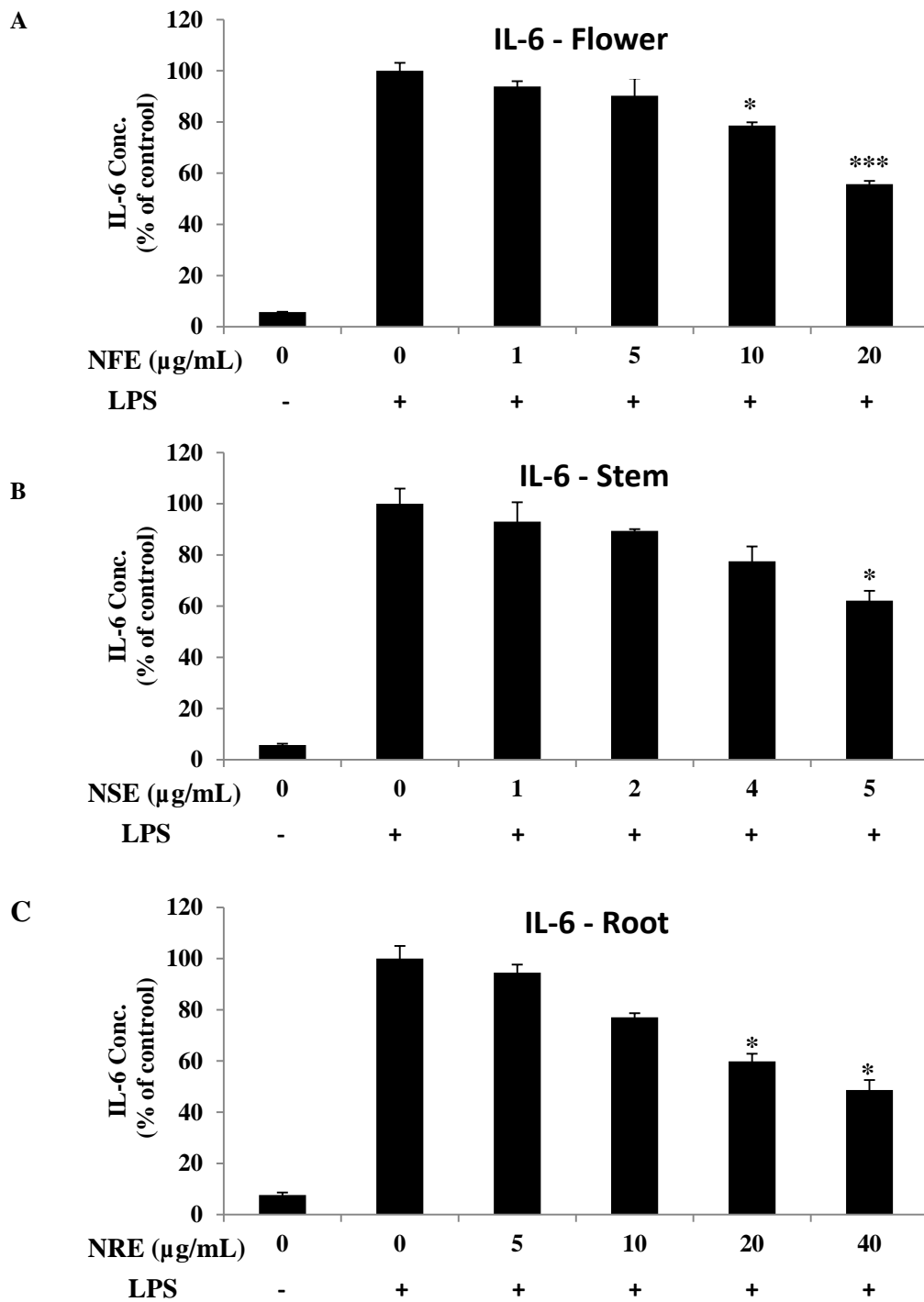
Figure 13. Inhibitory effect of NE on the proinflammatory cytokine production in LPS stimulated RAW 264.7 macrophage cells.

The production of IL-6 in LPS stimulated RAW 264.7 cells was determined by ELISA using the supernatant. Data are the means of ± S.E. for three independent experiments. (*p < 0.01, and ***p < 0.0001 compared with the control). (A) NFE (B) NSE (C) NRE
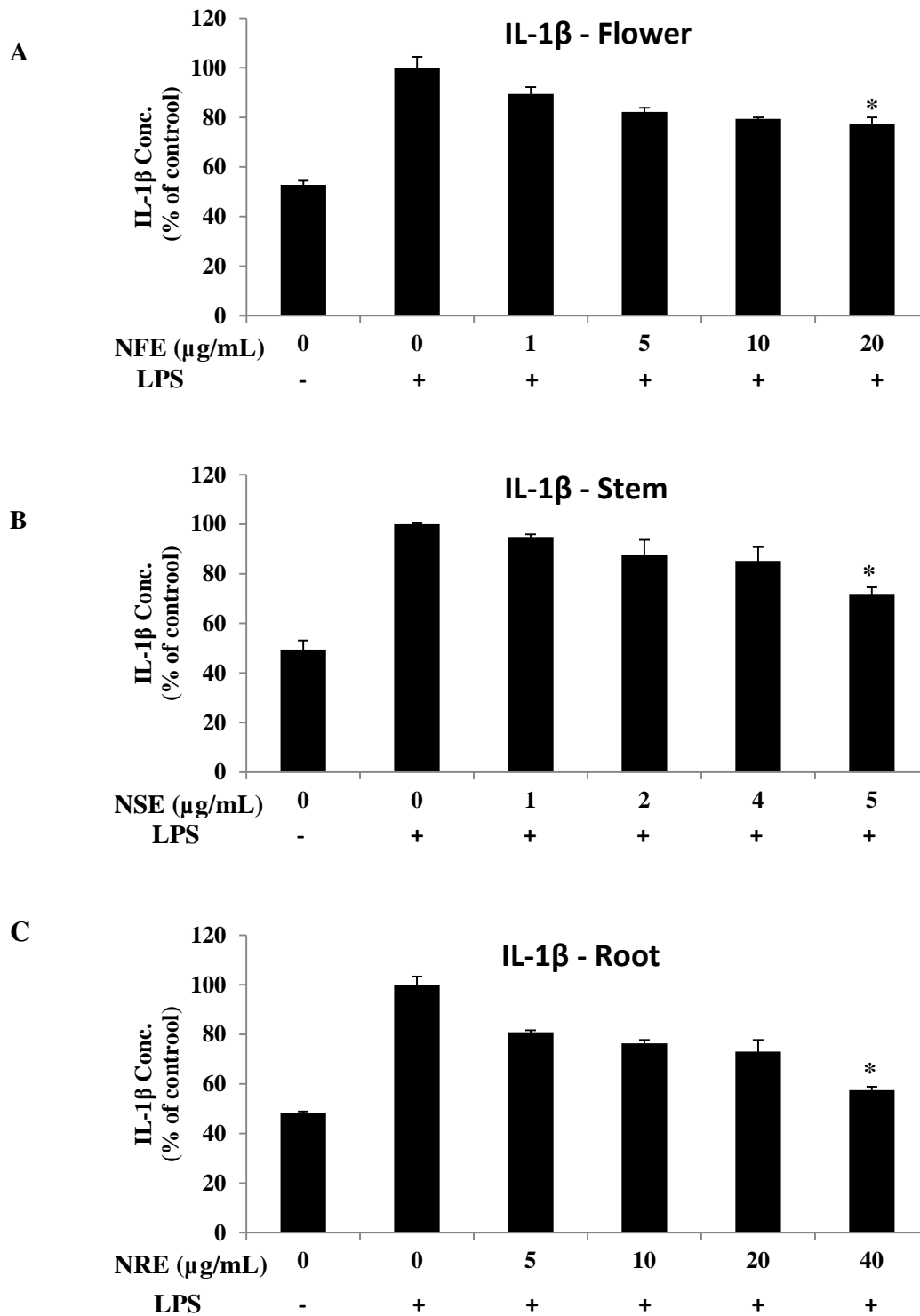
Figure 14. Inhibitory effect of NE on the proinflammatory cytokine production in LPS stimulated RAW 264.7 macrophage cells.

The production of IL-1β in LPS stimulated RAW 264.7 cells was determined by ELISA using the supernatant. Data are the means of ± S.E. for three independent experiments. (*p < 0.01 compared with the control). (A) NFE (B) NSE (C) NRE
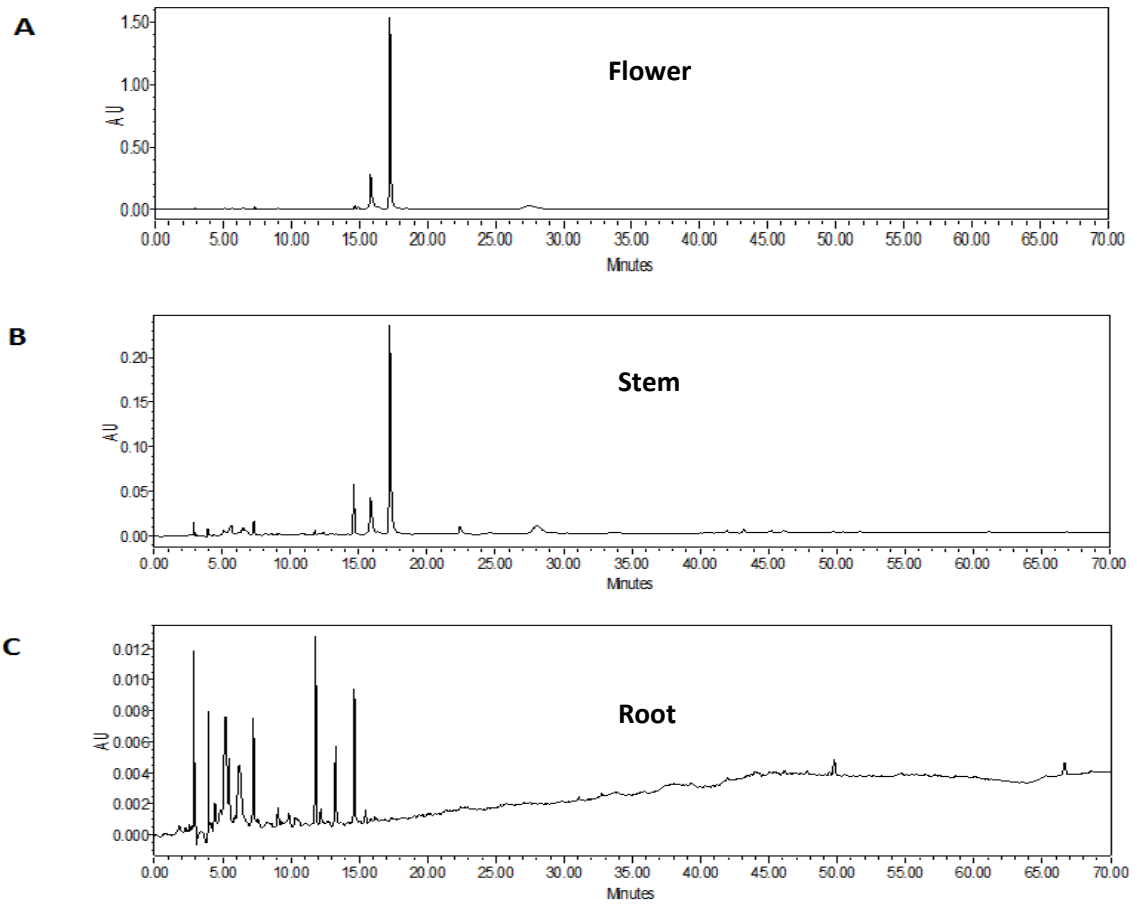
Figure 15. Chromatograms od analytical HPLC analysis of crude Narcissus tazetta var. Chinensis extracts (NE).

HPLC analysis was performed using Waters Model 2489 UV / Visible detector, a Model 2998 Photodiode Array Detector, and a Model 2707 Auto sampler. NE (80 mg / mL) were diluted with methanol to a final concentration of 5 mg / mL. A binary mobile phase SunFire Column, Reversed-Phase 5 μm Spherical Silica (4.6 mm x 250 mm column) consisted with solvent (A) acetonitrile and (B) distilled water was used. (0 to 60 min: 0: 100, 60 to 70 min: 100: 0). The eluate was measured at 230 nm with a VWD detector at a flow rate of 1 mL / min for 90 minutes and the temperature of the column was maintained at 30 ° C. **(A)** NFE **(B)** NSE **(C)** NRE
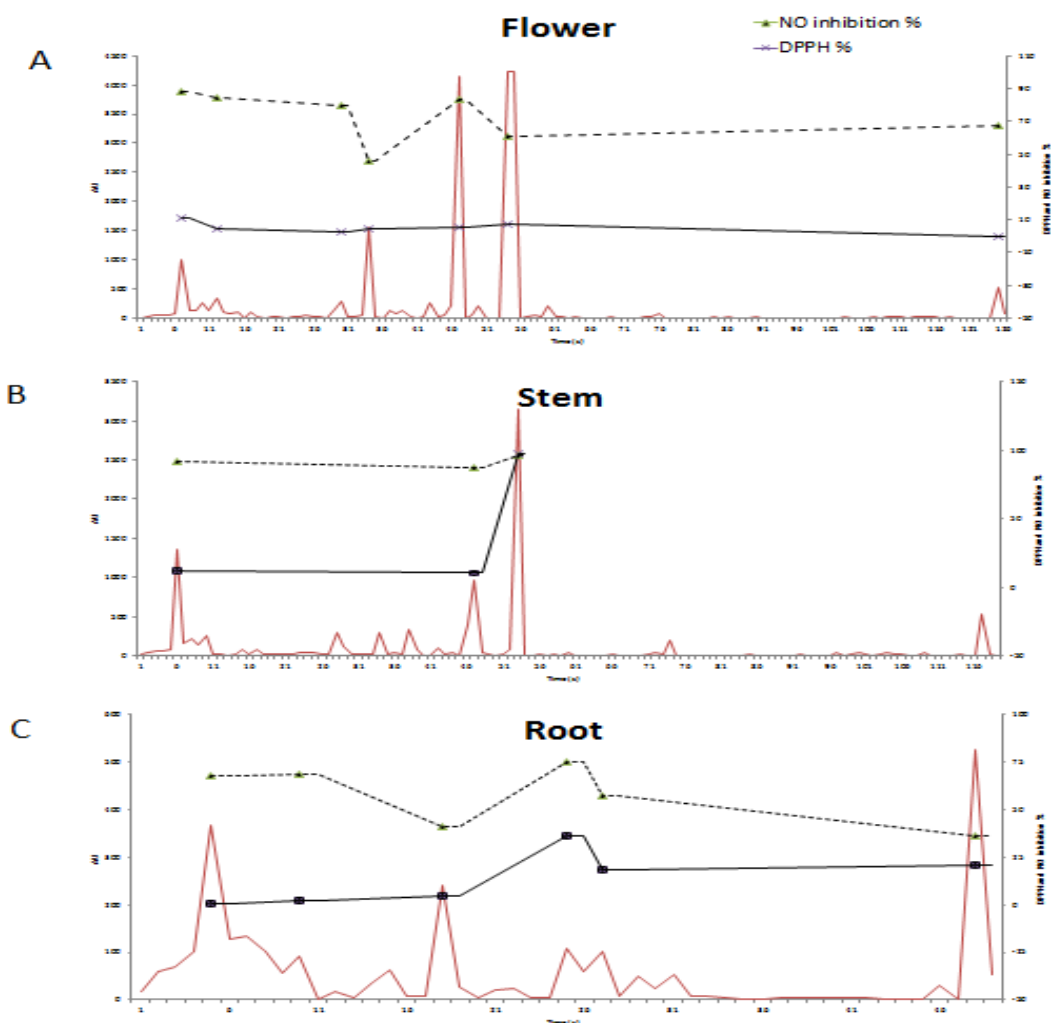
Figure 16. Conventional preparative HPLC chromatograms of the crude Narcissus tazetta var. Chinensis extracts (NE)

The PrepLC device was a 1220 Infinity II LC from Agilent Technologies (Agilent, Santa Clara, Calif., USA). Each daffodil flower, stem, and root extract (80 mg / mL) was diluted with methanol to a final concentration of 30 mg / mL. The column was a YMC-Pack ODS-A column (250 mm × 10.0 mm id, 5 μm, 12 nm column) and two mobile phases consisting of solvent (A) distilled water and acetonitrile (B) / Min (0 to 60 min: 0: 100, 60 to 70 min: 100: 0). The eluate was measured at a flow rate of 2 mL / min for 90 minutes with a VWD detector at 230 nm and the temperature of the column was maintained at 30 ° C **(A)** NFE **(B)** NSE **(C)** NRE

RNA sequencing quality analysis

RAW 264.7 cells were cultured in 6 well plates (1×10^6 cells/well) and incubated at 37°C, for 48 hrs. Cells were exposed to α-MSH and different concentrations of NE. Following RAW 264.7 cell cultivation and NE sample treatment, total RNA was isolated by dissolving cells in 500 μL of Trizol reagent/well (Invitrogen, USA) according to manufacturer's instructions, and were stored at -80°C until use. RNA quality of all 5 sample groups including (A) No LPS, (B) LPS, (C) NFE, (D) NSE, and (E) NRE were analyzed prior to further processing and labelling for microarray hybridization. RNA integrity number (RIN) values were checked to assess RNA quality using a mRNA Pico chip. The Agilent 2100 Bioanalyzer system with the RNA Integrity Number (RIN) provides a quantitative measure of RNA degradation. (A) No LPS, (B) LPS, (C) NFE, (D) NSE, and (E) NRE sample groups were qualified for further processing with RIN higher than 7. Based on (28s/18s) data Control (+),Control (-),Flower+LPS, Stem+LPS, and Root+LPS groups showed 1.9, 2, 2, 2.1, and 2 values respectively (Table 2).

Table 2. RNA QC Results

No.	Sample	ng/µl	Total (µg)	OD$_{260/280}$	OD$_{260/230}$	Ratio(28s/18s)	RIN	Result
1	Control (+)	5048.9	100.978	1.97	2.01	1.9	9.8	Qualified
2	Control (-)	7399.9	147.998	2.06	2.09	2.0	10.0	Qualified
3	Flower+LPS	4901.5	98.030	1.99	2.05	2.0	10.0	Qualified
4	Stem+LPS	7607.2	152.144	2.11	2.19	2.1	10.0	Qualified
5	Root+LPS	5134.4	102.688	1.97	2.02	2.0	9.9	Qualified
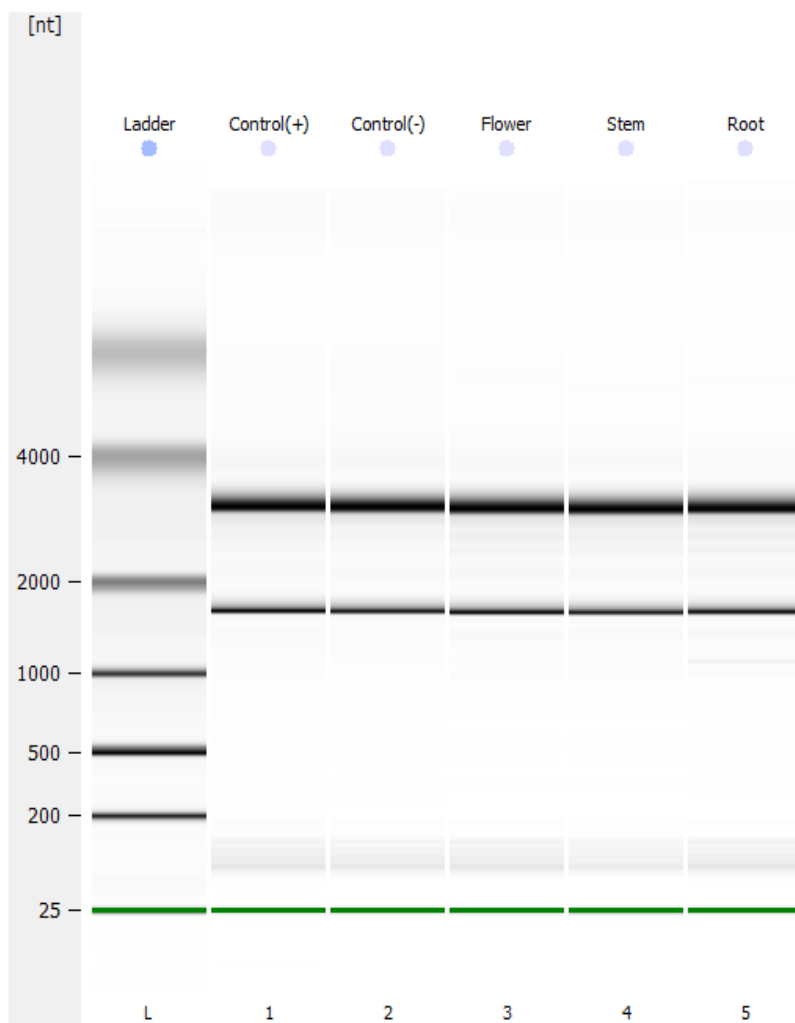
Figure 15. Migration patterns of RAW 264.7 cells treated with or without LPS and NE.

Gel electrophoresis of total RNA was isolated from LPS stimulated RAW 264.7 macrophage cells treated with NE and quality control assessment of total RNA (500ng) was determined using the Agilent 2100
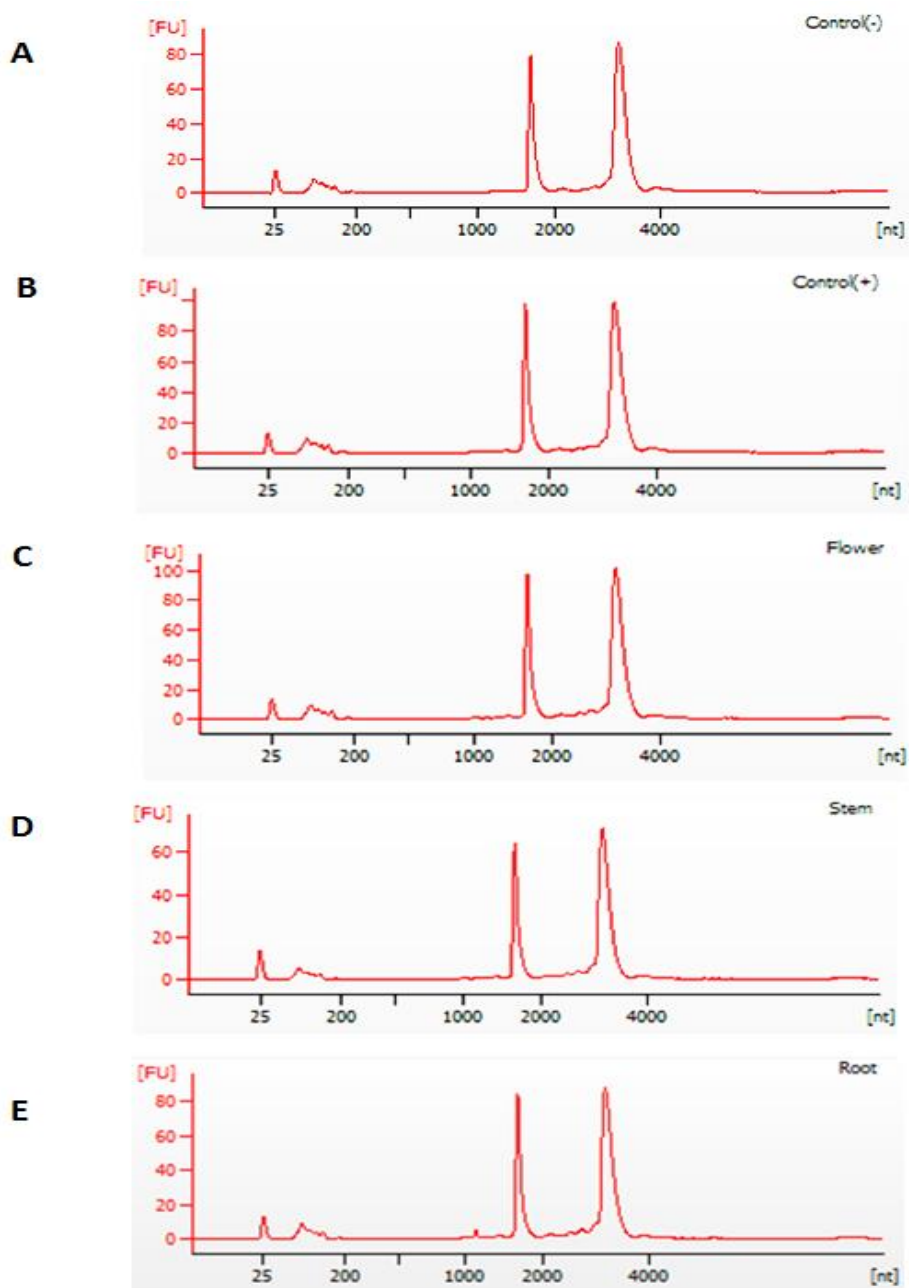
Figure 16. Peak patterns of RAW 264.7 cells treated with or without LPS and NE.

Electropherogram showing the evaluation of RNA integrity using the Agilent 2100 BioAnalyzer. Samples of total RNA preparations (500 ng) from LPS treated RAW 264.7 cells treated with NE were fractionated resolved. and integrity was evaluated. **(A)** No LPS **(B)** LPS **(C)** NFE+LPS **(D)** NSE+LPS **(E)** NRE+LPS

Gene Ontology analysis

Gene Ontology (GO) is an important bioinformatics tool to evaluate genome-scale protein function annotation. Roles of genes or proteins are explained by GO terms in eukaryotic cellular process. GO mainly has consists of three separate ontologies: cellular component, molecular function and biological process. GO categories of aging, angiogenesis, apoptotic process, cell cycle, cell death, cell differentiation, cell migration, cell proliferation, DNA repair, extracellular matrix, immune response, neurogenesis, RNA splicing, secretion, antioxidant activity, inflammatory responses and macrophage receptor activity genes up-regulated by LPS are summarized in Table3.

In particular, higher ratio of genes in GO categories of immune response (18-19%), and inflammatory response (17-21%) were up-regulated in all LPS treated cells compared to control (untreated cells) (Table 3).

Particularly, higher ratio of genes in GO categories of immune response (6-8%), and inflammatory response (8-12%) were down-regulated in all LPS treated cells compared to control (untreated cells) (Table 3).
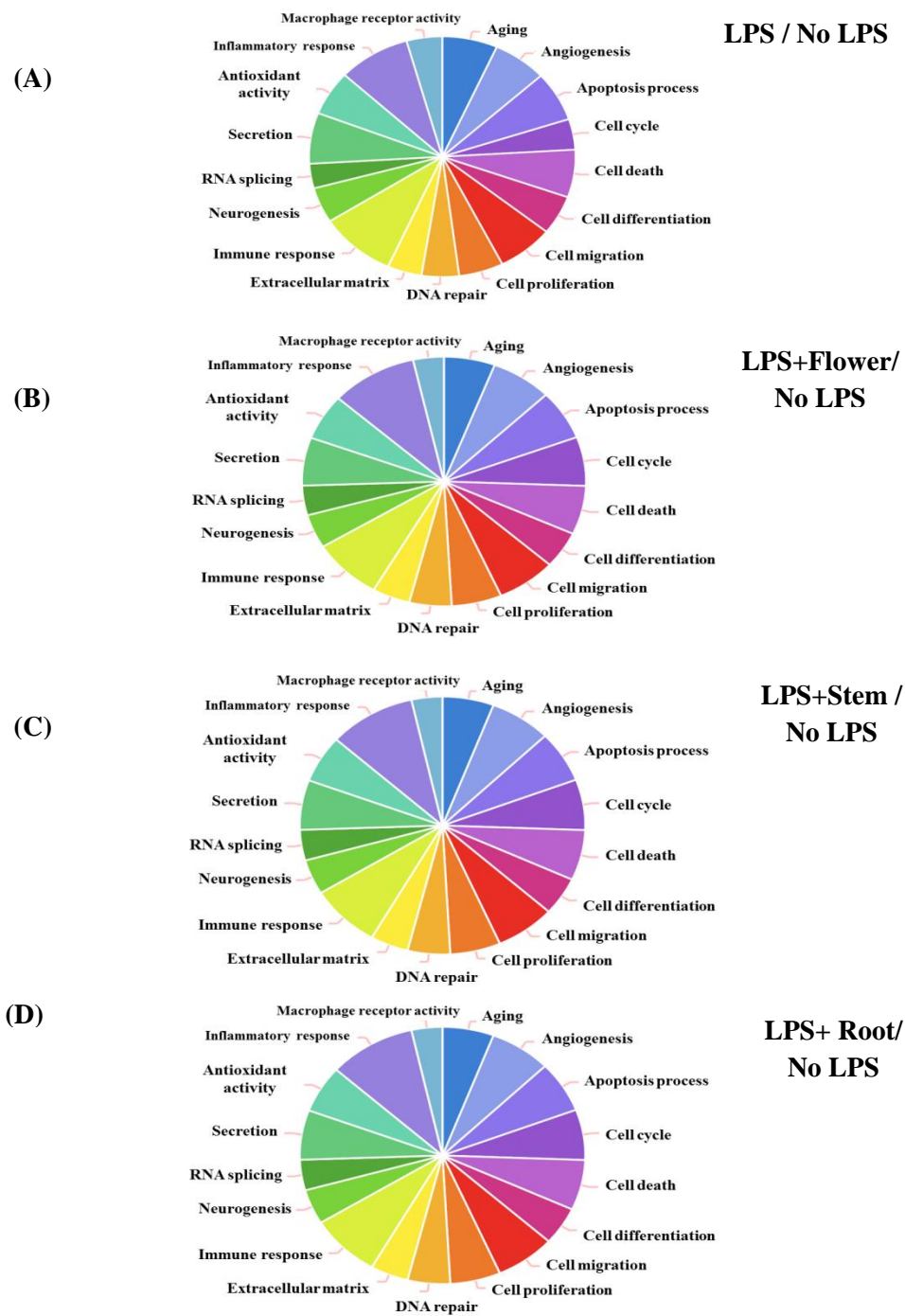
Figure 17. The Gene Ontology analysis of RAW 264.7 cells treated with or without LPS and NE as a percentage of total significant

The transcripts RAW 264.7 cells treated with or without LPS and NE were classified into GO categories of **(A)** LPS/ No LPS **(B)** NFE+LPS/ No LPS **(C)** NSE+LPS/ No LPS **(D)** NRE+LPS/ No LPS on the basis of GO terms as a percentage of total significant
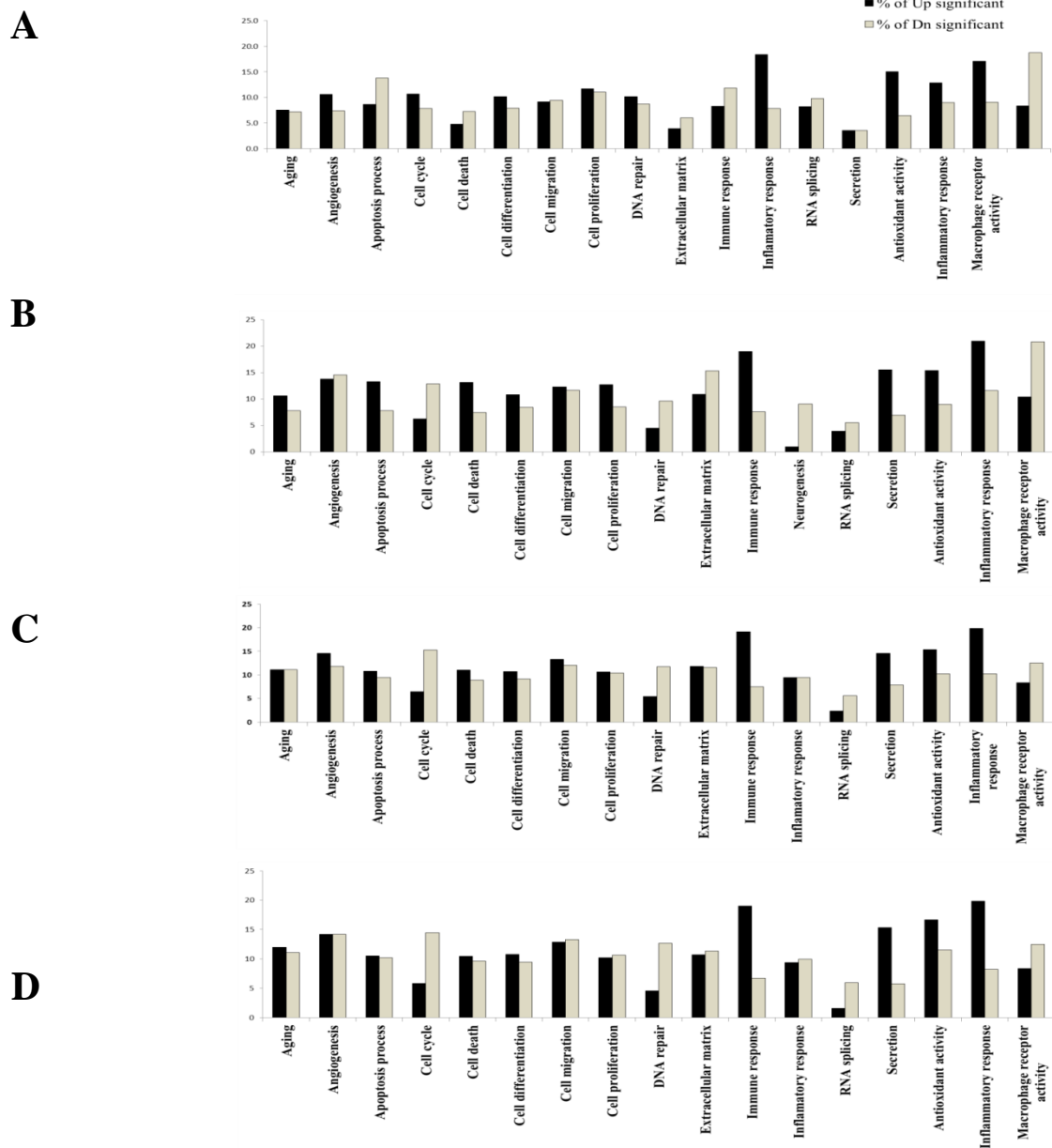
Figure 18. Gene Ontology annotation analysis of RAW 264.7 cells treated with or without LPS and NE as a percentage of up significant and percentage of down significant

The transcripts RAW 264.7 cells treated with or without LPS and NE were classified into GO categories of **(A)** LPS/ No LPS **(B)** NFE+LPS/ No LPS **(C)** NSE+LPS/ No LPS **(D)** NRE+LPS/ No LPS on the basis of GO terms as a percentage of up significant and percentage of down significant

46

Table 3. Differential gene expression of LPS stimulated RAW 264.7 macrophage cells

	Total	Aging	Angiogenesis	Apoptosis process	Cell cycle	Cell death	Cell differentiation	Cell migration	Cell proliferation	DNA repair	Extracellular matrix	Immune response	Neurogenesis	RNA splicing	Secretion	Antioxidant activity	Inflammatory response	Macrophage receptor activity
Gene Number	23282	217	254	638	895	698	2812	608	471	332	449	804	1277	252	418	78	439	48
% of Total	100.0	0.9	1.1	2.7	3.8	3.0	12.1	2.6	2.0	1.4	1.9	3.5	5.5	1.1	1.8	0.3	1.9	0.2
Up significant	1760	23	22	68	43	71	257	71	48	13	37	148	105	9	63	10	75	4
% of Up significant	7.6	10.6	8.7	10.7	4.8	10.2	9.1	11.7	10.2	3.9	8.2	18.4	8.2	3.6	15.1	12.8	17.1	8.3
Dn significant	1671	16	35	50	65	55	265	67	41	20	53	63	125	9	27	7	40	9
% of Dn significant	7.2	7.4	13.8	7.8	7.3	7.9	9.4	11.0	8.7	6.0	11.8	7.8	9.8	3.6	6.5	9.0	9.1	18.8

Table 4. Differential gene expression of LPS stimulated RAW 264.7 macrophage cells treated with NFE (5µg/mL)

	Total	Aging	Angiogenesis	Apoptosis process	Cell cycle	Cell death	Cell differentiation	Cell migration	Cell proliferation	DNA repair	Extracellular matrix	Immune response	Neurogenesis	RNA splicing	Secretion	Antioxidant activity	Inflammatory response	Macrophage receptor activity
Gene Number	23282	217	254	638	895	698	2812	608	471	332	449	804	1277	252	418	78	439	48
% of Total	100.0	0.9	1.1	2.7	3.8	3.0	12.1	2.6	2.0	1.4	1.9	3.5	5.5	1.1	1.8	0.3	1.9	0.2
Up significant	2056	23	35	85	56	92	305	75	60	15	49	153	13	10	65	12	92	5
% of Up significant	8.8	10.6	13.8	13.3	6.3	13.2	10.8	12.3	12.7	4.5	10.9	19.0	1.0	4.0	15.6	15.4	21.0	10.4
Dn significant	1507	17	37	50	115	52	237	71	40	32	69	61	116	14	29	7	51	10
% of Dn significant	6.5	7.8	14.6	7.8	12.8	7.4	8.4	11.7	8.5	9.6	15.4	7.6	9.1	5.6	6.9	9.0	11.6	20.8

Table 5. Differential gene expression of LPS stimulated RAW 264.7 macrophage cells treated with NSE (2µg/mL).

	Total	Aging	Angiogenesis	Apoptosis process	Cell cycle	Cell death	Cell differentiation	Cell migration	Cell proliferation	DNA repair	Extracellular matrix	Immune response	Neurogenesis	RNA splicing	Secretion	Antioxidant activity	Inflammatory response	Macrophage receptor activity
Gene Number	23282	217	254	638	895	698	2812	608	471	332	449	804	1277	252	418	78	439	48
% of Total	100.0	0.9	1.1	2.7	3.8	3.0	12.1	2.6	2.0	1.4	1.9	3.5	5.5	1.1	1.8	0.3	1.9	0.2
Up significant	1937	26	36	67	52	73	303	78	48	15	48	153	120	4	64	13	87	4
% Up significant	8.3	12.0	14.2	10.5	5.8	10.5	10.8	12.8	10.2	4.5	10.7	19.0	9.4	1.6	15.3	16.7	19.8	8.3
Dn significant	1708	24	36	65	129	67	266	81	50	42	51	54	127	15	24	9	36	6
% of Dn significant	7.3	11.1	14.2	10.2	14.4	9.6	9.5	13.3	10.6	12.7	11.4	6.7	9.9	6.0	5.7	11.5	8.2	12.5

Table 6. Differential gene expression of LPS stimulated RAW 264.7 macrophage cells treated with NRE (10µg/mL)

	Total	Aging	Angiogenesis	Apoptosis process	Cell cycle	Cell death	Cell differentiation	Cell migration	Cell proliferation	DNA repair	Extracellular matrix	Immune response	Neurogenesis	RNA splicing	Secretion	Antioxidant activity	Inflammatory response	Macrophage receptor activity
Gene Number	23282	217	254	638	895	698	2812	608	471	332	449	804	1277	252	418	78	439	48
% of Total	100.0	0.9	1.1	2.7	3.8	3.0	12.1	2.6	2.0	1.4	1.9	3.5	5.5	1.1	1.8	0.3	1.9	0.2
Up significant	2023	24	37	69	58	77	300	81	50	18	53	154	121	6	61	12	87	4
% Up significant	8.7	11.1	14.6	10.8	6.5	11.0	10.7	13.3	10.6	5.4	11.8	19.2	9.5	2.4	14.6	15.4	19.8	8.3
Dn significant	1745	24	30	60	137	62	257	73	49	39	52	60	121	14	33	8	45	6
% of Dn significant	7.5	11.1	11.8	9.4	15.3	8.9	9.1	12.0	10.4	11.7	11.6	7.5	9.5	5.6	7.9	10.3	10.3	12.5

Differential gene expression

The differential gene expression of RAW 264.7 cells treated with LPS and NE were observed using RNA sequencing analysis. Based on RNA sequencing results, among 23,282 of total genes in RAW 264.7 cells, 1,760 genes were up-regulated (higher than 2.0) and 1,671 genes were down-regulated (lower than 0.5) in LPS treated cells compared to control (untreated cells). In contrast, 2,056 genes were up-regulated and 1,507 genes were down-regulated in both LPS and 5 µg/mL NFE treated cells compared to control (Table 7). Considering NSE, 1,937 genes were up-regulated and 1,708 genes were down-regulated in both LPS and 2 µg/mL NSE treated cells compared to control (Table 8). In addition 2,023 genes were up-regulated and 1,745 genes were down-regulated in both LPS and 10 µg/mL NRE treated cells compared to control (Table 9).

Analysis of RNA sequencing data showed that 8 genes related to inflammatory response, immune response, antioxidant activity and macrophage receptor activity were screened using ExDEGA 1.1.9.0 software. The expression levels of 39, 43, 41 genes related to inflammation, were down-regulated in exposure to LPS and were normalized to control level by the addition of NFE, NSE and NRE respectively (Table 10, 11, 12). The expression levels of 8, 12, 12 genes related to inflammation were down-regulated in exposure to LPS and were normalized to control level by the addition of NFE, NSE and NRE respectively (Table 10, 11, 12).

Genes including Vpreb3, Nr1h4, IL12B, Cxcl9, Cxcl11, Ccl28, Tnfrsf13c, Sod2 and H2-Eb2 were up-regulated by more than 2 folds compared to the control level by addition of LPS. However, the levels were normalized to control level by the addition of NE. In particular, the expression levels of NF-κB1 and NF-Kb2 genes which are key regulating genes in inflammation were up-regulated by 3 and 2 fold compared to control level by LPS, and were normalized to control level by addition of NE (Table. 7, 8).

49

Genes related to inflammation including Apoe, Hp, Havcr2 were down-regulated by 0.2, 0.3, and 0.2 fold compared to control level by α-MSH, and were normalized to control level by addition of NE (Table. 7, 8, 9).

Table 7. Up-regulated genes in LPS treated RAW 264.7 cells and normalized by NFE

Gene Symbol	LPS /Control	LPS+NFE /Control	Gene Name
Vpreb3	3.617	1.000	Pre-B lymphocyte 3
Nr1h4	2.352	1.000	Nuclear receptor subfamily 1 group H member 4
Grap	4.257	1.258	GRB2-related adaptor protein
Hist1h2bf	2.049	0.879	Histone cluster 1, h2b
F12	2.550	1.000	Coagulation factor XII
Ccl28	2.352	1.000	C-C motif chemokine ligand 28
Slc30a8	3.687	1.000	Solute carrier family 30 member 8
Tnfrsf13c	2.458	1.000	TNF receptor superfamily member 13C
Ifnar1	2.155	1.089	Interferon alpha and beta receptor subunit 1
Mx1	3.509	1.079	MX dynamin like gtpase 1
Sod2	2.045	1.130	Superoxide dismutase 2, mitochondrial
H2-Eb2	3.617	1.000	Histocompatibility 2, class II antigen E beta2
Lta	4.878	0.989	Lymphotoxin alpha
H2-L	2.288	1.051	Histocompatibility 2, D region locus L
H2-Q7	3.221	1.062	Histocompatibility 2, Q region locus 7
Trem3	2.256	1.097	Triggering receptor expressed on myeloid cells 3
Camk4	4.555	1.192	Calcium/calmodulin dependent protein kinase IV
Malt1	2.035	1.207	MALT1 paracaspase
Nfkb2	2.121	1.491	Nuclear factor kappa B subunit 2
Card9	2.098	1.329	Caspase recruitment domain family, member 9
Zp3	3.918	1.000	Zona pellucida glycoprotein 3
Rasgrp1	2.352	1.000	RAS guanyl releasing protein 1
Cd1d1	2.748	1.457	CD1d1 antigen
Polr3c	3.286	0.971	Polymerase (RNA) III (DNA directed) polypeptide C
Cxcl9	3.617	1.000	Chemokine (C-X-C motif) ligand 9(
Gbp6	2.187	1.349	Guanylate binding protein 6
Oas1f	2.352	1.000	2'-5' oligoadenylate synthetase 1F
Irak2	2.777	1.395	Interleukin 1 receptor associated kinase 2
Tarm1	3.101	1.396	T cell-interacting, activating receptor on myeloid cells 1
Axl	2.307	0.691	AXL receptor tyrosine kinase
Isg20	2.894	1.397	Interferon-stimulated protein
Gcnt3	2.352	1.000	Glucosaminyl (N-acetyl) transferase 3, mucin type
Ltf	2.352	1.000	Lactotransferrin
Cxcr2	2.957	0.735	Chemokine (C-X3-C motif) receptor 1
Il13	2.352	1.000	Suppression inducing transmembrane adaptor 1
Cd300a	3.311	1.230	CD300a molecule
Cxcr6	2.352	1.000	C-X-C motif chemokine receptor 6
Hhipl1	2.352	1.000	Hedgehog interacting protein-like 1
Scara5	5.107	1.000	Scavenger receptor class A, member 5

51

Table 8. Up-regulated genes in LPS treated RAW 264.7 cells and normalized by NSE

Gene Symbol	LPS /Control	LPS+NSE /Control	Gene Name
Gja1	3.397	1.168	Gap junction protein alpha 1
Vpreb3	3.617	1.000	Pre-B lymphocyte 3
Nr1h4	2.352	1.000	Nuclear receptor subfamily 1 group H member 4
Il12b	3.686	1.000	Interleukin 12B
Cplx2	3.750	1.000	Complexin 2
Ccl28	2.352	1.000	C-C motif chemokine ligand 28
Ifnar1	2.155	0.920	Interferon alpha and beta receptor subunit 1
Sod2	2.045	0.931	Superoxide dismutase 2, mitochondrial
H2-Eb2	3.617	1.000	Histocompatibility 2, class II antigen E beta2
H2-T23	3.690	0.815	Histocompatibility 2, T region locus 23
Malt1	2.035	1.271	MALT1 paracaspase
Anxa1	4.026	1.083	Annexin A1
Fas	6.759	1.114	TNF receptor superfamily member 6
Kynu	2.408	1.000	Kynureninase
Nmi	2.143	1.321	N-myc (and STAT) interactor
Rasgrp1	2.352	1.000	RAS guanyl releasing protein 1
Cd1d1	2.748	1.337	CD1d1 antigen
Ripk2	2.637	1.061	Receptor interacting serine/threonine kinase 2
Exosc3	3.029	0.964	Exosome component 3
Tnfsf15	5.041	1.000	Tumor necrosis factor (ligand) superfamily, member 15
Ifnb1	12.395	1.000	Interferon beta 1
Nfkb1	3.033	1.424	Nuclear factor of kappa light polypeptide gene enhancer in B cells 1, p105
Cxcl9	3.617	1.000	Chemokine (C-X-C motif) ligand 9
Cxcl11	2.469	0.872	Chemokine (C-X-C motif) ligand 11
Gbp6	2.187	1.304	Guanylate binding protein 6
Oas1f	2.352	1.000	2'-5' oligoadenylate synthetase 1F
Irak2	2.777	1.367	Interleukin 1 receptor associated kinase 2
Psg17	2.458	1.000	Pregnancy specific glycoprotein 17
Axl	2.307	0.984	AXL receptor tyrosine kinase
Trim12a	2.458	1.000	Tripartite motif-containing 12A
Nxnl1	3.905	1.002	Nucleoredoxin-like 1
Gcnt3	2.352	1.000	Glucosaminyl (N-acetyl) transferase 3, mucin type
Ltf	2.352	1.000	Lactotransferrin
Cxcr2	2.957	0.836	C-X-C motif chemokine receptor 2
Il13	2.352	1.000	Interleukin 13
Cd300a	3.311	0.850	CD300a molecule
Il1rap	2.842	1.277	Interleukin 1 receptor accessory protein
Cxcr6	2.352	1.000	C-X-C motif chemokine receptor 6
Hhipl1	2.352	1.000	Hedgehog interacting protein-like 1

Table 9. Up-regulated genes in LPS treated RAW 264.7 cells and normalized by NRE

Gene Symbol	LPS /Control	LPS+NRE /Control	Gene Name
Gja1	3.397	0.964	Gap junction protein alpha 1
Vpreb3	3.617	1.000	Pre-B lymphocyte 3
Nr1h4	2.352	1.000	Nuclear receptor subfamily 1 group H member 4
Il12b	3.686	1.000	Interleukin 12B
Pxdn	2.590	1.000	Peroxidasin
Ccl28	2.352	1.000	C-C motif chemokine ligand 28
Slc30a8	3.687	1.000	Solute carrier family 30 member 8
Ifnar1	2.155	1.099	Interferon alpha and beta receptor subunit 1
Mx1	3.509	1.115	MX dynamin like gtpase 1
Sod2	2.045	1.000	Superoxide dismutase 2, mitochondrial
H2-Eb2	3.617	1.000	Histocompatibility 2, class II antigen E beta2
H2-Q7	3.221	1.404	Histocompatibility 2, Q region locus 7
Trem3	2.256	0.842	Triggering receptor expressed on myeloid cells 3
Camk4	4.555	1.332	Calcium/calmodulin dependent protein kinase IV
Malt1	2.035	1.070	MALT1 paracaspase
Anxa1	4.026	0.788	Annexin A1
Fas	6.759	1.031	TNF receptor superfamily member 6
Card9	2.098	1.124	Caspase recruitment domain family, member 9
Kynu	2.408	1.000	Kynureninase
Rasgrp1	2.352	1.000	RAS guanyl releasing protein 1
Ripk2	2.637	1.495	Receptor interacting serine/threonine kinase 2
Tnfsf15	5.041	1.000	Tumor necrosis factor (ligand) superfamily, member 15
Gbp2	5.037	0.773	Guanylate binding protein 2
Cxcl9	3.617	1.000	Chemokine (C-X-C motif) ligand 9
Oas1f	2.352	1.000	2'-5' oligoadenylate synthetase 1F
Irak2	2.777	1.249	Interleukin 1 receptor associated kinase 2
Styk1	3.238	1.490	Serine/threonine/tyrosine kinase 1
Tarm1	3.101	1.023	T cell-interacting, activating receptor on myeloid cells 1
Psg17	2.458	1.000	Pregnancy specific glycoprotein 17
Axl	2.307	1.138	AXL receptor tyrosine kinase
Slc7a2	3.514	0.791	Solute carrier family 7 member 2
Nxnl1	3.905	0.842	Nucleoredoxin-like 1
Gcnt3	2.352	1.000	Glucosaminyl (N-acetyl) transferase 3, mucin type
Ltf	2.352	1.000	Lactotransferrin
Sit1	2.305	1.330	Suppression inducing transmembrane adaptor 1
Il13	2.352	1.000	Interleukin 13
Cd300a	3.311	0.682	CD300a molecule
Cxcr6	2.352	1.000	C-X-C motif chemokine receptor 6
Hhipl1	2.352	1.000	Hedgehog interacting protein-like 1

Table 10. Down-regulated genes in LPS treated RAW 264.7 cells and normalized by NFE

Gene Symbol	LPS /Control	LPS+NFE /Control	Gene Name
Txnrd3	0.367	0.917	Thioredoxin reductase 3
Apoe	0.276	0.882	Apolipoprotein E
Cited1	0.380	1.198	Cbp/p300-interacting transactivator with Glu/Asp-rich carboxy-terminal domain 1
Cd24a	0.286	0.848	CD24a antigen
Tbxa2r	0.392	0.885	Thromboxane A2 receptor
Tlr4	0.338	0.850	Toll-like receptor 4
Tnfrsf4	0.442	0.854	Tumor necrosis factor receptor superfamily, member 4

Table 11. Down-regulated genes in LPS treated RAW 264.7 cells and normalized by NSE

Gene Symbol	LPS /Control	LPS+NSE /Control	Gene Name
Gper1	0.381	0.763	G protein-coupled estrogen receptor 1
Cyp26b1	0.238	1.146	Cytochrome P450, family 26, subfamily b, polypeptide 1
Star	0.467	0.848	Steroidogenic acute regulatory protein
Cd3d	0.245	1.002	CD3 antigen, delta polypeptide
Slc26a6	0.091	0.766	Solute carrier family 26, member 6
Cd24a	0.286	1.170	CD24a antigen
Stab1	0.330	0.724	Stabilin 1
Ahsg	0.392	1.002	Alpha-2-HS-glycoprotein
Thbs1	0.358	1.337	Thrombospondin 1
Havcr2	0.227	1.337	Hepatitis A virus cellular receptor 2

Table 12. Down-regulated genes in LPS treated RAW 264.7 cells and normalized by NRE

Gene Symbol	LPS /Control	LPS+NRE /Control	Gene Name
Txnrd3	0.367	0.922	Thioredoxin reductase 3
Apoe	0.276	0.723	Apolipoprotein E
Cx3cl1	0.491	1.394	Chemokine (C-X3-C motif) ligand 1
Hp	0.387	0.844	Haptoglobin
Cd3d	0.245	0.833	CD3 antigen, delta polypeptide
Cited1	0.380	0.852	Cbp/p300-interacting transactivator with Glu/Asp-rich carboxy-terminal domain 1
Cd24a	0.286	1.063	CD24a antigen
AI182371	0.425	0.811	Expressed sequence AI182371
Thbs1	0.358	0.801	Thrombospondin 1
Tnfrsf4	0.442	1.099	Tumor necrosis factor receptor superfamily, member 4
Vtn	0.404	0.826	Vitronectin
Loxl4	0.369	0.867	Lysyl oxidase-like 4
Tmprss13	0.431	0.801	Transmembrane protease, serine 13

STRING protein-protein analysis of differentially expressed proteins

To investigate the functional relationship among the differentially expressed genes, a network analysis of protein- protein interaction (PPI) was performed using STRING analysis. STRING (Search Tool for the Retrieval of Interacting Genes/Proteins) is a database program designed for protein-protein interaction analysis which generates a network of interactions from different sources, including various interaction databases, text mining, genetic interactions and shared pathway interactions [55]. The network of the interactions among 29 proteins related to inflammation which were up- or down-regulated by LPS and were normalized by NFE are depicted in Fig. 19. NF-κB2 is located in the middle of network of proteins related to inflammatory response. Another network of proteins related to chemotaxis (Cxcr2, Cxcr6, Ccl28, Cxcl9) are closely located to NF-κB network. In PPI network of 25 proteins which were normalized by NSE both NF-κB1 and Cxcl9 form "functional hubs" in the middle of network (Fig. 22). PPI network of 28 proteins which were up- or down-regulated by LPS and were normalized by NRE are shown in Fig. 25. Cxcl9 is located in the middle of PPI network and connects with other protein's function. PPI network explains the molecular mechanisms underlying the anti-inflammatory effect of NE.

IPA gene network analysis

As described above, NE treatment normalized the expression of genes related to inflammatory response in LPS stimulated RAW 264.7 macrophage cells. These genes were uploaded onto the IPA analysis program to identify the functional subsets, gene networks, and upstream regulators targeted by NE. Within these gene networks IPA denoted the main up-stream regulators which function is modulated by NE. Accordingly; IPA network constructed based on 29 genes affected by NFE includes NF-κB2, AXL, APOE, LDL, TLR4 IL-13 and pro-inflammatory cytokines Fig 23. Fig 23 depicts the network of the interactions among 25 proteins related to inflammation which were differentially expressed in presence of LPS and were normalized by NSE, which includes NF-κB1, IFNB1, IRAK2, NR1H4 and pro-inflammatory cytokines. In RAW 264.7 macrophage cells LDL, APOE, HDL, NR1H, NR1H4 and other pro-inflammatory cytokines are included in IPA network constructed based on 28 genes affected by NRE (Fig 26). Using the IPA gene network analysis tool, we predicted interacting molecular networks to further evaluate the broader potential effects of NE.

Regulator effect network analysis in IPA

Regulator effect network analysis in IPA tool integrates altered regulator results to build causal hypotheses to interpret influence of upstream to cause particular functional outcomes downstream. The master regulators for the inflammatory response and chemotaxis includes APOE, HLA-A, LTS, CXCR3, IL-13, CXCL9, TLR4, NF-Kb2 and TNFRSF4 proteins in NFE treated macrophages. The master regulators for the inflammatory response and chemotaxis includes NMI, LTF, CXCL9, CXCL11, RIPK2, CD1D, AXL, IFNAR1, CXCR2, 1L-13, 1L-12B, FAS, 1FNB1, CD300A, SOD2, and STAR proteins in NSE treated macrophages. 20 upper tier proteins regulated 12 downstream proteins related to inflammatory response, and chemotaxis in NSE treated macrophages. NF-Kb2 complex master regulated the cell death of macrophages in NRE trated macrophages. The master regulators for the death of macrophage includes APOE, SOD2, IL-13, CXCL1, and FAS proteins in NRE treated macrophages.
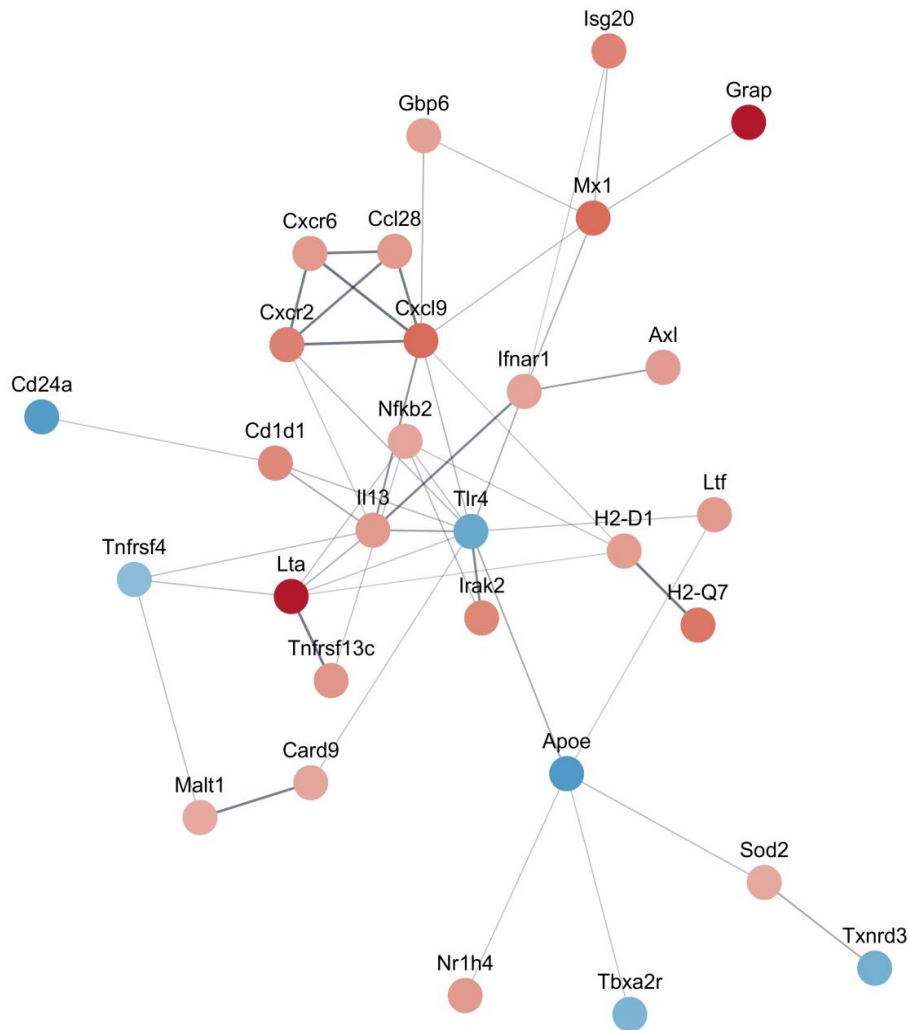
Figure 19. Protein-protein interaction (PPI) network constructed of differentially expressed genes (DEGs) identified in RAW 264.7 macrophage cells treated with LPS and NFE.

Network of the interactions between 29 proteins containing the most significant peptides. Bold lines represent the strongly connected genes in focus of inflammation. Different colors indicate different expression of genes. Red colour represents up-regulated gene expression and blue colour represents down-regulated gene expression.
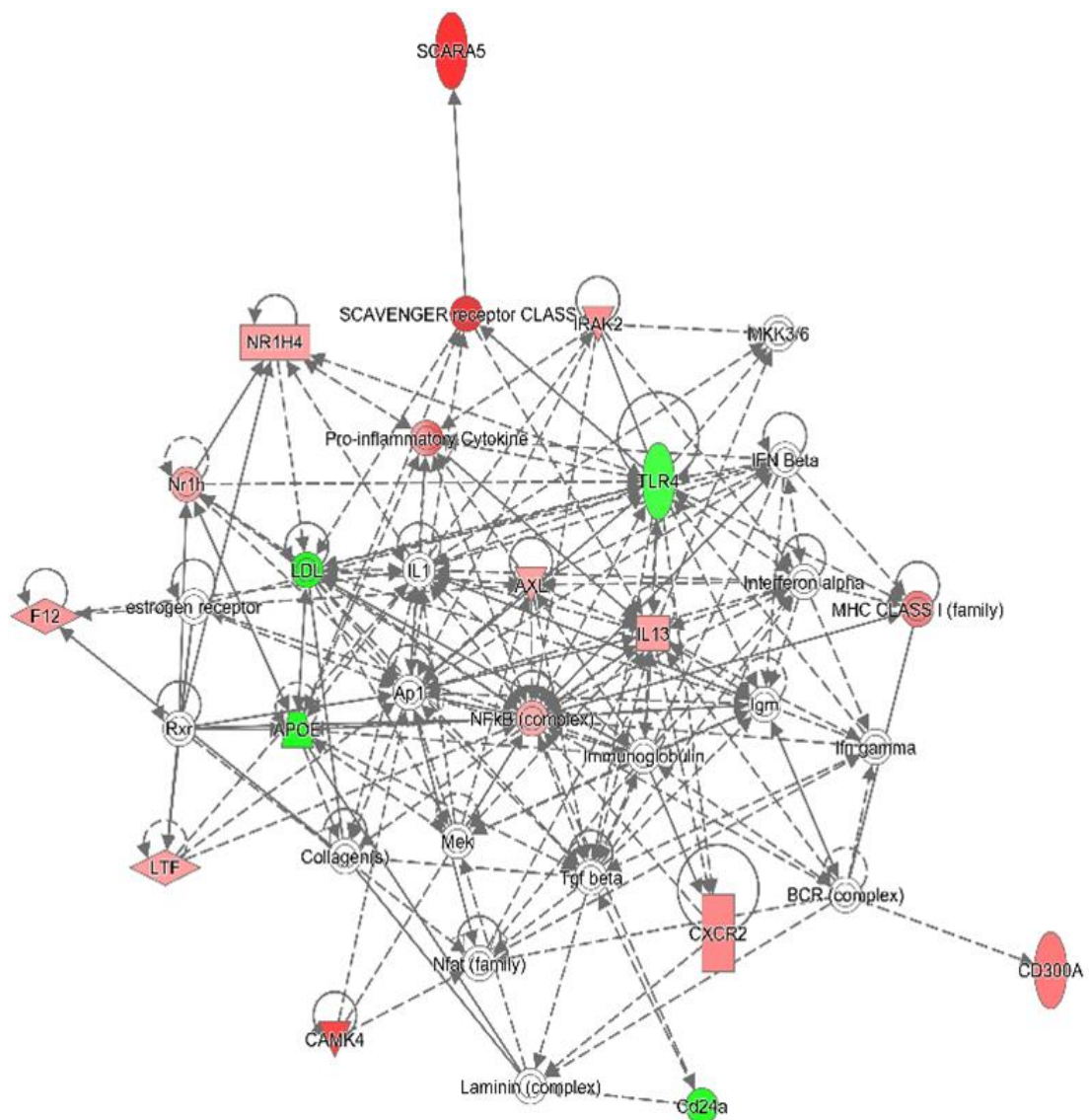
Figure 20. IPA gene network analysis of differentially expressed genes (DEGs) identified in RAW 264.7 macrophage cells treated with LPS and NFE.

Ingenuity pathway analysis (IPA) network analysis indicates interactions between 19 genes affected in RAW 264.7 macrophage cells by LPS and were normalized in presence of NFE. The intensity of the node color indicates the expression level as up- and down- regulated genes are indicated by red and green colour. Genes in uncolored notes were not differentially expressed by NFE and were integrated into the computationally generated networks.
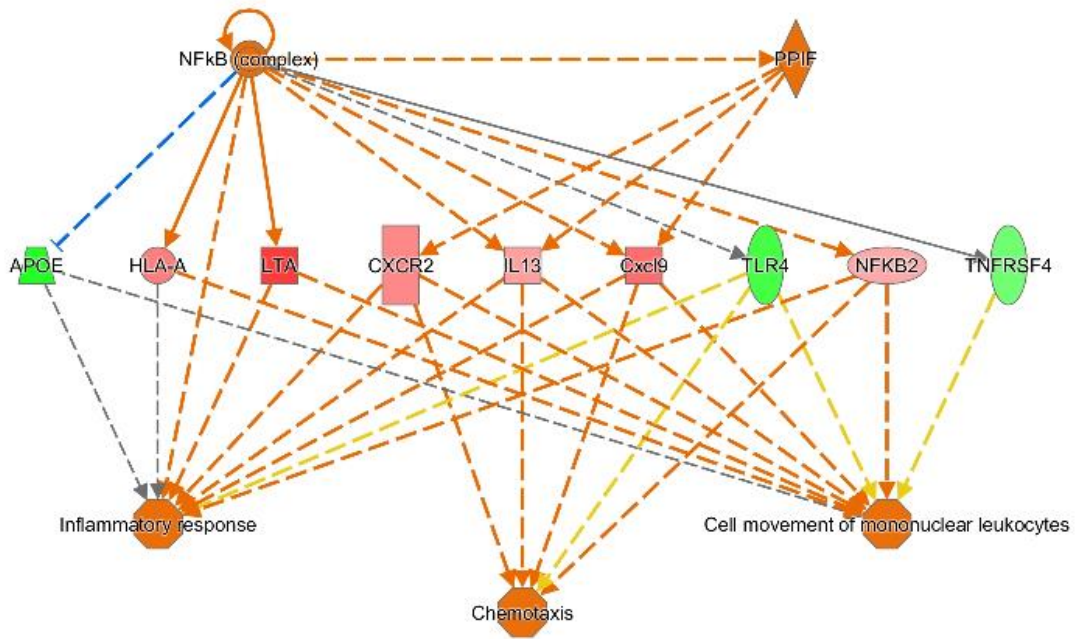
Figure 21. Upstream regulator effect analysis of chemotaxis and cell migration pathways of differentially expressed genes (DEGs) identified in RAW 264.7 macrophage cells treated with LPS and NFE.using Ingenuity Pathway Analysis (IPA).

The top tier in each network shows master regulators are predicted to be activated by NFE (orange color) and the middle tiers show the intermediate regulators through which the master regulators exert their effect on the regulated functions, which are indicated in the bottom tier. Up-regulated molecules in the middle tiers are colour coded red and down-regulated molecules in green. The shape of each molecule indicates its molecular function. Orange (predicted to be activated) and blue (predicted to be inhibited) lines represent relationships with causal consistency
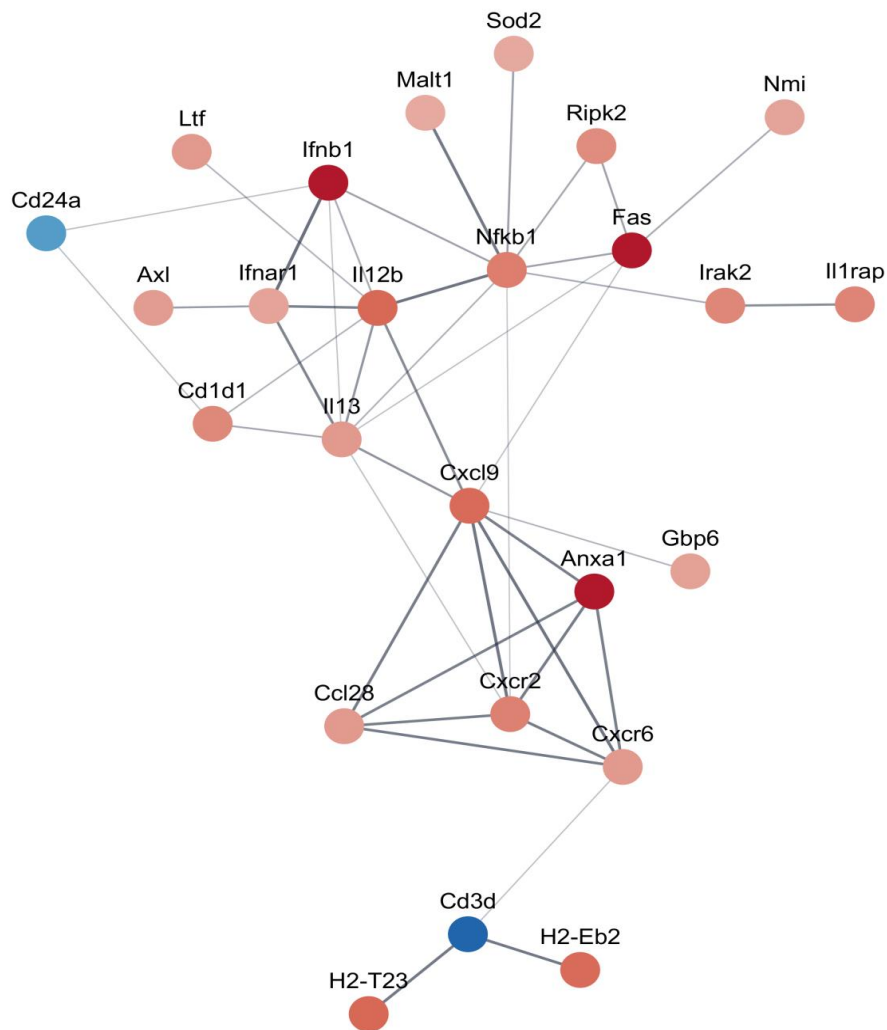
.

Figure 22. Protein-protein interaction (PPI) network constructed of differentially expressed genes (DEGs) identified in RAW 264.7 macrophage cells treated with LPS and NSE.

Network of the interactions between 25 proteins containing the most significant peptides. Bold lines represent the strongly connected genes in focus of inflammation. Different colors indicate different expression of genes. Red colour represents up-regulated gene expression and blue colour represents down-regulated gene expression.
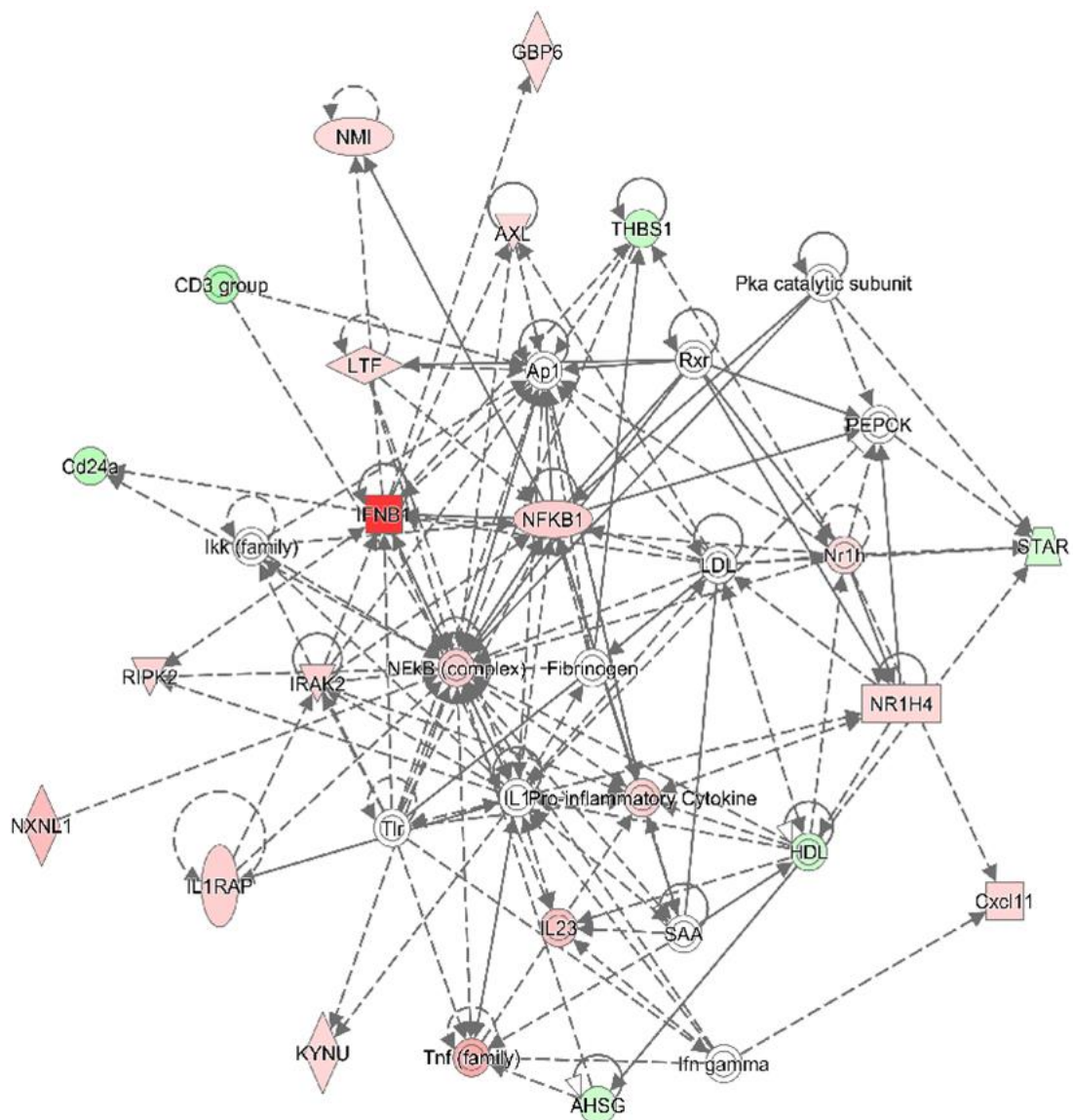
Figure 23. IPA gene network analysis of differentially expressed genes (DEGs) identified in RAW 264.7 macrophage cells treated with LPS and NSE.

Ingenuity pathway analysis (IPA) network analysis indicates interactions between 24 genes affected in RAW 264.7 macrophage cells by LPS and were normalized in presence of NFE. The intensity of the node color indicates the expression level as up- and down- regulated genes are indicated by red and green colour. Genes in uncolored notes were not differentially expressed by NFE and were integrated into the computationally generated networks.
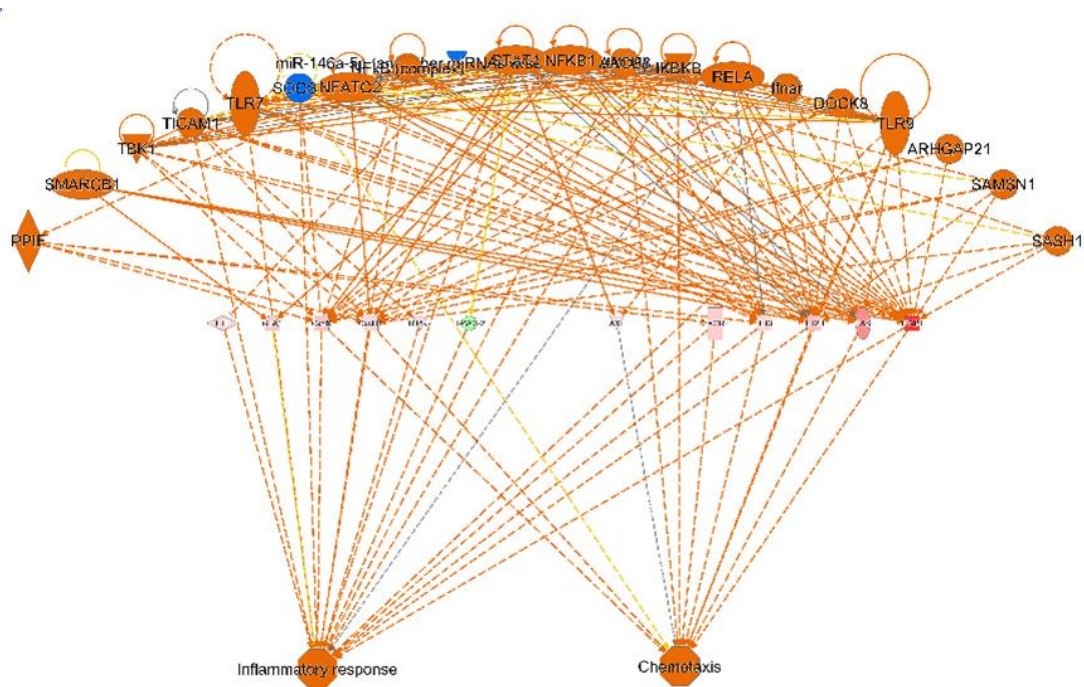
62

Figure 24. Upstream regulator effect analysis of chemotaxis and cell migration pathways of differentially expressed genes (DEGs) identified in RAW 264.7 macrophage cells treated with LPS and NSE.using Ingenuity Pathway Analysis (IPA).

The top tier in each network shows master regulators are predicted to be activated by NSE (orange color) and the middle tiers show the intermediate regulators through which the master regulators exert their effect on the regulated functions, which are indicated in the bottom tier. Up-regulated molecules in the middle tiers are colour coded red and down-regulated molecules in green. The shape of each molecule indicates its molecular function. Orange (predicted to be activated) and blue (predicted to be inhibited) lines represent relationships with causal consistency.
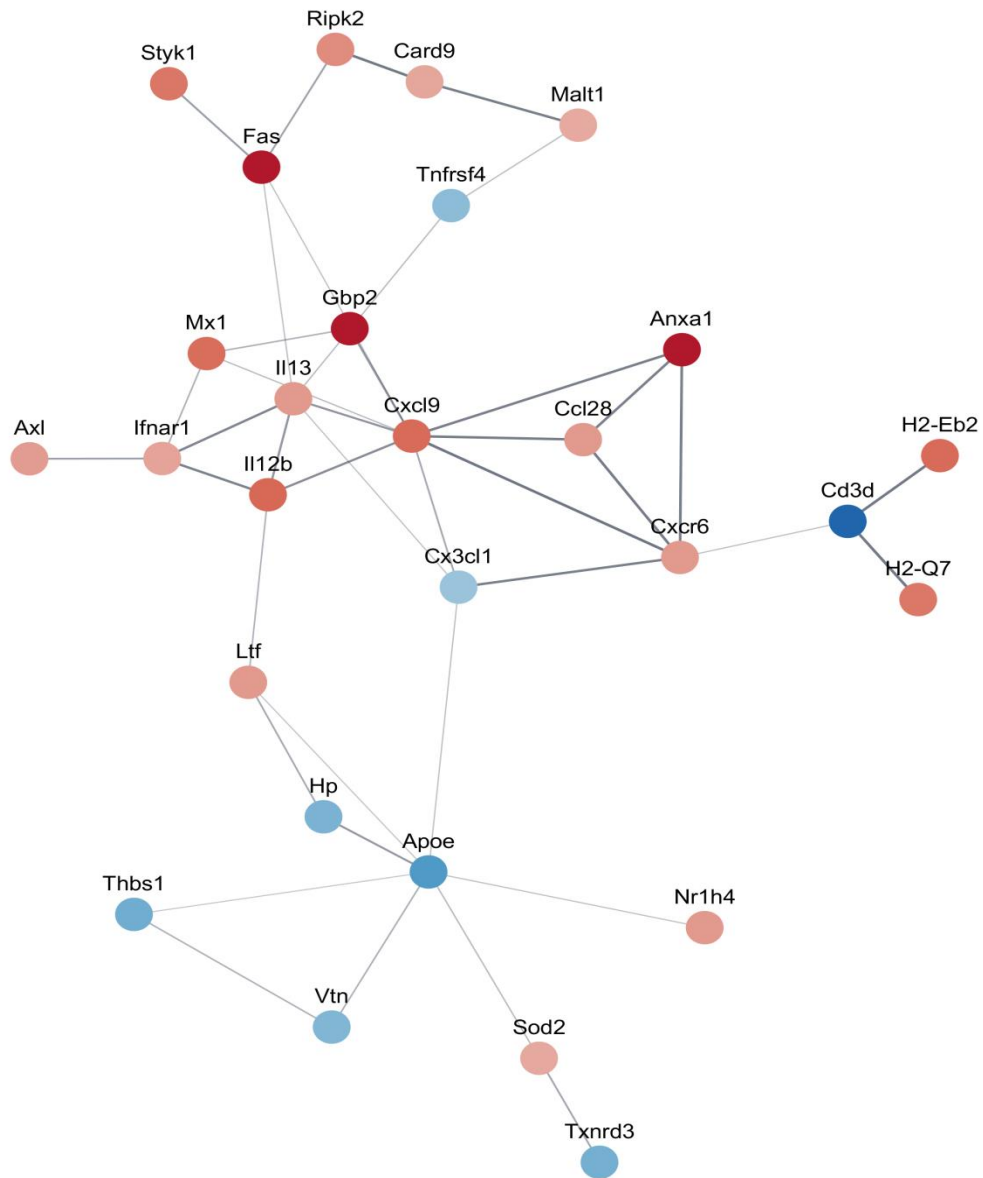
Figure 25. Protein-protein interaction (PPI) network constructed of differentially expressed genes (DEGs) identified in RAW 264.7 macrophage cells treated with LPS and NRE.

Network of the interactions between 28 proteins containing the most significant peptides. Bold lines represent the strongly connected genes in focus of inflammation. Different colors indicate different expression of genes. Red colour represents up-regulated gene expression and blue colour represents down-regulated gene expression.
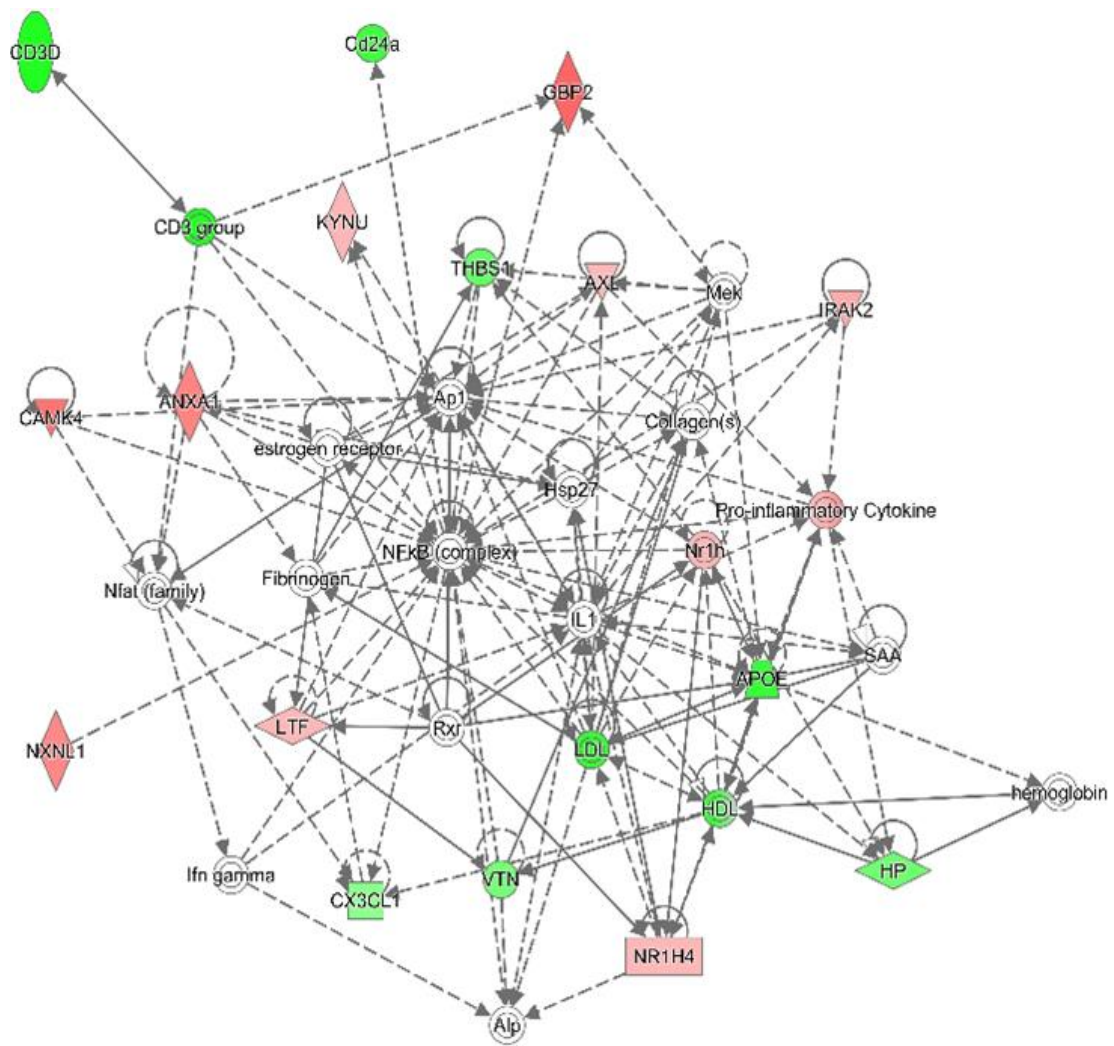
Figure 26. IPA gene network analysis of differentially expressed genes (DEGs) identified in RAW 264.7 macrophage cells treated with LPS and NRE.

Ingenuity pathway analysis (IPA) network analysis indicates interactions between 21 genes affected in RAW 264.7 macrophage cells by LPS and were normalized in presence of NFE. The intensity of the node color indicates the expression level as up- and down- regulated genes are indicated by red and green colour. Genes in uncolored notes were not differentially expressed by NFE and were integrated into the computationally generated networks.
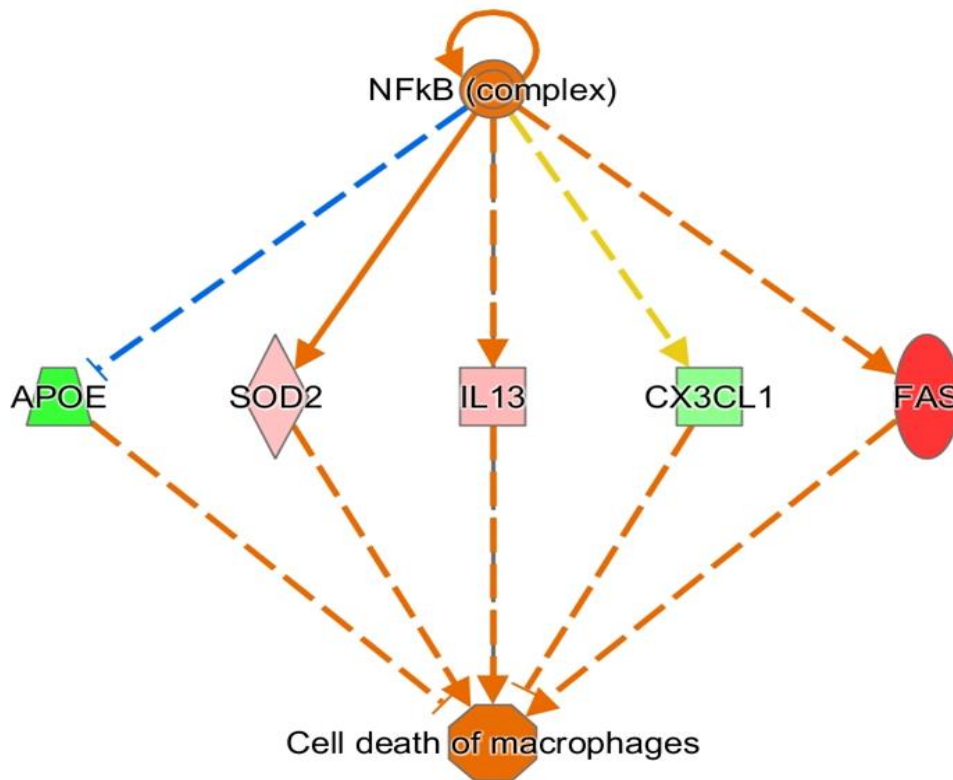
Figure 27. Upstream regulator effect analysis of chemotaxis and cell migration pathways of differentially expressed genes (DEGs) identified in RAW 264.7 macrophage cells treated with LPS and NRE.using Ingenuity Pathway Analysis (IPA). The top tier in each network shows master regulators are predicted to be activated by NRE (orange color) and the middle tiers show the intermediate regulators through which the master regulators exert their effect on the regulated functions, which are indicated in the bottom tier. Up-regulated molecules in the middle tiers are colour coded red and down-regulated molecules in green. The shape of each molecule indicates its molecular function. Orange (predicted to be activated) and blue (predicted to be inhibited) lines represent relationships with causal consistency.

Cellular toxicity

To determine the cytotoxicity of NE, B16-F10 melanoma cells were treated with varying concentrations of NE for 24 hrs, and observed the cell viabilities using an MTT assay. No cytotoxicity was observed in B16-F10 melanoma cells up to NFE 20 μg/mL where as cytotoxicity was increased significantly by 39% at 40 μg/mL of NEF in B16-F10 melanoma cell (Fig. 28 A). NSE showed no cytotoxicity less than10 μg/mL of NSE whereas the cytotoxicity was increased significantly by 9% at 10 μg/mL of NSE in B16-F10 melanoma cell (Fig. 28 B). B16-F10 melanoma cells had no cytotoxicity up to 20 μg/mL of NRE whereas the cytotoxicity was significantly increased by 30% at the concentration of 40 μg/mLof NRE in B16-F10 melanoma cell respectively (Fig. 28 C).

A
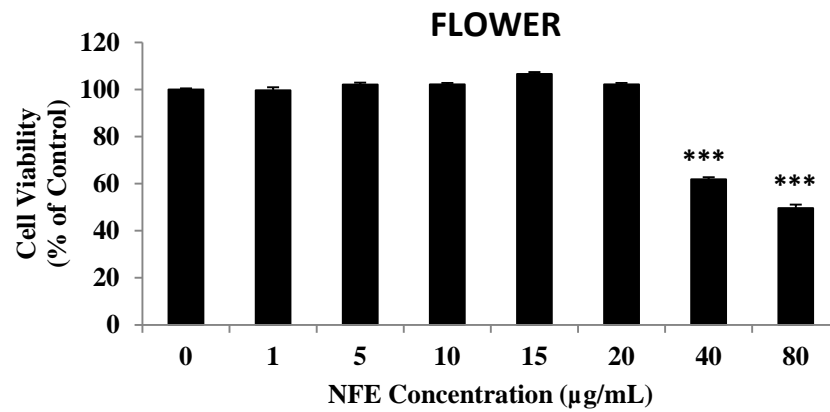
B
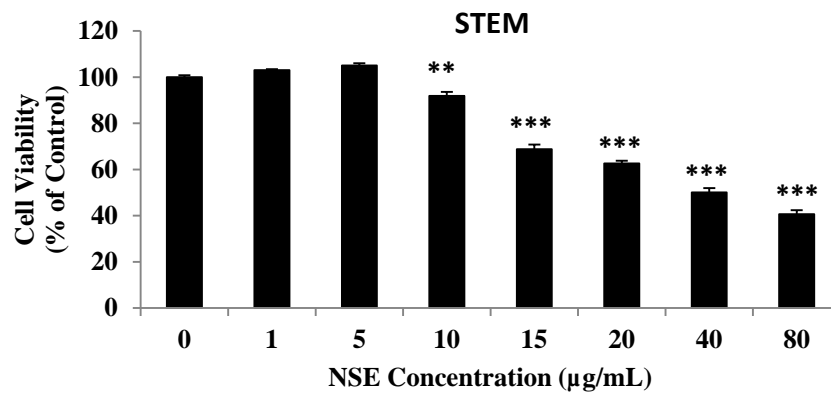
C

Figure 28. Effects of NE on B16-F10 melanoma cell viability.

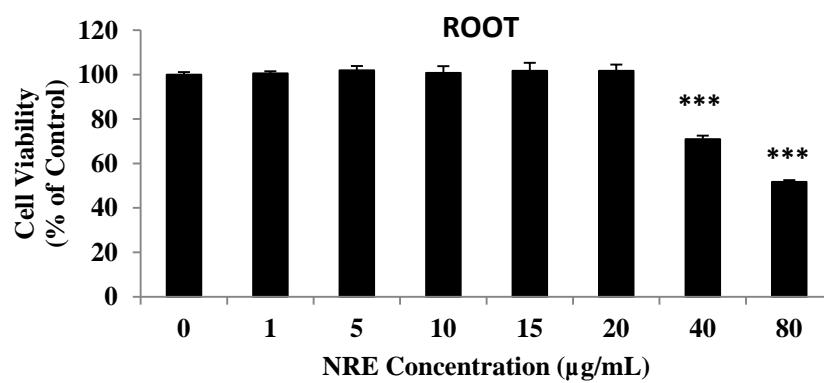**(A)** B16-F10 melanoma cell viability in different concentrations of NFE, **(B)** NSE, and **(C)** NRE. Data are the means of ± S.E. for three independent experiments. (**p < 0.001, and ***p < 0.0001 compared with the control).

Inhibitory effect on mushroom tyrosinase activity

Inhibitory effect of NE on mushroom tyrosinase activity was observed as described in Materials and Methods. As shown in Fig. 25, NF inhibited mushroom tyrosinase activity in a dose-dependent manner. Mushroom tyrosinase inhibition at 1,000, 2,000, 4,000 and 8,000 µg/mL of concentrations samples were estimated to be 10%, 19%, 29% and 36% for NFE respectively (Fig. 29B). The enzyme activity was inhibited by 14%, 16%, 17% and 29% for corresponding concentration of NSE (Fig. 25B) and for NRE, mushroom tyrosinase activity was inhibited by 12%, 14%, 15% and 17% for corresponding concentration of NRE respectively (Fig. 29C). Arbutin, (10 mM) a well-known tyrosinase inhibitor was used as a positive control, which showed 53% of mushroom tyrosinase inhibition indicating the direct inhibition of tyrosinase activity. The IC50 values of NFE, NSE, and NRE for 1250 U/mL mushroom tyrosinase were estimated to be 6680 µg/mL, 3585 µg/mL, and 4185 µg/mL. These results suggest NE has direct inhibitory effect on tyrosinase activity.
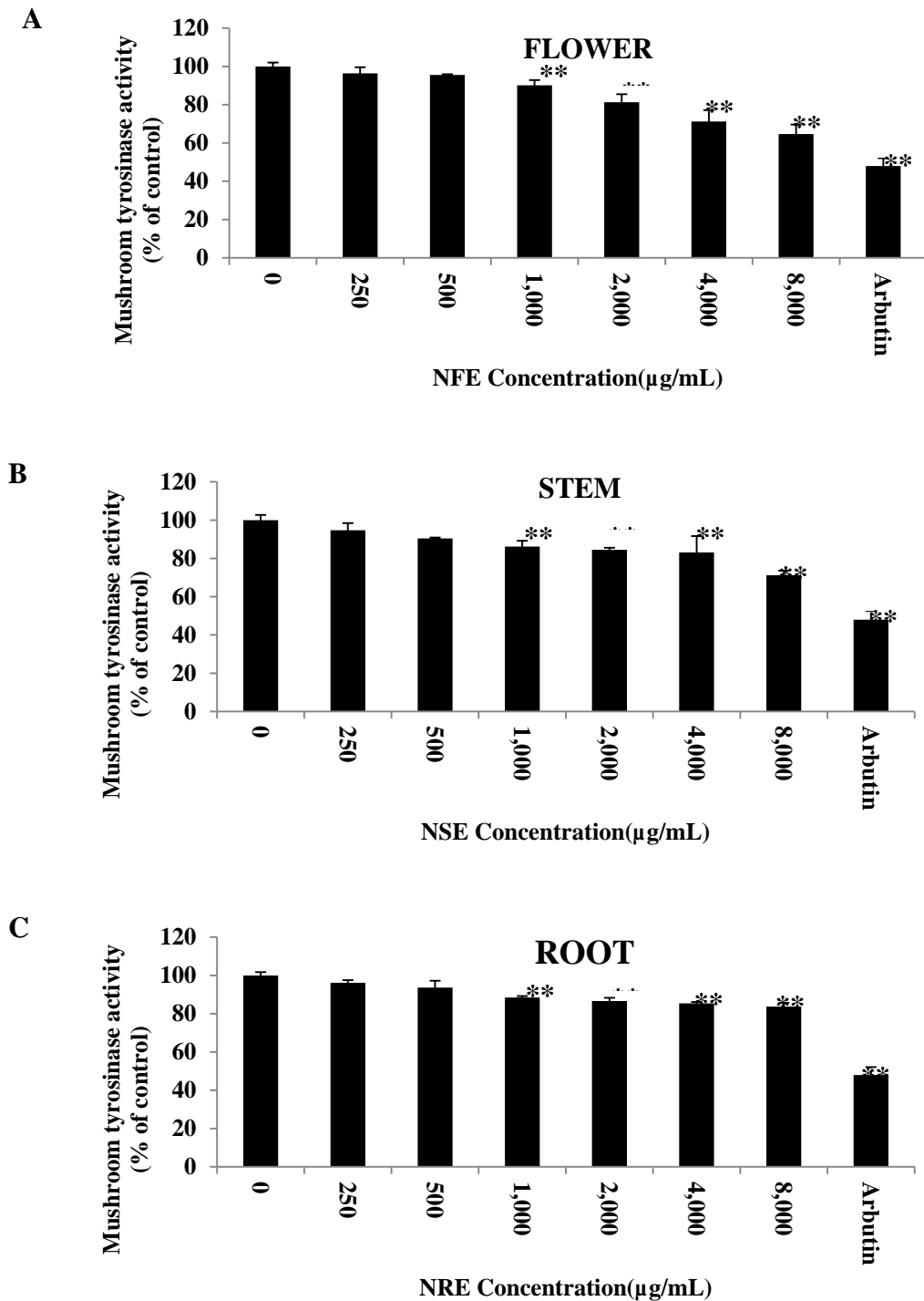
Figure 29. Inhibitory effect of NE on mushroom tyrosinase activity

Mushroom tyrosinase activity was examined at varying concentrations of **(A)** NFE, **(B)** NSE and **(C)** NRE. Values represent the mean ± S.E. for three independent experiments (***p < 0.0001 compared with the control).

Inhibitory effect on cellular tyrosinase activity

Inhibitory effect of NE on cellular tyrosinase activity was evaluated in ɑ-MSH stimulated B16-F10 melanoma. The enzyme activity was significantly increased in exposure to α-MSH, whereas the activities were inhibited in a concentration dependent manner of NE. Cellular tyrosinase activity was inhibited by 9%, 19%, 27% and 57% at 1, 10, 20 and 40 µg/mL of NFE (Fig. 30A). The enzyme activity was inhibited by 11%, 19%, 36% and 61% at 1, 2, 5 and 10 µg/mL of NSE (Fig. 30B). 1, 10, 20 and 40 µg/mL of NRE showed the inhibition of cellular tyrosinase activity by 6%, 8%, 22% and 39% respectively (Fig. 30C). The IC50 values of NFE, NSE, and NRE for cellular tyrosinase were estimated to be 38 µg/mL, 14 µg/mL, and 51 µg/mL.
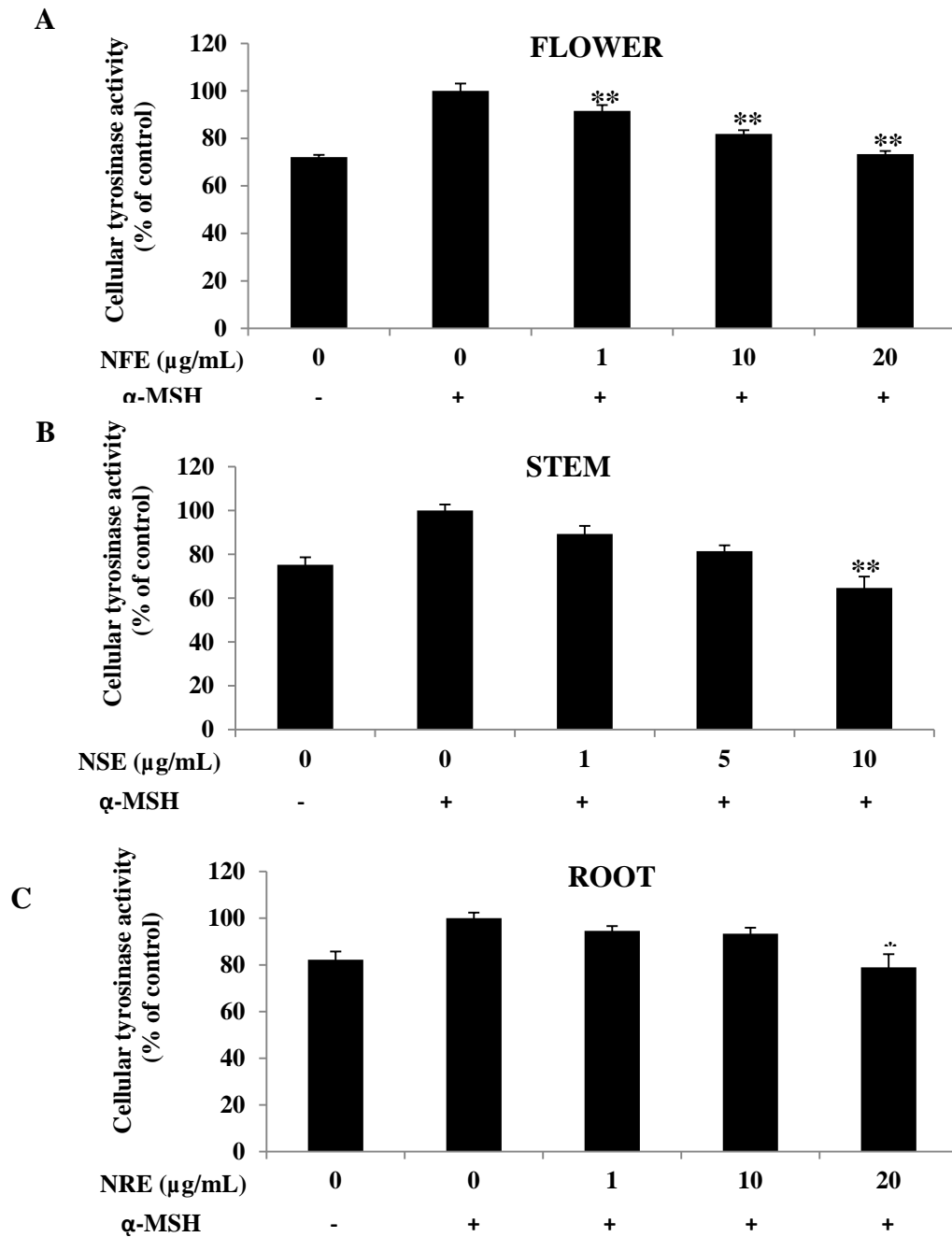
Figure 30. Inhibitory effect of NE on α-MSH-stimulated cellular tyrosinase activity in B16-F10 melanoma cells.

Cellular tyrosinase activity in B16-F10 melanoma cell was observed after treatment of α-MSH (20 nM) and varying concentrations of **(A)** NFE, **(B)** NSE and **(C)** NRE. Values represent the mean ± S.E. for three independent experiments (***p < 0.0001 compared with the control).

Inhibitory effect on melanin synthesis

α-MSH stimulated B16-F10 melanoma cells were used to observe the inhibitory effect of NE on melanin synthesis. Melanin synthesis was markedly increased in the presence of α-MSH, whereas diminishing pattern of melanin was observed in exposure to increasing concentration range of NE (Fig. 31A). 1, 10, 20 and 40 µg/mL of NFE suppressed melanin synthesis by 11%, 25%, 42% and 70% respectively (Fig. 31B). 1, 2, 5 and 10 µg/mL of NSE suppressed melanin synthesis by 5%, 8%, 28% and 36% (Fig. 31C). 1, 10, 20 and 40 µg/mL of NRE suppressed melanin synthesis by 15%, 16%, 30% and 44% respectively. The IC50 values of NFE, NSE, and NRE for cellular melanin synthesis were estimated to be 24µg/mL, 19 µg/mL, and 37 µg/mL.
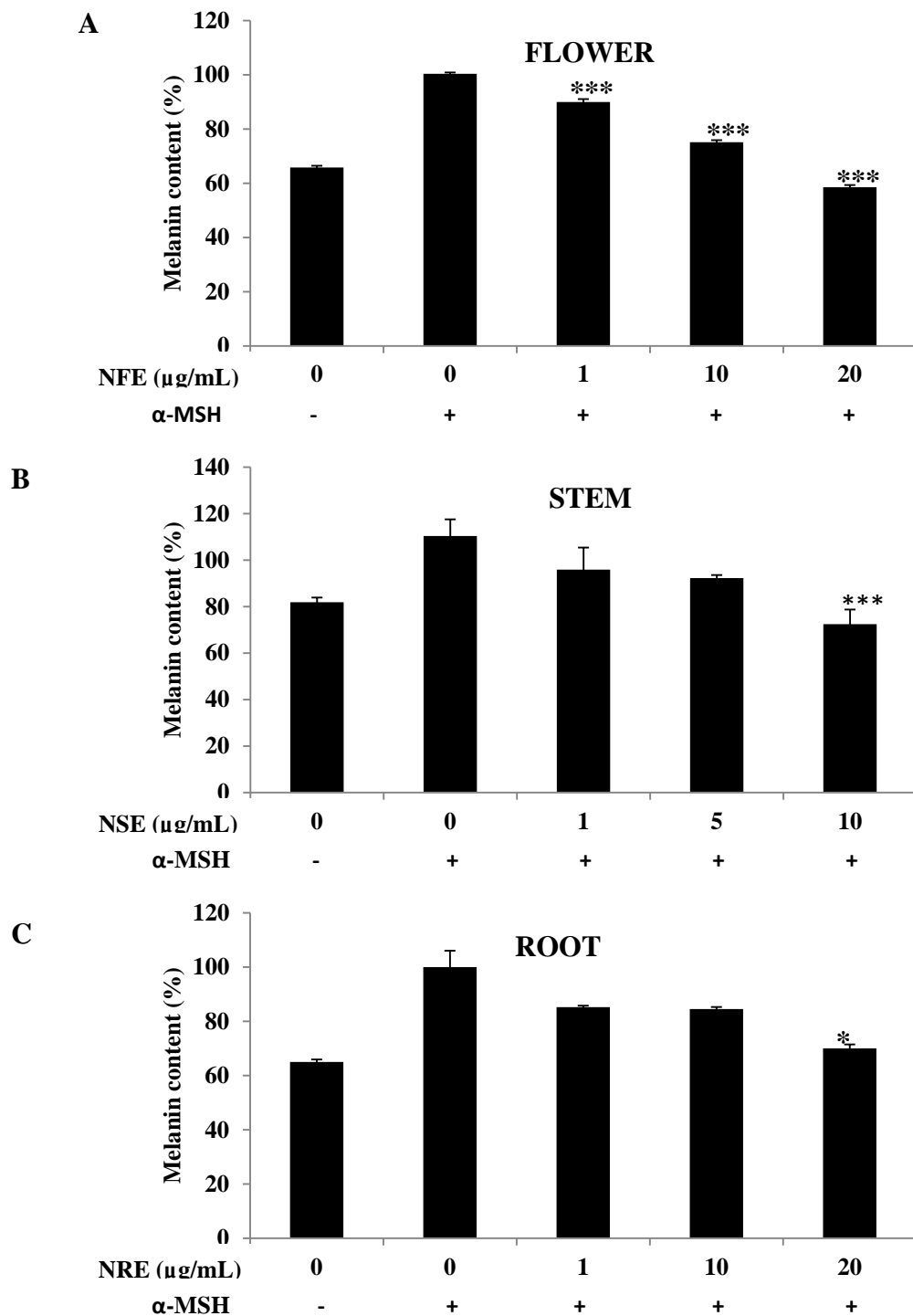
Figure 31. Inhibitory effect of NE on α-MSH-stimulated melanogenesis in B16-F10 melanoma cells.

Melanin synthesis inhibitory activity of B16-F10 melanoma cells exposed to α-MSH (20 nM) and varying concentrations of **(A)** NFE **(B)** NSE and **(C)** NRE were observed. Values

represent the mean ± S.E. for three independent experiments (**p < 0.001, and ***p < 0.0001 compared with the control).

Figure 32. Microscopic images (100X) of α-MSH-stimulated B16-F10 melanoma cells incubated with varying concentration of (A) NFE (B) NSE and (C) NRE

제주대학교 중앙도서관
JEJU NATIONAL UNIVERSITY LIBRARY

DISCUSSION

The present study evaluated the inhibitory activity of extracts of *Narcissus tazetta var. Chinensis* on inflammation in RAW 264.7 macrophage and melanin synthesis in B16-F10 melanoma cells. NE scavenged DPPH free radicals in a dose-dependent manner. Based on western blot analysis, NE significantly reduced the expression levels of iNOS and COX-2, with concomitant reductions in the production of NO in LPS stimulated RAW 264.7 cells. In addition, NE inhibited pro-inflammatory cytokine levels including TNF-α, IL-1β, and IL-6 in LPS stimulated RAW 264.7 cells. RNA sequencing analysis showed differential gene expression patterns in genes related to immune response, inflammatory res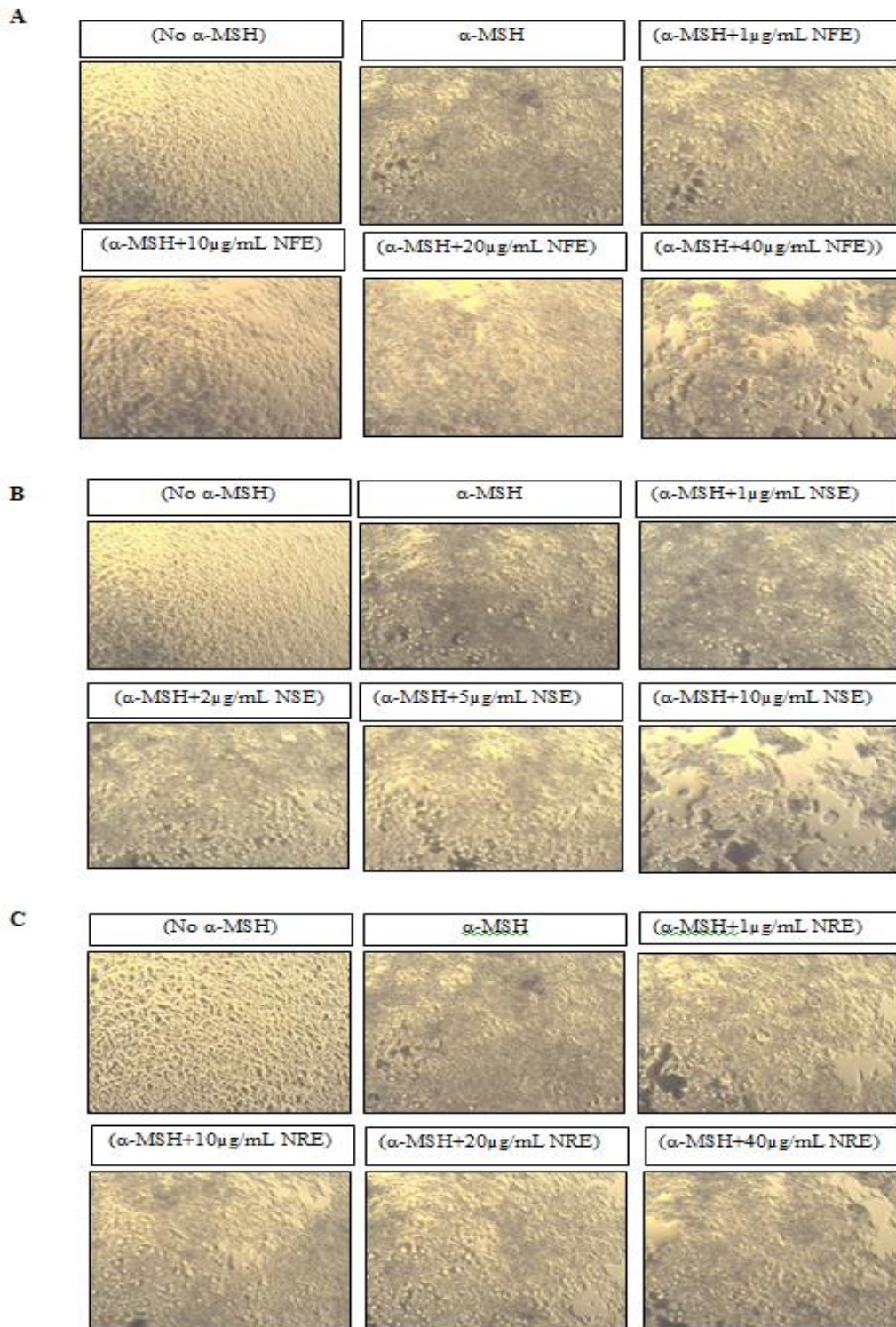ponse and antioxidant activity in LPS stimulated RAW 264.7 cells. NE inhibited both melanin synthesis and tyrosinase activity in α-MSH stimulated B16-F10 melanoma cells in a dose dependent manner. The present study observed that NE have anti-inflammatory effects via normalizing the expression of genes related to inflammation which were perturbed by LPS in RAW cells, and anti-melanogenesis effects on α-MSH stimulated B16-F10 melanoma cells through inhibition of cellular tyrosinase activity.

Phytochemicals have been reported to possess a variety of physiological activities, such as anti-oxidative activities anti-inflammation and anti-melanogenesis effects [33]. In the present study, the inhibitory effects of NE against LPS-induced RAW 264.7 macrophage cell inflammatory response and α-MSH induced B16-F10 melanoma cell melanogenesis were investigated.

In this study, NE displayed DPPH free radical scavenging activity in a dose-dependent manner. Previous studies revealed that the skin is vulnerable to oxidative attack due to the exposure of UV and ROS. High levels of reactive oxygen species (ROS) are generated from inflammation by leukocytes and macrophages in inflamed skin, UV rays

from sun, environment pollutants and natural process of aging stimulate the inflammatory process in the skin which induce complex biological reactions leading to DNA damage and overwhelms cellular scavenging systems [58, 85]. ROS causes up-regulation of tyrosinase activity in melanocytes, which activate α-MSH/MC1R or MITF signaling pathway and mediate elevation of melanogenesis [56]. Therefore, ROS scavengers will reduce skin inflammation and hyperpigmentation.

The current study observed that, NE significantly suppressed the expression levels of iNOS and COX-2, with concomitant reductions in the production of NO in LPS stimulated RAW 264.7 cells. Based on previous studies, NO which is synthesized by iNOS could activate the proteins and enzymes critical to inflammation including NF-κB [14]. Production of prostaglandin is regulated by COX-1, COX-2 which promote pain, fever, and inflammation [66]. Therefore, NE have anti-inflammatory effects on LPS stimulated RAW 264.7 macrophage cells by reducing inflammatory mediators including iNOS and COX-2 proteins.

In the present study, NE significantly suppressed the production of pro-inflammatory cytokines including TNF-α, IL-6 and IL-1β in RAW 264.7 macrophage cells in a concentration dependent manner. TNF-α is considered to be key mediators of inflammatory diseases, which is overexpressed in some pathogenic conditions and possesses a toxic effect that results in hypersensitivity reactions causing chronic inflammation [80]. IL-6 plays a major role in the acute inflammation and possess variety of clinical and biological features such as the production of acute phase proteins and believed to be an endogenous mediator of LPS-induced fever [22, 80]. IL-1β is a pro-inflammatory cytokine that has been involved in pain, inflammation and autoimmune conditions [65]. Macrophages secrete pro-inflammatory cytokines including TNF-α IL-6 and IL-1β as a host defense response, to modulate inflammatory response and overproduction of pro-inflammatory cytokines causes extreme

78

tissue damage [11, 45]. Therefore, mitigating overproduction of pro-inflammatory cytokines is an important healing procedure in inflammation. Data revealed that NE has anti-inflammatory effects on LPS stimulated RAW 264.7 macrophage cells by suppressing the production of pro-inflammatory cytokines including TNF-α, IL-6 and IL-1β.

In the present study, NSE normalized NF-κB1 and NFE normalized NF-κB2 which were elevated in LPS induced RAW 264.7 cells. NF-κB1 and NF-κB2 proteins (p105 and p100) serve as both NF-κB precursors and inhibitors of NF-κB dimers [73]. NF-κB plays a significant role in the LPS-induced expression of many inflammation-related genes. NF-κB translocate into the nucleus and trigger the transcription of inflammation-associated genes following phosphorylation of IκBs by IκB kinases in exposure to a cytokines or LPS [51, 67]. Activated NF-κB involves in the pathogenesis including proliferation, survival, and secretion of proinflammatory cytokines [7].NF-κB has two contrasting roles; as increased and sustained NF-κB activation induces inflammation and tissue damage, and on the other hand NF-κB signaling disturbs immune homeostasis, triggering inflammation and disease [89]. Tight regulation of NF-κB ensures the homeostasis in immune system [62]. Therefore, inhibition of NF-κB activation is a promising therapeutic target and an agent inhibiting the overexpression of NF-κB has a beneficial role as anti-inflammatory agents. In the present study, both NFE and NSE normalized up-regulated NF-κB gene to the control level in LPS stimulated RAW 264.7 macrophage cells assuring the anti-inflammatory effects of NE.

STRING analysis developed based on RNA sequencing data of this study shows a protein-protein interaction (PPI) network constructed of differentially expressed genes (DEGs) identified in LPS stimulated RAW 264.7 cells. STRING analysis uncovered interaction of 29, 25 and 28 genes which are related to inflammation, immune response or anti-oxidant activity were up or down-regulated by LPS and were standardized by NFE, NSE and NRE respectively. In PPI network, either NF-Kb or NF-κB2 forms "functional hubs" in

the middle of network which explains the molecular mechanisms underlying the anti-inflammatory of NE.

In the present study, LPS induced RAW 264.7 cells overexpressed chemokine family genes including CXCL9, CXCL11, CCL28 CXCR2, and CXCR6 which were normalized into control level by NE. Previous studies revealed that, CXC family chemokines CXCL9 and CXCL11 recruit immune cells at the inflammation site, and develope autoimmune diseases by creating local amplification loops of inflammation which induce worsening of clinical manifestation and involved in pathogenesis of a variety of physiological diseases [16, 40]. CCL28 is expressed and increased by pro-inflammatory cytokines and bacterial products, and recruits effector cells to site of injury and could cause autoimmune condition in overexpressed conditions [18]. Chemokine receptor CXCR2 is the major receptor which regulates inflammatory neutrophil recruitment in acute and chronic inflamed tissues and contributes to autoimmune condition [16]. Chemokine receptor CXCR6 regulates the recruitment of pro-inflammatory IL-17A-producing T cells and contribute in autoimmune condition [5]. Therefore, NE have anti-inflammatory effects on LPS stimulated RAW 264.7 macrophage cells by regulating chemokine family gene expressions.

In the current study, NE standardized LTA, CARD9, and ANXA1 genes which were up-regulated by LPS in RAW 264.7 macrophage cells. It is reported that LTA is the closest homolog to TNFα and binds following phosphorylation of MAPKs p38, ERK1/2, PI3K, and Akt. CARD9 initiates cytokine cascade in myeloid cells, plays the positive roles in fighting fungal and viral infections in activated macrophage, and up-regulates IL-1β synthesis [92]. ANXA1 modulates both chronic and acute inflammation, several inflammatory diseases, and autoimmune diseases [23, 75].

In our study, elevated expression of IFNB1, IFNAR1, IFNB1, IL-12B, IL-13 and SOD genes in LPS stimulated RAW 264.7 macrophage cells were normalized into control

level by NE. Previous studies revealed that IFNB1 modulates expression of cytokines and cytokine receptors, affects leukocyte trafficking. In addition it affects bone marrow–derived macrophages and NK cells migration to secondary sites during infections [69]. IFNAR1 alters migration of inflammatory monocytes and neutrophils to the infected site [17]. IL-13 stimulates skin inflammation and tissue remodeling at sites of T helper (Th) 2 inflammation [52]. IL-12 stimulates IFN-γ production and of the develop of T helper (Th) 1 autoimmune response and IL-12B encodes proteins in interleukin-12 (IL-12) superfamily of cytokines [9, 57]. LTF activates macrophages and induce secretion of TNF-α, IL-8, NO and increase inflammation [79]. SOD mediates neutrophil-mediated inflammation through SOD induced neutrophil apoptosis [90]. Our findings suggest NE has anti-inflammatory effects by regulating above genes following LPS stimulation in RAW 264.7 macrophage cells.

Several reports have demonstrated that RIPK2 plays a central role in the nucleotide binding and oligomerization domain (NOD) signaling pathway, promotes infiltration of immune cells, and mounts inflammatory cytokine response upon NOD stimulation [48]. IRAK2 gene has a unique role in mediating LPS-induced cytokine and chemokine production which is essential for TLR4 induced septic shock [86]. FAS plays a critical role in delivering death signals to the immune system, and regulates death signal pathway leading to lymphocyte apoptosis, whereas down regulation of FAS cause lymphocyte proliferation and autoimmune disease [60]. NE is a potent anti-inflammatory agent in LPS induced RAW 264.7 macrophage cells by normalizing above genes related to inflammation.

NE normalized genes which were down-regulated in LPS stimulated RAW 264.7 macrophage cells into control level. Previous studies reported APOE gene induces anti-inflammatory phenotype in macrophages and NE normalized APOE gene expression to control level in LPS induced RAW 264.7 cells further confirming anti-inflammatory effect of NE in RAW 264.7 macrophage cells.

81

In this present study, NE inhibited both mushroom tyrosinase activity and cellular tyrosinase activity in α-MSH stimulated B16-F10 melanoma cells in a dose dependent manner. Direct inhibitory effects of NE on tyrosinase activity were exhibited by mushroom tyrosinase activity inhibition. Previous studies revealed that tyrosinase plays a major role in the melanogenic pathway by oxidizing L-DOPA dopaquinone, an intermediate that is common to both eumelanogenic and pheomelanogenic pathways [78]. Tyrosinase is processed in the endoplasmic reticulum and Golgi, and is trafficked to melanosomes to synthesize melanin in melanocytes [59]. Since tyrosinase is a key enzyme in melanin synthesis, directly inhibition of tyrosinase catalytic activity is a prominent and successful therapeutic target for melanogenesis inhibition [59]. NE showed anti-melanogenesis effects on α-MSH stimulated B16-F10 melanoma cells through inhibition of cellular tyrosinase activity.

Fractions collected from preparative liquid chromatography significantly scavenged DPPH free radicles and inhibited NO production in LPS induced RAW 264.7 macrophage cells. Previous studies revealed that Narcissus is a source of new pharmaceutical compounds which contains Amaryllidaceae alkaloids including lycorine, galanthamine, tazettine, narciclasine, crinine, montaine, homolycorine and plicamine [83]. Lycorine blockes LPS induced production of pro-inflammatory mediators including iNOS and COX-2 suppresses the release of NO, PGE2, TNF- α, and IL-6 in LPS-treated RAW264.7 macrophage cells, and further inhibited LPS-induced activation of P38 MAPK and Jak-STAT signaling pathways [8]. Narcissus flower contained phenylethanoid and phenylpropanoid glycosides which have melanogenesis inhibitory activity and demonstrated inhibitory effects on melanogenesis in theophylline stimulated murine B16-F10 melanoma cells [47]. Therefore, anti-oxidant, anti-inflammatory and anti-melanogenesis effects of NE in current study could be due to the beneficial bioactive compounds including galanthamine, tazettine, narciclasine, crinine, lycorine, montaine, homolycorine and plicamine.

Overall results suggest that NE scavenged DPPH free radicles dose dependently, exhibited anti-inflammatory effects via attenuating iNOS, COX-2 protein expression, TNF-α, IL-6 and IL-1β pro-inflammatory cytokines expression and normalizing the expression of genes related to inflammation which were perturbed by LPS in RAW 264.7 macrophage cells, and showed anti-melanogenesis effects on α-MSH stimulated B16-F10 melanoma cells by suppressing the cellular tyrosinase activity and melanin synthesis in B16-F10 melanoma cells. Bioactive compounds in NE can be applied for the development of anti-inflammatory drugs in pharmaceutical industry and for the development of anti-melanogenesis drugs in cosmetic industry.
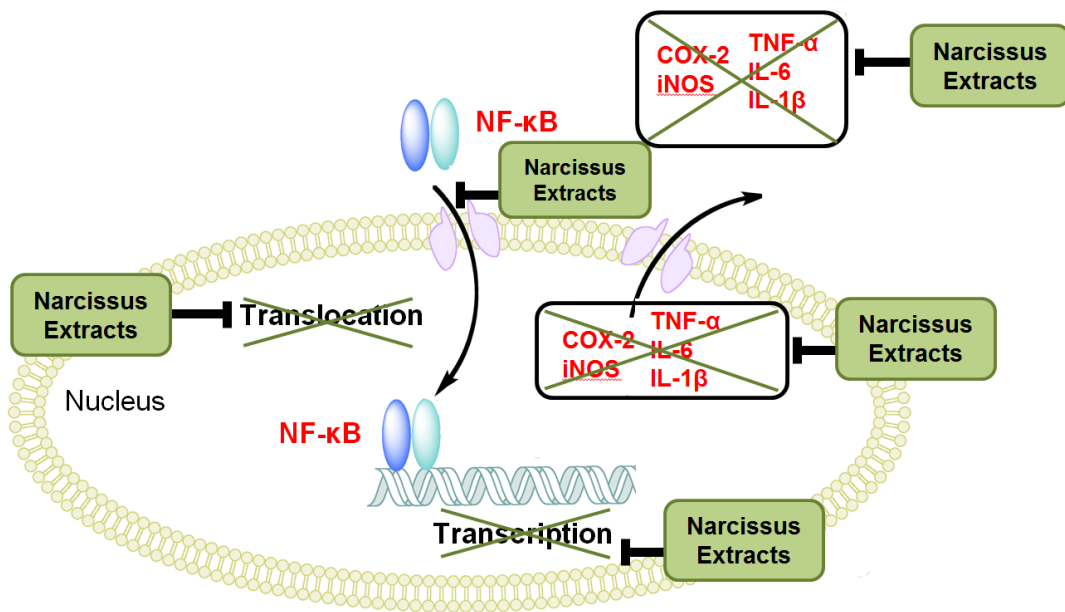

Figure 33. Model of the effects of NE on LPS stimulated RAW 264.7 macrophage cells
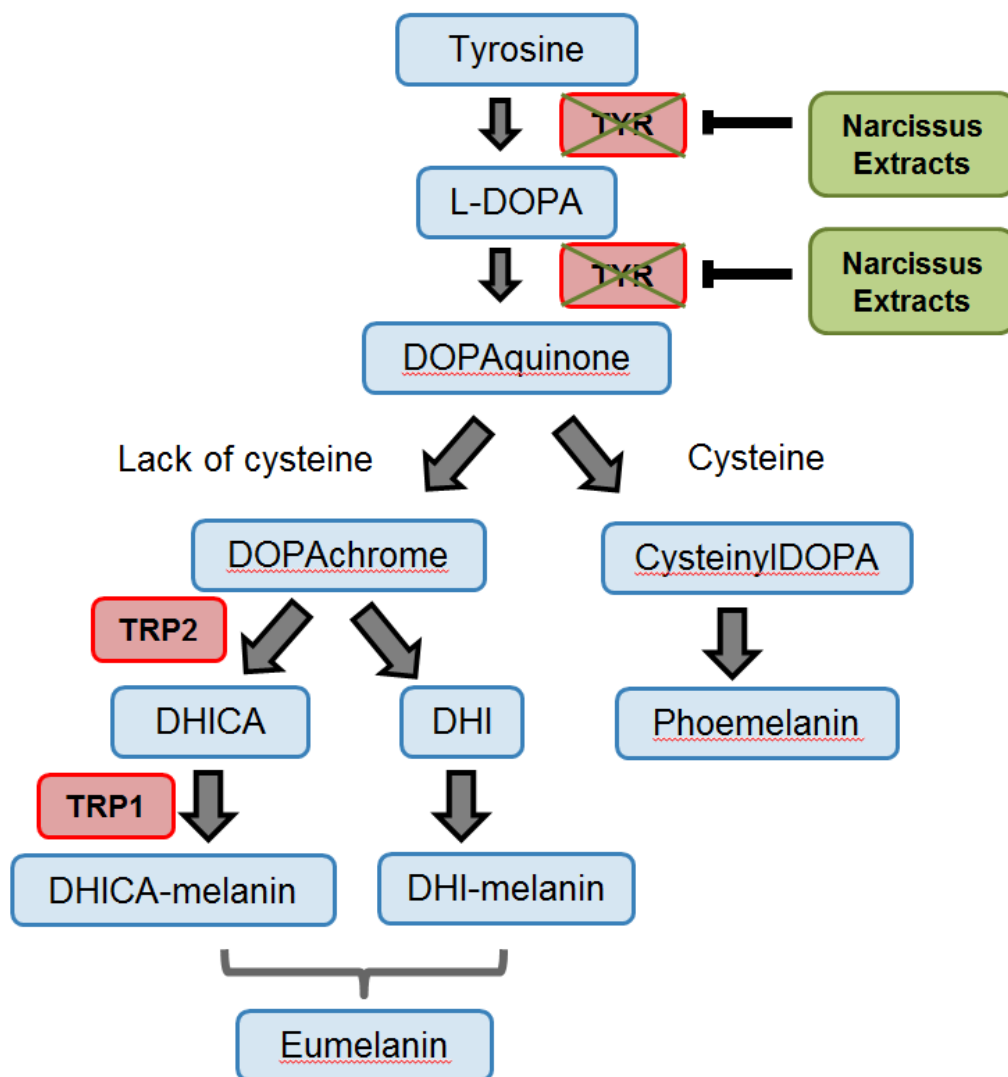
Figure 34. Model of the effects of NE on α-MSH stimulated B16-F10 melanoma cell

CONCLUSION

The present study investigated the effects of NE on LPS stimulated RAW 264.7 macrophages and α-MSH induced melanogenesis in B16-F10 melanoma cells. NE scavenged DPPH free radicles dose dependently, exhibited anti-inflammatory effects via attenuating iNOS, COX-2 protein expression, TNF-α, IL-6 and IL-1β pro-inflammatory cytokines expression and normalizing the expression of genes related to inflammation which were perturbed by LPS in RAW 264.7 macrophage cells, and showed anti-melanogenesis effects on α-MSH stimulated B16-F10 melanoma cells by suppressing the cellular tyrosinase activity and melanin synthesis in B16-F10 melanoma cells. Bioactive compounds in NE can be applied for the development of anti-inflammatory drugs in pharmaceutical industry and for the development of anti-melanogenesis drugs in cosmetic industry

REFERENCES

1.   **Ahn S, Siddiqi MH, Noh H-Y, Kim Y-J, Kim Y-J, Jin C-G, Yang D-C**. Anti-inflammatory activity of ginsenosides in LPS-stimulated RAW 264.7 cells. Sci Bull 2015, **60**, 773-784.

2.   **Baldwin Jr AS**. The NF-κB and IκB proteins: new discoveries and insights. Annu Rev Immunol 1996, 649-681.

3.   **Barnes PJ, Karin M**. Nuclear factor-κB—a pivotal transcription factor in chronic inflammatory diseases. N Engl J Med 1997, **336**, 1066-1071.

4.   **Brenner M, Hearing VJ**. The protective role of melanin against UV damage in human skin. Photochem Photobiol 2008, **84**, 539-549.

5.   **Butcher MJ, Wu C-I, Waseem T, Galkina EV**. CXCR6 regulates the recruitment of pro-inflammatory IL-17A-producing T cells into atherosclerotic aortas. Int Immunol 2015, **28**, 255-261.

6.   **Calkins CM, Bensard DD, Shames BD, Pulido EJ, Abraham E, Fernandez N, Meng X**. IL-1 regulates in vivo C—X—C chemokine induction and neutrophil sequestration following endotoxemia. J Endotoxin Res 2002, **8**, 59-67.

7.   **Calmon-Hamaty F, Combe B, Hahne M, Morel J**. Lymphotoxin α revisited: general features and implications in rheumatoid arthritis. Arthritis Res Ther 2011, **13**, 232.

8.   **Cao Z, Yang P, Zhou Q**. Multiple biological functions and pharmacological effects of lycorine. Sci China Chem 2013, **56**, 1382-1391.

9.   **Chang M, Saiki RK, Cantanese JJ, Lew D, van der Helm-van Mil A, Toes RE, Huizinga TW**. The inflammatory disease–associated variants in IL12B

and IL23R are not associated with rheumatoid arthritis. Arthritis Rheum 2008, **58**, 1877-1881.

10.   **Chen H, Weng QY, Fisher DE**. UV signaling pathways within the skin. J Invest Dermatol 2014, **134**, 2080-2085.

11.   **Cinel I, Opal SM**. Molecular biology of inflammation and sepsis: a primer. Crit Care Med 2009, **37**, 291-304.

12.   **Costin GE, Hearing VJ**. Human skin pigmentation: melanocytes modulate skin color in response to stress. FASEB J 2007, **21**, 976-994.

13.   **D'Agostino P, Ferlazzo V, Milano S, La Rosa M, Di Bella G, Caruso R, Barbera C**. Anti-inflammatory effects of chemically modified tetracyclines by the inhibition of nitric oxide and interleukin-12 synthesis in J774 cell line. Int Immunopharmacol 2001, **1**, 1765-1776.

14.   **DeFranco A, Hambleton J, McMahon M, Weinstein S**. Examination of the role of MAP kinase in the response of macrophages to lipopolysaccharide. Prog Clin Biol Res 1995, **392**, 407-420.

15.   **DiDonato J, Mercurio F, Rosette C, Wu-Li J, Suyang H, Ghosh S, Karin M**. Mapping of the inducible IkappaB phosphorylation sites that signal its ubiquitination and degradation. Mol Cell Biol 1996, **16**, 1295-1304.

16.   **Ding Q, Lu P, Xia Y, Ding S, Fan Y, Li X, Han P**. CXCL9: evidence and contradictions for its role in tumor progression. Cancer Med 2016, **5**, 3246-3259.

17.   **Dorhoi A, Yeremeev V, Nouailles G, Weiner J, Jörg S, Heinemann E, Oberbeck-Müller D**. Type I IFN signaling triggers immunopathology in tuberculosis-susceptible mice by modulating lung phagocyte dynamics. Eur J Immunol 2014, **44**, 2380-2393.

18.   **Eksteen B, Miles A, Curbishley SM, Tselepis C, Grant AJ, Walker LS, Adams DH**. Epithelial inflammation is associated with CCL28 production and the recruitment of regulatory T cells expressing CCR10. J Immunol 2006, **177**, 593-603.

19.   **Englaro W, Bahadoran P, Bertolotto C, Dérijard B, Livolsi A, Peyron J-F, Ortonne J-P**. Tumor necrosis factor alpha-mediated inhibition of melanogenesis is dependent on nuclear factor kappa B activation. Oncogene 1999, **18**, 1553.

20.   **Fang H, Pengal RA, Cao X, Ganesan LP, Wewers MD, Marsh CB, Tridandapani S**. Lipopolysaccharide-induced macrophage inflammatory response is regulated by SHIP.   J Immunol 2004, **173**, 360-366.

21.   **Fu KL, Li X, Ye J, Lu L, Xu XK, Li HL, Zhang WD**. Chemical constituents of Narcissus tazetta var. chinensis and their antioxidant activities. Fitoterapia 2016, **113**, 110-116.

22.   **Gabay C**. Interleukin-6 and chronic inflammation. Arthritis Res Ther 2006, **8**, S3.

23.   **Gavins FNE, Hickey MJ**. Annexin A1 and the regulation of innate and adaptive immunity. Front Immunol 2012, **3**, 354.

24.   **Gentleman RC, Carey VJ, Bates DM, Bolstad B, Dettling M, Dudoit S, Ellis B**. Bioconductor: open software development for computational biology and bioinformatics. Genome Biol 2004, **5**, R80.

25.   **Ghosh S, May MJ, Kopp EB**. NF-κB and Rel proteins: evolutionarily conserved mediators of immune responses. Annu Rev Immunol 1998, **16**, 225-260.

26.   **Guha M, Mackman N**. LPS induction of gene expression in human monocytes. Cell signal 2001, **13**, 85-94.

27.   **Guzik T, Korbut R, Adamek-Guzik T**. Nitric oxide and superoxide in inflammation. J physiol pharmacol 2003, **54**, 469-487.

28.   **Guzik T, Korbut R, Adamek-Guzik T**. Nitric oxide and superoxide in inflammation. J physiol pharmacol 2003, **54**, 469-487.

29.   **Ishida Y, Gao J-L, Murphy PM**. Chemokine receptor CX3CR1 mediates skin wound healing by promoting macrophage and fibroblast accumulation and function. J Immunol 2008, **180**, 569-579.

30.   **Janeway CA, Jr., Medzhitov R**. Innate immune recognition. Annu Rev Immunol 2002, **20**, 197-216.

31.   **Jeong J-W, Hwang SJ, Han MH, Lee D-S, Yoo JS, Choi I-W, Cha H-J**. Fucoidan inhibits lipopolysaccharide-induced inflammatory responses in RAW 264.7 macrophages and zebrafish larvae. Mol cell toxicol 2017, **13**, 405-417.

32.   **Jones BA, Beamer M, Ahmed S**. Fractalkine/CX3CL1: a potential new target for inflammatory diseases. Mol Interv 2010, **10**, 263.

33.   **Kashif M, Akhtar N, Mustafa R**. An overview of dermatological and cosmeceutical benefits of Diospyros kaki and its phytoconstituents. Rev bras farmacogn 2017.

34.   **Kato K, Kawaguchi Y, MizuNo T**. Structural analysis of suisen glucomannan. Carbohydr Res 1973, **29**, 469-476.

35.   **Kim DH, Chung JH, Yoon JS, Ha YM, Bae S, Lee EK, Jung KJ**. Ginsenoside Rd inhibits the expressions of iNOS and COX-2 by suppressing NF-kappaB in LPS-stimulated RAW264.7 cells and mouse liver. J Ginseng Res 2013, **37**, 54-63.

36.   **Kim Y, Kim K, Lee H, Han S, Lee Y-S, Choe J, Kim Y-M**. Celastrol binds to ERK and inhibits FcεRI signaling to exert an anti-allergic effect. Eur J Pharmacol 2009, **612**, 131-142.

37.   Kirkham P. Oxidative stress and macrophage function: a failure to resolve the inflammatory response. Portland Press Limited; 2007. p.

38.   **Koh TJ, DiPietro LA**. Inflammation and wound healing: the role of the macrophage. Expert Rev Mol Med 2011, **13**.

39.   **Kondo T, Hearing VJ**. Update on the regulation of mammalian melanocyte function and skin pigmentation. Expert Rev Dermatol 2011, **6**, 97-108.

40.   **Lacotte S, Brun S, Muller S, Dumortier H**. CXCR3, inflammation, and autoimmune diseases. Ann N Y Acad Sci 2009, **1173**, 310-317.

41.   **Langmead B, Salzberg SL**. Fast gapped-read alignment with Bowtie 2. Nature methods 2012, **9**, 357-359.

42.   **Lee SY, Kim HJ, Han JS**. Anti-inflammatory Effect of Oyster Shell Extract in LPS-stimulated Raw 264.7 Cells. Prev Nutr Food Sci 2013, **18**, 23-29.

43.   **Liu J, Li Y, Ren W, Hu WX**. Apoptosis of HL-60 cells induced by extracts from Narcissus tazetta var. chinensis. Cancer Lett 2006, **242**, 133-140.

44.   **Liu X-H, Kirschenbaum A, Yao S, Stearns ME, Holland JF, Claffey K, Levine AC**. Upregulation of vascular endothelial growth factor by cobalt chloride-simulated hypoxia is mediated by persistent induction of cyclooxygenase-2 in a metastatic human prostate cancer cell line. Clin Exp Metastasis 1999, **17**, 687-694.

45.   **Medzhitov R**. Origin and physiological roles of inflammation. Nature 2008, **454**, 428.

46.   **Morikawa T, Ninomiya K, Kuramoto H, Kamei I, Yoshikawa M, Muraoka O**. Phenylethanoid and phenylpropanoid glycosides with melanogenesis inhibitory activity from the flowers of Narcissus tazetta var. chinensis. J Nat Med 2016, **70**, 89-101.

47.   **Morikawa T, Ninomiya K, Kuramoto H, Kamei I, Yoshikawa M, Muraoka O**. Phenylethanoid and phenylpropanoid glycosides with melanogenesis inhibitory activity from the flowers of Narcissus tazetta var. chinensis. J Nat Med 2016, **70**, 89-101.

48.   **Nachbur U, Stafford CA, Bankovacki A, Zhan Y, Lindqvist LM, Fiil BK, Khakham Y**. A RIPK2 inhibitor delays NOD signalling events yet prevents inflammatory cytokine production. Nat Commun 2015, **6**, 6442.

49.   **Nachbur U, Stafford CA, Bankovacki A, Zhan Y, Lindqvist LM, Fiil BK, Khakham Y**. A RIPK2 inhibitor delays NOD signalling events yet prevents inflammatory cytokine production. Nat Commun 2015, **6**, 6442.

50.   **Napoli C, de Nigris F, Williams-Ignarro S, Pignalosa O, Sica V, Ignarro LJ**. Nitric oxide and atherosclerosis: an update. Nitric oxide 2006, **15**, 265-279.

51.   **Oeckinghaus A, Ghosh S**. The NF-κB family of transcription factors and its regulation. Cold Spring Harb Perspect Biol 2009, **1**, a000034.

52.   **Oh M-H, Oh SY, Yu J, Myers AC, Leonard WJ, Liu YJ, Zhu Z**. IL-13 induces skin fibrosis in atopic dermatitis by thymic stromal lymphopoietin. J Immunol 2011, **186**, 7232-7242.

53.   **Ortonne J**. The effects of ultraviolet exposure on skin melanin pigmentation. J Int Med Res 1990, **18**, 8C-17C.

54.   **Oseguera-Toledo ME, de Mejia EG, Dia VP, Amaya-Llano SL**. Common bean (Phaseolus vulgaris L.) hydrolysates inhibit inflammation in LPS-induced

macrophages through suppression of NF-κB pathways. Food chem 2011, **127**, 1175-1185.

55. **Pang M, Bai XY, Li Y, Bai JZ, Yuan LR, Ren SA, Hu XY**. Label-free LC-MS/MS shotgun proteomics to investigate the anti-inflammatory effect of rCC16. Mol Med Rep 2016, **14**, 4496-4504.

56. Panich U. Antioxidant Defense and UV-Induced Melanogenesis: Implications for Melanoma Prevention. Current Management of Malignant Melanoma: InTech; 2011.

57. **Paunović V, Carroll H, Vandenbroeck K, Gadina M**. Signalling, inflammation and arthritis: crossed signals: the role of interleukin (IL)-12,-17,-23 and-27 in autoimmunity. Rheumatology 2008, **47**, 771-776.

58. **Pillai S, Oresajo C, Hayward J**. Ultraviolet radiation and skin aging: roles of reactive oxygen species, inflammation and protease activation, and strategies for prevention of inflammation-induced matrix degradation–a review. Int J Cosmet Sci 2005, **27**, 17-34.

59. **Pillaiyar T, Manickam M, Namasivayam V**. Skin whitening agents: Medicinal chemistry perspective of tyrosinase inhibitors. J Enzyme Inhib Med Chem 2017, **32**, 403-425.

60. **Pinhu L, Qin Y, Xiong B, You Y, Li J, Sooranna SR**. Overexpression of Fas and FasL is associated with infectious complications and severity of experimental severe acute pancreatitis by promoting apoptosis of lymphocytes. Inflammation 2014, **37**, 1202-1212.

61. **Pushpakumar S, Ren L, Kundu S, Gamon A, Tyagi SC, Sen U**. Toll-like Receptor 4 Deficiency Reduces Oxidative Stress and Macrophage Mediated Inflammation in Hypertensive Kidney. Sci rep 2017, **7**, 6349.

62. **Qu L, Ji Y, Zhu X, Zheng X**. hCINAP negatively regulates NF-κB signaling by recruiting the phosphatase PP1 to deactivate IKK complex. J MOL CELL BIOL 2015, **7**, 529-542.

63. **Rabeta M, Vithyia M**. Effect of different drying methods on the antioxidant properties of Vitex negundo Linn. tea. IFRJ 2013, **20**, 3171-3176.

64. **Razik A, Adly F, Moussaid M, Berhal C, Moussaid H, Elamrani A, Bellahcen TO**. Antimicrobial, Antioxidant and Anti-Inflammatory Activities of the extract of a Moroccan endemic Narcissus: Narcissus broussonetii. IJSRST 2016, **2**, 6-11.

65. **Ren K, Torres R**. Role of interleukin-1β during pain and inflammation. Brain Res Rev 2009, **60**, 57-64.

66. **Ricciotti E, FitzGerald GA**. Prostaglandins and inflammation. Arterioscler Thromb Vasc Biol 2011, **31**, 986-1000.

67. **Rigoglou S, Papavassiliou AG**. The NF-κB signalling pathway in osteoarthritis. Int J Biochem Cell Biol 2013, **45**, 2580-2584.

68. **Roger T, Chanson AL, Knaup-Reymond M, Calandra T**. Macrophage migration inhibitory factor promotes innate immune responses by suppressing glucocorticoid-induced expression of mitogen-activated protein kinase phosphatase-1. Eur J immunol 2005, **35**, 3405-3413.

69. **Salazar-Mather TP, Lewis CA, Biron CA**. Type I interferons regulate inflammatory cell trafficking and macrophage inflammatory protein 1α delivery to the liver. Eur J Clin Invest 2002, **110**, 321-330.

70. Salvemini D, Ischiropoulos H, Cuzzocrea S. Roles of nitric oxide and superoxide in inflammation. Inflammation Protocols: Springer; 2003. p. 291-303.

71.   **Sánchez-Moreno C, Larrauri JA, Saura-Calixto F**. A procedure to measure the antiradical efficiency of polyphenols. J Sci Food Agric 1998, **76**, 270-276.

72.   **Satooka H, Cerda P, Kim H-J, Wood WF, Kubo I**. Effects of matsutake mushroom scent compounds on tyrosinase and murine B16-F10 melanoma cells. Biochem Biophys Res Commun 2017, **487**, 840-846.

73.   **Savinova OV, Hoffmann A, Ghosh G**. The Nfkb1 and Nfkb2 proteins p105 and p100 function as the core of high-molecular-weight heterogeneous complexes. Mol cell 2009, **34**, 591-602.

74.   **Schiaffino MV**. Signaling pathways in melanosome biogenesis and pathology. Int J Biochem Cell Biol 2010, **42**, 1094-1104.

75.   **Sena AA, Glavan T, Jiang G, Sankaran-Walters S, Grishina I, Dandekar S, Goulart LR**. Divergent Annexin A1 expression in periphery and gut is associated with systemic immune activation and impaired gut immune response during SIV infection. Sci Rep 2016, **6**, 31157.

76.   **Seo H, Cho YC, Ju A, Lee S, Park BC, Park SG, Kim JH**. Dual-specificity phosphatase 5 acts as an anti-inflammatory regulator by inhibiting the ERK and NF-kappaB signaling pathways. Sci Rep 2017, **7**, 17348.

77.   **Sheng H, Shao J, Morrow JD, Beauchamp RD, DuBois RN**. Modulation of apoptosis and Bcl-2 expression by prostaglandin E2 in human colon cancer cells. Cancer Res 1998, **58**, 362-366.

78.   **Slominski A, Zmijewski MA, Pawelek J**. L-tyrosine and L-dihydroxyphenylalanine as hormone-like regulators of melanocyte functions. Pigment Cell Melanoma Res 2012, **25**, 14-27.

79.   **Sorimachi K, Akimoto K, Hattori Y, Ieiri T, Niwa A**. Activation of macrophages by lactoferrin: secretion of TNF-α, IL-8 and NO. IUBMB Life 1997, **43**, 79-87.

80.   **Soromou LW, Zhang Z, Li R, Chen N, Guo W, Huo M, Guan S**. Regulation of inflammatory cytokines in lipopolysaccharide-stimulated RAW 264.7 murine macrophage by 7-O-methyl-naringenin. Molecules 2012, **17**, 3574-3585.

81.   **Sprague AH, Khalil RA**. Inflammatory cytokines in vascular dysfunction and vascular disease. Biochem Pharmacol 2009, **78**, 539-552.

82.   Sunar K, Kumar U, Deshmukh S. Recent Applications of Enzymes in Personal Care Products. Recent Applications of Enzymes in Personal Care Products: Elsevier; 2016. p. 279-298.

83.   **Takos AM, Rook F**. Towards a molecular understanding of the biosynthesis of Amaryllidaceae alkaloids in support of their expanding medical use. Int J Mol Sci 2013, **14**, 11713-11741.

84.   **Tomita Y, MAEDA K, TAGAMI H**. Melanocyte-stimulating properties of arachidonic acid metabolites: possible role in postinflammatory pigmentation. Pigment Cell Res 1992, **5**, 357-361.

85.   **Trenam CW, Blake DR, Morris CJ**. Skin inflammation: reactive oxygen species and the role of iron. J Investig Dermatol 1992, **99**, 675-682.

86.   **Wan Y, Xiao H, Affolter J, Kim TW, Bulek K, Chaudhuri S, Carlson D**. Interleukin-1 receptor-associated kinase 2 is critical for lipopolysaccharide-mediated post-transcriptional control. J Biol Chem 2009, **284**, 10367-10375.

87.   **Wang K-H, Lin R-D, Hsu F-L, Huang Y-H, Chang H-C, Huang C-Y, Lee M-H**. Cosmetic applications of selected traditional Chinese herbal medicines. J Ethnopharmacol 2006, **106**, 353-359.

88.   **Wasmeier C, Hume AN, Bolasco G, Seabra MC**. Melanosomes at a glance. J Cell Sci 2008, **121**, 3995-3999.

89.   **Wullaert A, Bonnet MC, Pasparakis M**. NF-kappaB in the regulation of epithelial homeostasis and inflammation. Cell Res 2011, **21**, 146-158.

90.   **Yasui K, Kobayashi N, Yamazaki T, Agematsu K, Matsuzaki S, Ito S, Nakata S**. Superoxide dismutase (SOD) as a potential inhibitory mediator of inflammation via neutrophil apoptosis. Free Radic Res 2005, **39**, 755-762.

91.   **Yoon NY, Eom T-K, Kim M-M, Kim S-K**. Inhibitory effect of phlorotannins isolated from Ecklonia cava on mushroom tyrosinase activity and melanin formation in mouse B16F10 melanoma cells. J Agric Food Chem 2009, **57**, 4124-4129.

92.   **Zhong X, Chen B, Yang L, Yang Z**. Molecular and physiological roles of the adaptor protein CARD9 in immunity. Cell Death Dis 2018, **9**, 52.

ACKNOWLEDGEMENTS